Lake Carmi Feasibility Study on the Inactivation of Phosphorus in Lake Bottom Sediments

Prepared for
Vermont Department of Environmental Conservation

Draft

March 28, 2024

DRAFT

Lake Carmi Feasibility Study on the Inactivation of Phosphorus in Lake Bottom Sediments

March 28, 2024

Contents

List of Tables

List of Figures

List of Appendices

Abbreviations

°C	degree Celsius
µg	microgram
µS/cm	microSiemens per cm
Al-P	aluminum-bound phosphorus
BMP	best management practice
cm	cm
CN	curve number
CPH	catch per hour
DO	dissolved oxygen
DP	dissolved phosphorus
EPA	U.S. Environmental Protection Agency
Fe-P	iron-bound phosphorus
g	gram
HCl	hydrochloric acid
HDPE	high-density polyethylene
hr	hour
in	inch
kg	kilogram
km	kilometer
km^2	square kilometer
L	liter
m	meter
M	molar
mg	milligram
mL	milliliter
MN	Minnesota
mV	millivolts
NaOH	sodium hydroxide
nm	nanometer
P	phosphorus
PVC	polyvinyl chloride
SRP	soluble reactive phosphorus
TDP	total dissolved phosphorus
TKN	total Kjeldahl nitrogen
TMDL	total maximum daily load
TN	total nitrogen
TP	total phosphorus
VT DEC	Vermont Department of Environmental Conservation

Executive Summary

A comprehensive feasibility study was conducted to evaluate the expected water quality benefits and costs of an in-lake aluminum treatment to control internal phosphorus (P) loading in Lake Carmi. This study also evaluated other aspects of the treatment such as potential effects on fish (toxicological and trophic), expected changes in macrophyte growth, compliance with aluminum criteria, potential effects on benthic invertebrates, and rough fish (carp) effects on treatment. Alternatives were also considered, including dredging, inflow alum treatment at the largest tributary, and further BMP implementation of watershed controls. The analysis consisted of extensive sediment coring across Lake Carmi, laboratory incubation microcosm to evaluate the rate of internal loading under anaerobic conditions, and aluminum addition experiments to quantify the mass of aluminum need to inactivate phosphorus in the bottom sediment and significantly reduce internal loading.

The effectiveness of the aluminum treatments on Lake Carmi water quality was evaluated using a one dimensional hydrodynamic and water quality model that was calibrated to conditions prior to installation of the aerator and after installation of the aerator. From the modeling effort, several conclusions were made: (1) 71 percent of all P loading to Lake Carmi is from internal P loading, (2) cyanobacteria blooms in the lake are largely the consequence of internal P loading and nitrogen limitation, (3) operation of the aerator has not reduced internal P loading in Lake Carmi, and (4) aluminum treatment to control internal P loading will reduce P concentrations and phytoplankton blooms significantly and lake clarity will also improve significantly.

An application dose of 67 grams of aluminum per square meter (g/m^2) of lake bottom area is recommended for lake depths of six meters and greater. The total treatment area is 775 acres. Treatment should occur as a volumetric 2 to 1 mixture of alum and sodium aluminate. There may be some marginal benefits of splitting the dose into two different treatment years but splitting the dose is not a recommendation. A "double pass" approach may be necessary to meet applicable in-lake acute and chronic water quality criteria for aluminum. The opinion of probable cost to conduct the treatment is $2,629,728. However, this cost will be greater if a "double pass" treatment approach is required to comply with permit conditions.

1 Introduction and Study Scope

This report presents the results of a diagnostic feasibility study that evaluates the use of aluminum to treat lake bottom sediments to reduce phosphorus (P) release from the lake bottom (i.e., internal P loading). This study is part of a broader effort outlined in the Lake Carmi Crisis Response Plan (Plan) (Vermont DEC, 2022), which describes a range of implemented and planned watershed and in-lake best management activities. As indicated in the Plan and other supporting information that can be accessed on the Lake Carmi website (https://dec.vermont.gov/watershed/restoring/carmi), despite watershed P loading reductions having been largely achieved in accordance with the total maximum daily load (TMDL) (Vermont Agency of Natural Resources, 2008), phosphorus has remained persistently high with frequent summer algal blooms dominated by cyanobacteria (e.g., harmful algal blooms). Monitoring conducted after installing an aeration system in 2019 also demonstrates that aeration has not been capable of reducing internal P loading and has not prevented the occurrence of significant and frequent blooms.

The scope of work identified by the Vermont Department of Environmental Conservation (VT DEC) included seven tasks outlined below and mapped to their respective report sections.

Task 1 (Report Section 2): "Identification and Validation of Phosphorus Inactivation Approach" pertains to an evaluation of those factors that contribute to internal loading, potential treatment area (e.g., anoxic zone), and effectiveness.

Task 2 (Report Section 4): "Phosphorus Load Reduction Analysis" includes an analysis of the effect of external and internal load reductions on P, phytoplankton (as chlorophyll *a*), and lake clarity. This analysis includes modeling using the Barr Lake Model to accurately quantify sources and sinks of nutrients, make predictions with load reduction, as well as modeling conducted to be consistent with the TMDL. Both external and internal P loading were quantified as part of this analysis.

Task 3 (Report Section 3): "Complete Analyses to Identify Approach for a Future Phosphorus Inactivation Treatment" includes the results of sediment coring on Lake Carmi, phosphorus fractionation, laboratory mesocosm experiments to quantify phosphorus release rates under anaerobic and aerobic conditions, and aluminum addition experiments to develop alum doses (applied as alum and sodium aluminate). The results of this work were used as inputs in the modeling effort in Task 2.

Task 4 (Report Section 5): "Complete a Phosphorus Inactivation Treatment Design, Including Application Approach Options and Dosing Plan" provides a recommendation for doses, lake areas where aluminum application will be most effective, a treatment plan, and consideration of aluminum criteria with the treatment plan. Results of the in-lake response analysis identified in this task are provided in Section 4.

Task 5 (Report Section 3 and 5): "Complete a Cost-Benefit Analysis and Treatment Cost Analysis" includes an estimate of in-lake treatment cost based upon the dose determined in Tasks 3 and 4, potential application strategies such as split dosing, and cost per pound of phosphorus removed.

Task 6 (Report Section 6): "Assess Potential Impacts of Phosphorus Inactivation Treatment on Aquatic Biota" is an evaluation of the potential effect of the aluminum treatment on fish with respect to aluminum toxicity and a reduced trophic state with phosphorus reduction, and invertebrates with respect to chemical and physical toxicity.

Task 7 (Report Section 7): "Address Other Concerns Described Below Related to a Potential Phosphorus Inactivation Treatment in Lake Carmi" address the following additional concerns or considerations with aluminum treatment: site access, permitting, alternatives analysis, sulfate, post-project monitoring, and tributary phosphorus inactivation treatment.

2 Identification and Validation of Phosphorus Inactivation Approach

Phosphorus observed in the surface waters of Lake Carmi predominately originates from watershed inputs (including septic), atmospheric deposition, and sediments that have accumulated on the bottom of Lake Carmi (e.g., internal P loading). A significant fraction of P from watershed inputs deposit on the lake bottom as solids, or in the case of dissolved P (DP), it is first taken up by phytoplankton, which then settle to the lake bottom. Clearly, historical P inputs (i.e., legacy inputs) in Lake Carmi have enriched the lake bottom sediments with P, and these lake bottom sediments are now measurably affecting Lake Carmi water quality (Lake Carmi | Department of Environmental Conservation (vermont.gov)). Long-term water quality improvement of Lake Carmi will result from changes to the magnitude of external and internal phosphorus load and the successful implementation of management actions to reduce those loads. The longevity of internal load controls will also depend upon the effectiveness of watershed management activities.

For Lake Carmi, the dynamics of internal loading are a function of the inherent properties of the lake:

1. Large surface area (1400 acres, 567 hectares), which promotes mixing
2. Long fetch (13,120 feet, 4,000 meters) (i.e., the length of the lake segment across which wind travels) with a predominant northeast-to-southwest wind direction also promotes mixing
3. Relatively shallow average (20 feet/6 meters) and maximum (33 feet/10 meters) depths
4. High ratio of lake area to depth which leads to weak stratification
5. High oxygen demand of the lake bottom sediments
6. Chemistry of lake bottom sediments (see Section 3 of this report)

The effect of these lake characteristics on Lake Carmi P concentrations is the focus of Section 4.

2.1 Historical Summary of Lake Carmi Management Activity

The 2008 TMDL (Vermont Agency of Natural Resources, 2008) provided an account of phosphorus loading sources and management activities conducted prior to the TMDL publication. The management activities identified included:

1. Funding support to three watershed farms since 1998 for integrated crop management
2. Septic tank pumping cost-share program in operation since 2002 (Franklin Watershed Committee)
3. Septic surveys
4. Roadside stabilization
5. Three streambank stabilization projects in 2007

The TMDL assessed sources, including the watershed, septic systems, roads, Lake Carmi State Park wastewater treatment system, atmospheric deposition, and internal loading. Internal loading was underestimated in the TMDL study.

An updated account of watershed and in-lake management activities between 2008 and 2023 include[1] the following:

Watershed Management Activities

1. Participation in the VT DEC Lake Wise Program encouraging shoreline owners to embrace Best Management Practices (BMPs) such as vegetated buffers, proper stormwater drainage, and proper septic maintenance
2. Boat greeter program to prevent the spread of invasive species
3. Ongoing septic socials that advised owners of proper septic maintenance
4. Septic pump-out rebate program to assist shoreline owners with funding for septic pumping
5. Installation of a state-of-the-art, contained wastewater treatment system within Lake Carmi State Park
6. Private roads inventory to identify improvements in stormwater drainage
7. Stream walks of all the major tributaries to identify where buffers and floodplains can be installed to prevent unwanted sediment from entering the lake
8. Pursuant to the Lake in Crisis, Crisis Response Plan, the University of Vermont Extension has been working with farmers in the watershed to install Best Management Agricultural Practices (this has included the use of injection manure equipment and cover cropping)
9. In 2022 and 2023, ditch/stream bank stabilization projects were constructed (e.g., Black Wood Drive, Sandy Bay Road, and Patton Shore Road)
10. Installation of four drip-line infiltration trenched and permeable pavers as part of Lake Wise program evaluations

In-lake Management Activities

1. Installation of a lake aeration system in 2019. Mechanical issues with the southern compressor influenced operation duration in 2020, but the aerator has been operating during the open water season since 2021.
2. Aquatic plant harvesting is conducted in designated littoral areas of Lake Carmi in the south, southeast, southwest, northeast, and northwest regions of the lake. Plant harvesting targets the removal of the invasive aquatic species Eurasian water milfoil.
3. Fisheries management is ongoing at Lake Carmi with walleye fishery regulations ongoing for the open season from the first Saturday in May through March 15 (the following year). The regulations include a minimum length of 381 mm (15 inches) with a 432 to 508 mm (17 to 20 inches) protected slot and a limit of five fish per day. Invasive species that exist in Lake Carmi

[1] Special thanks to the Lake Carmi Campers Association for a thorough account of management activities.

include Alewife and common carp (presumably, although conversations with lake residents and VT DEC have not confirmed that carp are present and VT DEC fisheries reports have not reported on carp). To date, no management activities have been implemented to remove the invasive fish species.

2.2 Geomorphological Characterization

Several geomorphological properties of the Lake Carmi watershed are important to this study. The Lake Carmi watershed of approximately 23.8 km^2 is not large relative to the size (surface area) of the lake, which is 5.7 km^2 (1,400 acres). Using an annual watershed yield (Stroud Water Research Center, n.d.) of 35.9 cm and a lake volume of approximately 32,000,000 m^3, the residence time of Lake Carmi is 3.5 years. It is also notable that 84% of the runoff occurs in January through April and October through December (e.g., the non-summer months). Hence, the residence time is shorter in the spring and fall and longer in the summer. According to the 2008 TMDL, the three major watershed land use areas include agriculture (44%), forest (33%), and other water surfaces (9%). The soils are classified predominantly as C and D (slow infiltration)[4]. Hydraulic residence time, land use, and seasonal runoff patterns combined with the speciation (e.g., dissolved versus particulate) of nutrients in runoff provide some insight into how Lake Carmi will respond to different types of watershed nutrient control and the effectiveness of these controls relative to sediment treatment to reduce internal loading. Some general observations include:

- Watershed inflows contain, on average (not weighted by flow) and across all sites, predominantly dissolved phosphorus. For example, in 2022, 67 percent of the phosphorus was dissolved for all monitored inflows. This affects the type of watershed BMPs that can be employed to reduce watershed loads. These BMPs will need to be able to bind dissolved phosphorus or reduce the source of dissolved phosphorus.

- Watershed inflows that are predominantly dissolved also affect how phosphorus is captured in Lake Carmi. Since runoff occurs primarily in the spring and fall, much of this dissolved phosphorus will pass through the lake. The particulate form will settle. However, this suggests that a slower rate of phosphorus capture by Lake Carmi will enhance the longevity of the sediment treatments. Since the primary mechanism of phosphorus capture in Lake Carmi is algal growth, reduced algal growth with sediment treatment will also reduce phosphorus deposition on the lake bottom.

- The relatively long hydraulic residence time of Lake Carmi also suggests that internal load controls will be effective. A longer hydraulic residence time will also increase longevity.

- Overall, the geomorphology of Lake Carmi is favorable for sediment treatments that control internal loading.

The geomorphology of Lake Carmi promotes water column mixing, vertical transport, and longitudinal transport of water and chemistry in the water column. Several lines of evidence support this conclusion. Lake Carmi is oriented in a northeast to southwest direction (see the bathymetry map on Figure 2-1). The wind rose plots in Appendix A show that the prevailing wind direction is north-east to south-west. Hence, the prevailing wind direction directionally aligns with the longest fetch (approximately 4,000 meters) in

Lake Carmi. The length of a lake's fetch can have a measurable effect on the mixed layer[2] of a lake. This is important because any exchanges between lake bottom sediment and the water column in the mixed layer will be readily transported to the lake surface and made available for phytoplankton. Hence, if phosphorus is released from these sediments, it will rapidly be made available for algal blooms. Whether P is released from sediments in the mixed layer is complicated by the fact that oxygen is typically elevated in the mixed layer during the day. At night, phytoplankton respiration may depress oxygen and stimulate internal P loading. Thus, nutrient dynamics in the mixed layer can be complicated to determine spatially and over time.

A review of temperature profile data collected in 2018 (taken as an example of stratification dynamics prior to the installation of the aeration system) shows that the mixed layer depth in Lake Carmi during the summer months is approximately 6 meters (Appendix B). Although the mixed layer extends from 0 to 6 meters, stratification below 6 meters (between 6 and 10 meters) is not strong, and the temperature differential between layers is small. This implies that mixing bottom waters into the mixed layer likely occurred frequently before installing the aeration system.

Figure 2-1 shows the cumulative area (e.g., sediment surface area) of Lake Carmi as a function of depth. The mixed layer (approximately 0 to 6 meters) corresponds to about half of the total lake area. For each incremental 1-meter descent in depth in Lake Carmi, there is a corresponding area of sediment that is in contact with this layer. Lateral transport from the sediment to water in this layer provides an opportunity for phosphorus released from sediment to be used across the lake.

The aeration system has deepened the mixed layer of Lake Carmi. A review of temperature profile data collected in 2022 (taken as an example of stratification dynamics after installing the aeration system) shows that the mixed layer depth during the summer months extends to the bottom of the lake. This may have increased phosphorus transport from bottom waters or increased the depth within the sediment where anoxic conditions prevail and internal loading occurs. More analysis is provided in the Axonia Investigation section below.

[2] The mixed layer is defined as the maximum lake depth to which all depths above are the same or very nearly the same water temperature.

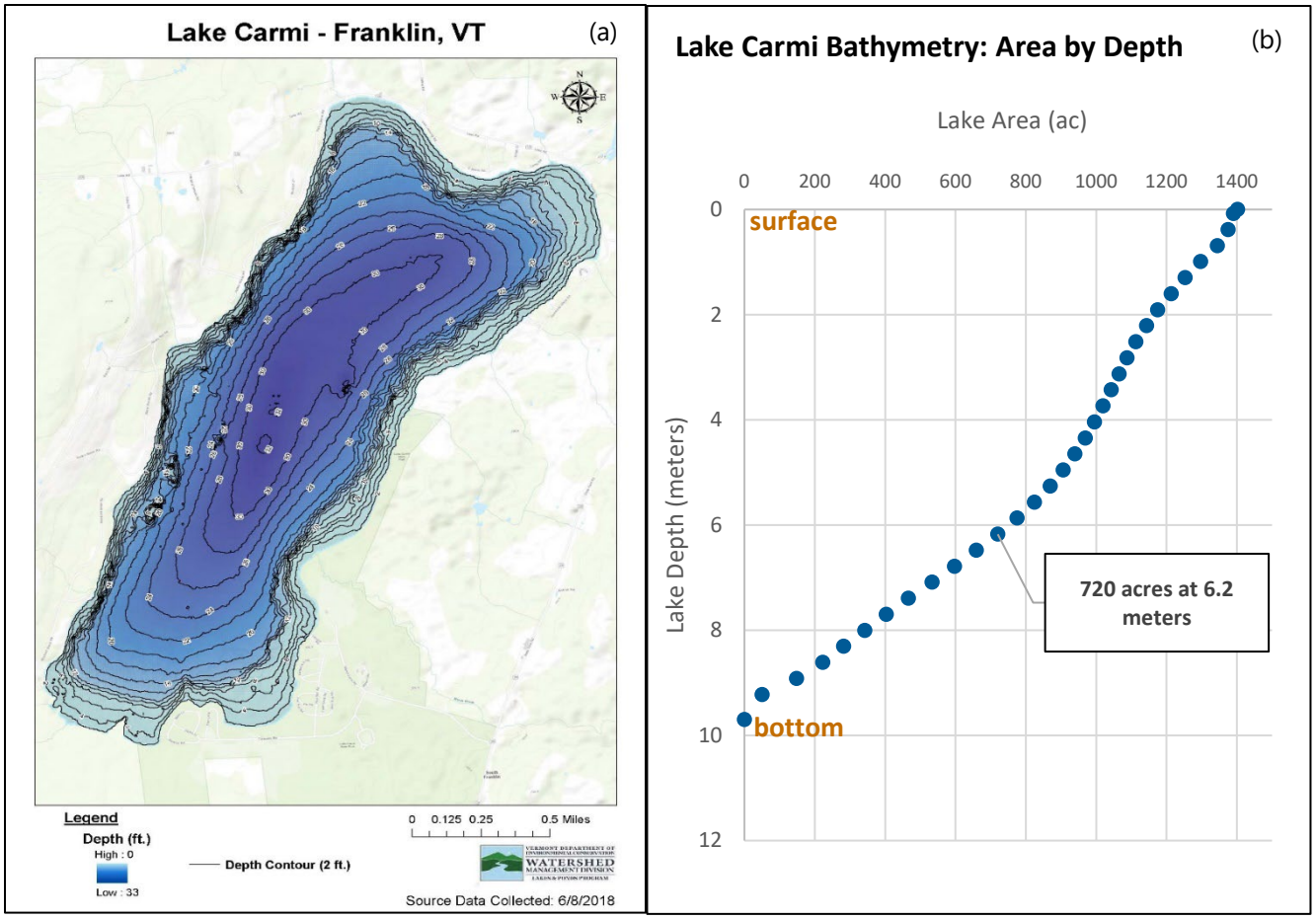

Figure 2-1 Bathymetry of Lake Carmi presented as a map (a) and depth to total area (b)

2.3 Anoxia Investigation

It is quite remarkable how phosphorus concentrations in Lake Carmi consistently begin to increase each year starting near June 1, and the rate of increase is steady through mid-September. Figure 2-2 (before aeration) and Figure 2-3 (with aeration) show that this steady increase in phosphorus concentration was observed before and after aeration was installed. Pike River flows are provided in these graphs to show that the phosphorus concentrations on Figures Figure 2-2 and Figure 2-3 are largely unaffected by prevailing hydrologic conditions (e.g., implied watershed inflows to Lake Carmi) and, therefore, are more strongly influenced by internal loading conditions.

Dissolved oxygen concentrations in the water column indicate anoxia in the bottom sediments and at what lake depths internal P loading potential is greatest. However, interpretations of the relationship between anoxia (low oxygen) and internal P loading potential can be affected by mixing, transport, and reaeration of surface waters. Ultimately, water column dissolved oxygen measurements are what is available to understand potential anoxia in bottom sediment.

For Lake Carmi, the plots in Appendix C show that dissolved oxygen is uniform and oxygenated to about 5 to 6 meters deep for much of the summer except for mid-July through late August (monitoring years 2018 (no aeration) and 2022 (aeration) provided as examples). From mid-July through late August, concentrations in the bottom waters (>9 to 6 meters) are at or approach DO of 0 milligrams per liter (mg/L). Calculations were conducted to determine the frequency of prevailing oxygen conditions by depth and lake area to begin quantifying the lake area where internal P treatment will be most effective. Table 2-1 through Table 2-4 provide the results of this analysis.

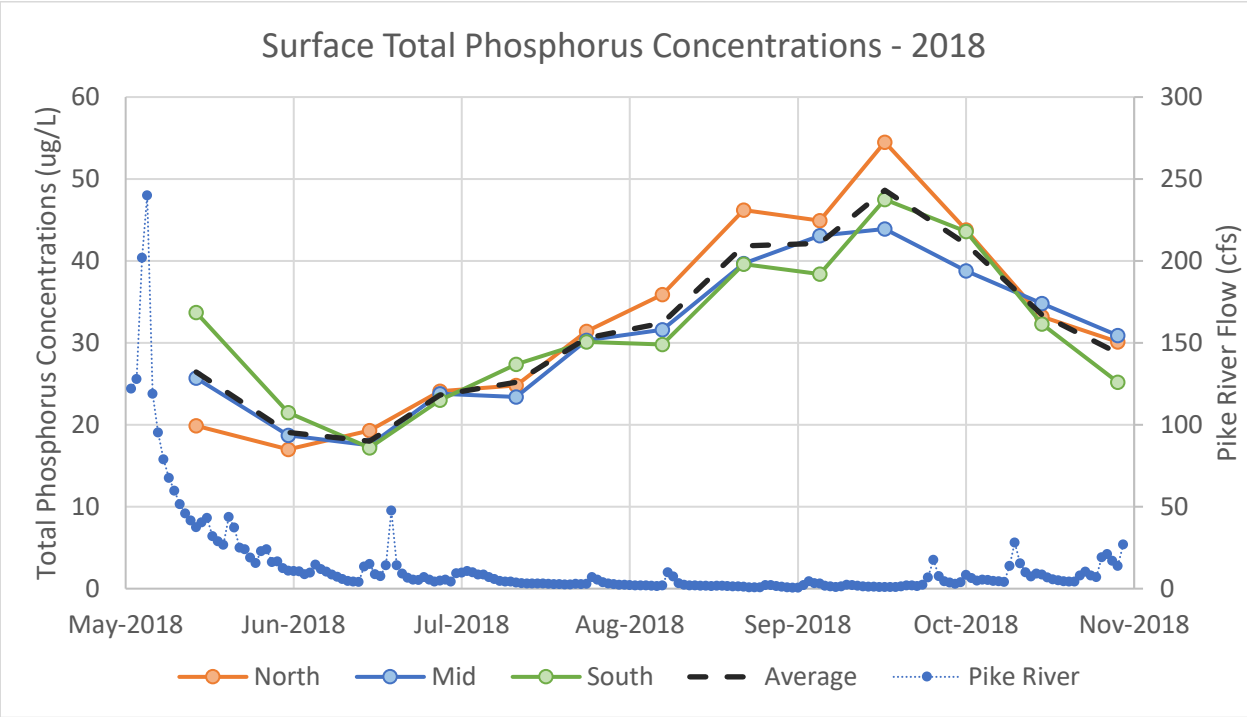

Figure 2-2 Phosphorus in Lake Carmi surface waters in 2018

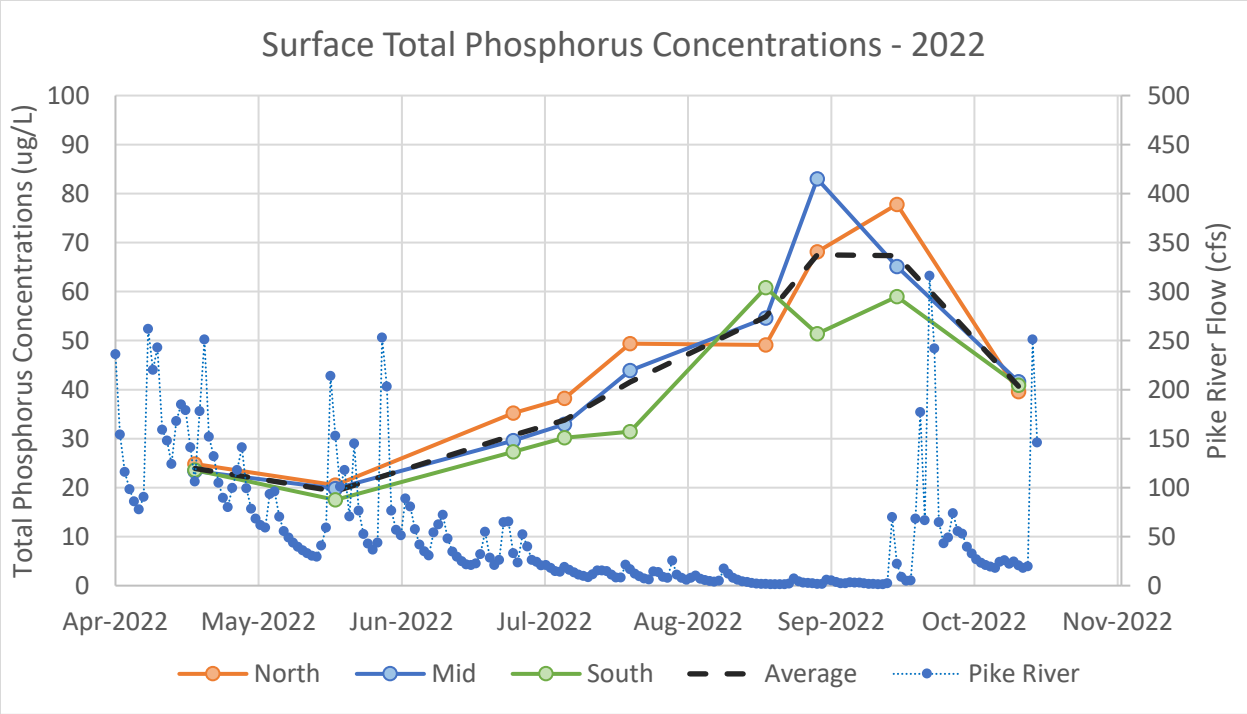

Figure 2-3 Phosphorus in Lake Carmi surface waters in 2022

As an example of pre-aeration conditions, Table 2-1 and Table 2-2 show 2017 and 2018 lake bottom area corresponding to prevailing dissolved oxygen conditions of less than 2, 4, 6, and 8 mg/L. As a starting point in this analysis, it can be assumed that internal loading occurs where dissolved oxygen is less than 2 mg/L. During pre-aeration conditions, it can be seen that a significant area of the lake had dissolved oxygen of less than 2 mg/L. In July 2017, the maximum area with less than 2 mg/L was 217 hectares. In July 2018, 318 hectares of lake bottom area were in contact with water containing dissolved oxygen less than 2 mg/L.

As an example of post-aeration conditions, Table 2-3 and Table 2-4 show 2021 and 2022 lake bottom areas corresponding to prevailing dissolved oxygen conditions of less than 2, 4, 6, and 8 mg/L. It can be seen that a significant area of the lake had dissolved oxygen of less than 2 mg/L. However, the anaerobic area (<2 mg/L) was less than pre-aeration conditions, and the low oxygen condition was less persistent. In August 2021, the maximum area with less than 2 mg/L was 169 hectares. In June 2022, 82 hectares of lake bottom area contacted water with dissolved oxygen less than 2 mg/L.

However, it appears that the dynamic between measured dissolved oxygen in the water column and internal loading was changed after aeration. For example, phosphorus concentrations were higher in 2022 compared to 2018 despite the fact that in 2022, notably less lake bottom area experienced oxygen less than 2 mg/L compared to 2018. With aeration, dissolved oxygen concentrations in the water column do not appear to provide a clear signal of prevailing anoxia in sediment. This suggests that the sediment oxygen demand of Lake Carmi sediments is high enough to maintain anoxic conditions favorable to internal loading even with the higher water column dissolved oxygen conditions. Modeling (Section 4)

conducted in this study for 2018 confirmed that approximately 94 percent of internal loading occurs at depths of 6 meters or greater.

Because aeration systems mix surface waters with bottom waters, lake bottom temperatures tend to be higher with aeration. This also appears to be the case for Lake Carmi (Figure 2-4). Internal loading rates increase with increasing temperature. Hence, although aeration may be delivering oxygen to the lake bottom, increased water (and sediment) temperature can be expected to increase respiration of lake bottom sediment. This, in turn, increases anaerobic conditions within the sediment and may work against the intended benefit of aeration, which is oxidation of the sediments to reduce internal loading.

Table 2-1 2017 lake areas corresponding to prevailing dissolved oxygen condition

Average Lake Condition	Depth of DO Condition (m)					Lake Area by DO Condition (Hectare)			
Month	Dissolved Oxygen (mg/L)					Dissolved Oxygen (mg/L)			
	<2	<4	<6	<8		<2	<4	<6	<8
April	none	none	none	none		-	-	-	-
May	none	9.1	8.2	3.9		-	64	145	414
June	none	7.8	6.7	1.1		-	173	271	532
July	7.3	6.6	5.0	2.3		217	277	376	471
August	8.1	7.8	6.5	1.7		147	178	283	497
September	8.3	7.7	6.7	3.2		133	182	269	436
Max	***8.3***	***9.1***	***8.2***	***3.9***		***217***	***277***	***376***	***532***
Min	***7.3***	***6.6***	***5.0***	***1.1***		***133***	***64***	***145***	***414***
Average	***7.8***	***7.8***	***6.6***	***2.5***		***175***	***171***	***260***	***473***

Table 2-2 2018 lake areas corresponding to prevailing dissolved oxygen condition

Average Lake Condition	Depth of DO Condition (m)					Lake Area by DO Condition (Hectare)			
Month	Dissolved Oxygen (mg/L)					Dissolved Oxygen (mg/L)			
	<2	<4	<6	<8		<2	<4	<6	<8
April	none	none	none	9.3		-	-	-	40
May	none	8.5	6.1	4.2		-	117	313	404
June	7.6	7.0	6.5	1.1		195	243	287	532
July	6.0	5.5	5.1	2.6		318	352	372	458
August	6.9	6.0	4.0	2.7		255	318	411	453
September	8.2	6.6	4.3	2.0		145	279	403	481
Max	***8.2***	***8.5***	***6.5***	***9.3***		***318***	***352***	***411***	***532***
Min	***6.0***	***5.5***	***4.0***	***1.1***		***145***	***117***	***287***	***40***
Average	***7.1***	***7.0***	***5.2***	***5.2***		***232***	***235***	***349***	***286***

Table 2-3 2021 lake areas corresponding to prevailing dissolved oxygen condition

Average Lake Condition	Depth of DO Condition (m)					Lake Area by DO Condition (Hectare)			
Month	Dissolved Oxygen (mg/L)					Dissolved Oxygen (mg/L)			
	<2	<4	<6	<8		<2	<4	<6	<8
April	none	none	none	none		-	-	-	-
May	none	none	none	8.2		-	-	-	141
June	9.2	9.0	8.2	4.7		53	79	141	389
July	none	8.0	7.1	3.9		-	157	232	414
August	7.9	7.4	5.8	4.1		169	208	332	407
September	none	none	none	4.6		-	-	-	392
Max	***9.2***	***9.0***	***8.2***	***8.2***		***169***	***208***	***332***	***414***
Min	***7.9***	***7.4***	***5.8***	***3.9***		***53***	***79***	***141***	***141***
Average	***8.5***	***8.2***	***7.0***	***6.1***		***111***	***144***	***236***	***277***

Table 2-4 2022 lake areas corresponding to prevailing dissolved oxygen condition

Average Lake Condition	Depth of DO Condition (m)					Lake Area DO Condition (Hectare)			
Month	Dissolved Oxygen (mg/L)					Dissolved Oxygen (mg/L)			
	<2	<4	<6	<8		<2	<4	<6	<8
April	none	none	none	none		-	-	-	-
May	9.4	8.0	6.8	3.8		33	161	259	418
June	8.9	8.6	6.9	1.1		82	111	249	532
July	none	8.9	7.6	1.7		-	89	195	496
August	none	8.3	7.1	3.2		-	131	232	437
September	none	none	7.0	1.1		-	-	243	532
Max	***9.4***	***8.9***	***7.6***	***3.8***		***82***	***161***	***259***	***532***
Min	***8.9***	***8.0***	***6.8***	***1.1***		***33***	***89***	***195***	***418***
Average	***9.1***	***8.4***	***7.2***	***2.5***		***57***	***125***	***227***	***475***

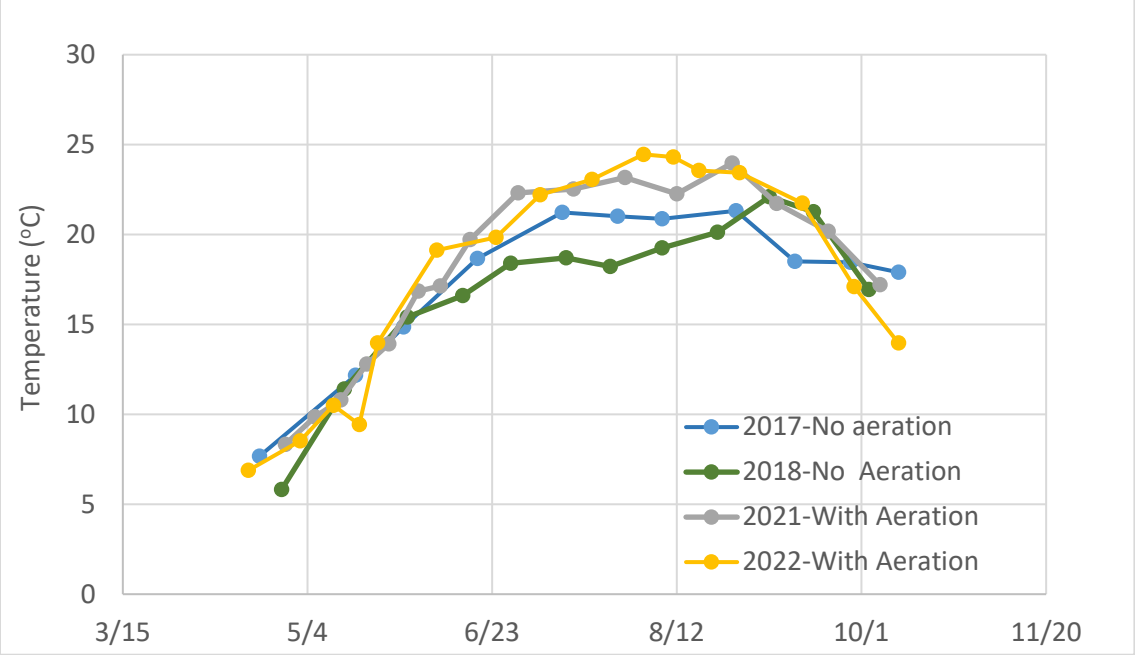

Figure 2-4 Average temperature of Lake Carmi waters at a depth of 7 meters or greater

3 Sediment Investigation

A sediment investigation was conducted for Lake Carmi to achieve several objectives, including:

- Spatially (across Lake Carmi and vertically within the lake sediment) define the concentration of phosphorus in lake sediments for iron-bound P (Fe-P), aluminum-bound P (Al-P), organically bound P (Org-P), and calcium-bound P (Ca-P) fractions.
- Conduct a laboratory microcosm experiment to estimate the maximum potential rate of phosphorus release from lake bottom sediments under anaerobic and oxic conditions.
- Conduct an aluminum addition and fractionation test with Lake Carmi sediment to define the relationship between aluminum dose, Fe-P loss, and conversion of Fe-P to Al-P.

The results of these investigations informed the modeling work (Section 4) and the treatment strategy (Chapter 5).

3.1 Sediment Collection

Sediment cores were collected on October 10 and 11, 2023 at the locations identified in Figure 3-1. In accordance with the project scope of work, a total of 10 cores (denoted "SC" on the figure) were collected and sliced to 20-cm depth in 2-cm sections in preparation for fractionation (Figure 3-2). Six additional cores (denoted Ex) were collected and a composite sample collected for the top 4 cm. A total of eight intact sediment cores were collected at four locations (these were duplicate cores) and prepared for transport to the Barr Engineering laboratory for the microcosm P release experiments.

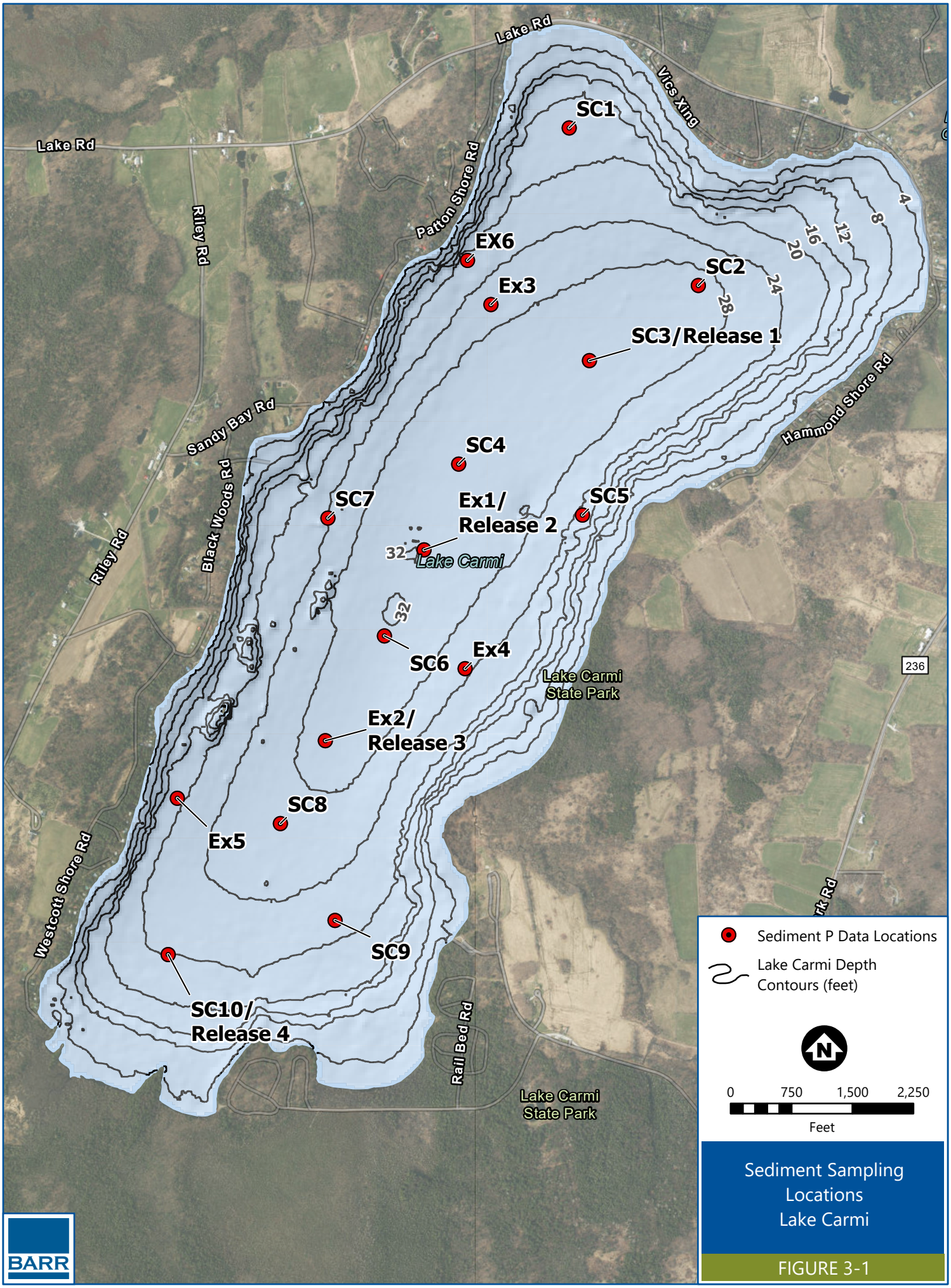

Barr Footer: ArcGISPro 3.1.3, 2024-02-20 11:25 File: I:\Projects\45\12\1001\Maps\Memos\Sediment\Sediment Phosphorus Figures.aprx Layout: Layout Figure 3-1 Sampling Locations User: TJA

Figure 3-2 Photograph demonstrating the sediment coring tube, stand, and slicing device used in this study

3.2 Phosphorus Release Experiments

The microcosm experiments were conducted in duplicate with six cores incubated under anaerobic conditions and two cores incubated under oxic conditions. The purpose of this effort was to identify the rate of P release from sediment expressed as milligrams per square meter of lake bottom area per day. This P release rate is considered a maximum potential rate (i.e., U_{max}) at a near zero DO concentration that can be adjusted using Michaelis-Menten kinetics and prevailing dissolved oxygen conditions in Lake Carmi.

3.2.1 Methods

Sediment core tubes were transported to Barr's laboratory space in Edina, MN. The clear plastic cores tubes are approximately 7 cm in diameter and 50 cm in length. Each core tube was filled approximately half full (20-25 cm) with sediment in the field. A rubber stopper was inserted in the bottom of the tube, and a second stopper was inserted within the tube at the surface of the sediment in the field, to hold the sediment in place within the tube during transport.

Once the sediment cores arrived at the laboratory, the rubber stoppers at the top of sediment were carefully removed, minimizing further sediment disturbance. Sediment remained in the core tubes, and

the tubes were placed in a rack to hold them vertically for the column release experiment. The columns were kept in a climate-controlled room (20°C) with no windows, and only exposed to fluorescent light during the brief periods of sample collection. Water collected from the surface of the lake was filtered through a 0.45-µm cartridge filter using a peristaltic pump. Filtered lake water was stored in a refrigerator at 4°C. Each column had filtered lake water slowly added to each core tube above the sediment, being careful to minimize sediment disturbance. Water was added to a depth of 20 cm above top of sediment. An air headspace of 5-10 cm remained in the top of the columns. A plastic slip cap, with three pre-drilled holes, was fit over the top of each core tube. A 3/8-inch diameter polyvinyl chloride (PVC) tubing was passed through the cap, and an aeration stone was attached. The aeration stone was lowered into the center of the water column in each tube, such that the aeration stone was positioned 10 cm above the sediment-water interface. A 4-inch piece of 3/8-inch diameter PVC tubing was inserted through the slip cap to allow venting of air or nitrogen gas from the column. A third hole through the cap acts as a port to allow for insertion of a sampling pipette, which remained covered with electrical tape when not being used to collect water samples, to help ensure a nitrogen gas head space in the anoxic.

Nitrogen gas was bubbled slowly from the aeration stone in each anoxic column. The gas flow rate was monitored daily and adjusted when necessary to provide a light but steady stream of bubbles. The continuous flow of nitrogen gas, combined with small orifice for gas to escape the top of column, ensured that the headspace above the water remained oxygen free. For the oxygenated cores, an aquarium air pump was used to provide a light but steady stream of air bubbles from the aeration stones.

Water samples were collected from each column within the first hour of setup in the laboratory. Water samples were collected by inserting a 25 milliliter (mL) volumetric glass pipette through the top cap of the column. A 50-mL volume sample was collected for each sampling event. An equal volume of filtered lake water, stored at 4°C, was added to replace the volume of removed water. The collected water samples were immediately filtered through a 0.45-µm filter (disk filter attached to a plastic syringe) and stored in small-volume high-density polyethylene (HDPE) plastic vials.

Filtered water samples were analyzed for soluble reactive phosphorus (SRP) following Standard Method 4500-P. SRP samples were analyzed immediately after collection (i.e., less than two hours). The remaining sample volume was stored in a refrigerator at 4°C.

3.2.2 Results

The prevailing conditions in the water above sediment in the microcosm are provided in Table 3-1. The anaerobic columns with a nitrogen headspace include columns 1 through 3, while column 4 is the oxic column.

Table 3-1 Physical and chemical conditions measured at the end of the incubation experiment

Column	Oxygenated Condition	Temperature (°C)	Specific Conductance (µS/cm)	pH	Dissolved Oxygen (mg/L)	Oxidation Reduction Potential (mV)
4A	Oxic	20.3	134	7.13	8.9	174
4B		20.1	133	6.91	9.0	236
3B	Anaerobic	20.1	158	7.80	0.44	219
3A		20.2	144	8.06	0.33	177
2B		20.1	159	8.43	0.31	178
2A		20.2	171	8.23	0.30	171
1B		20.2	147	8.48	0.28	146
1A		20.3	157	8.18	0.26	133

After day two, dissolved phosphorus (ortho-phosphate) measured in the anaerobic columns steadily increased throughout the 14-day test (Figure 3-3). Some of the columns lagged others with respect to release but appeared to catch up by day 11. Some of the columns had greater benthic activity (worms, chironomids) and this may have affected the timing of release. It should also be noted that for measurements taken at each timestep, water was removed with high P and then replaced with water with low P to keep water volumes balanced during this test. This effectively removed mass which was used to calculate release rates in addition to the change in P between timesteps. The rate of P release calculated between the timesteps is shown in Figure 3-3a and summarized for the entire testing period in Figure 3-4. The average rate of P release in the aerobic microcosms ranged from nearly zero to 0.88 milligrams per square meter per day. This suggests that there is very little to no aerobic P release for areas of Lake Carmi with high enough oxygen diffusion into the sediments to prevent the dissolution of Fe-P.

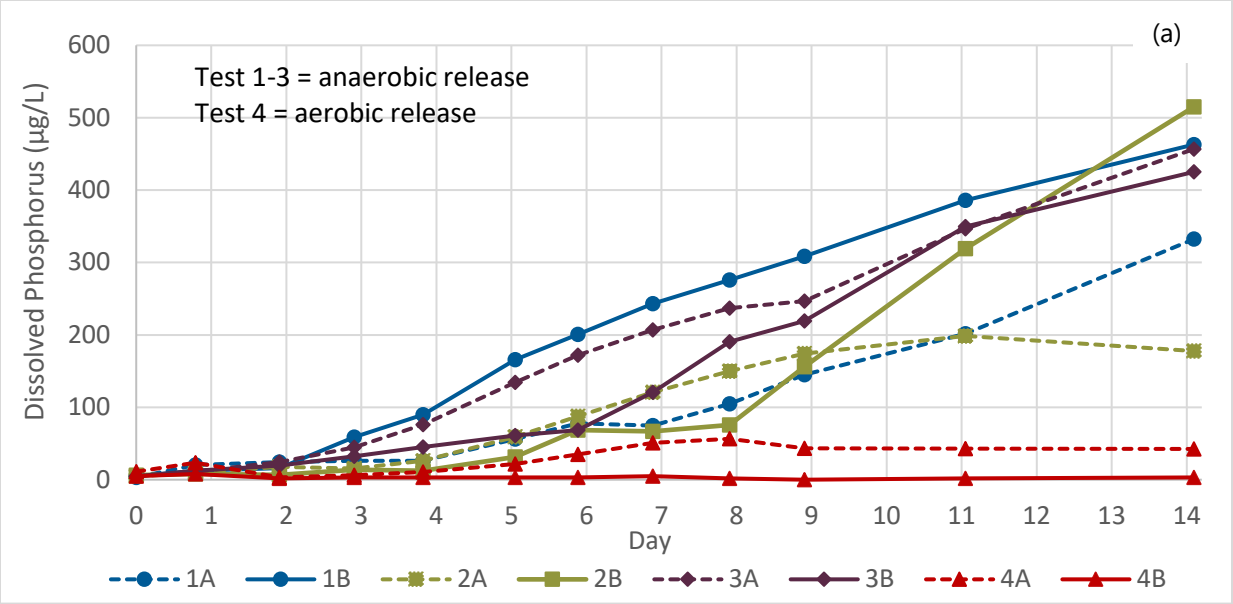

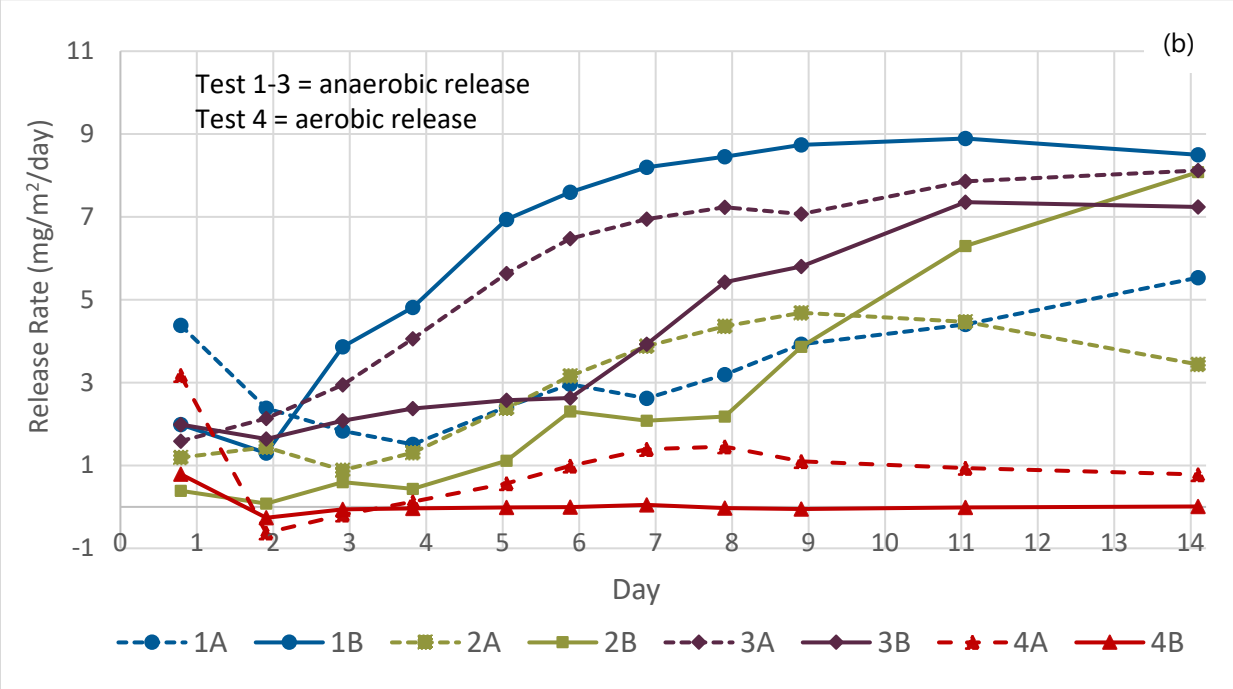

Figure 3-3 **Change in phosphorus in each column (a) and the corresponding release rate for each day (b)**

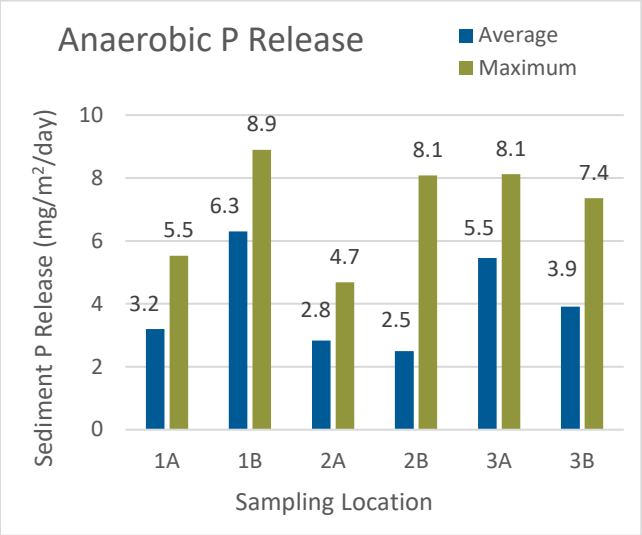

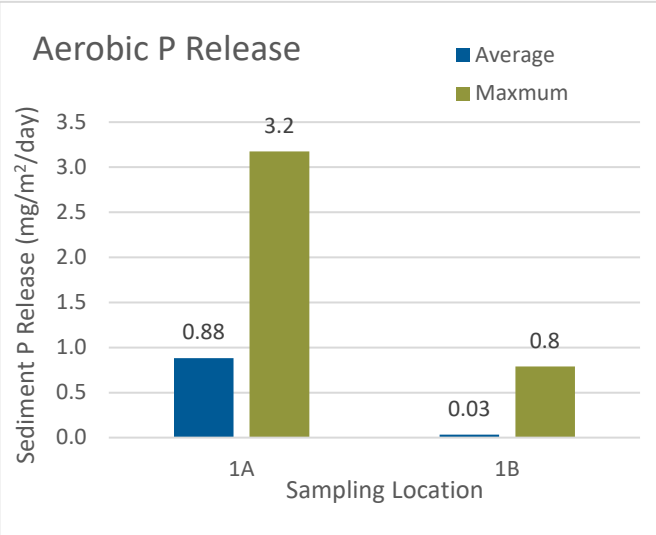

Figure 3-4 Summary of anaerobic and aerobic P release rates measured in the microcosm

The overall arithmetic average anaerobic release rate during the microcosm experiment for all of the cores was 4.0 milligrams phosphorus per square meter per day. The maximum rates ranged from 4.7 to 8.9 milligrams per square meter per day depending on sample location. The average rate is likely reflective of the overall rate of release during the summer in Lake Carmi, whereas the maximum rates measured in the microcosm are more likely to occur in July and early August. These microcosm results are consistent with the model results discussed in Chapter 4. For example, the average modeled P release rate from May 5 to October 8, 2018 for lake depths greater than 6 meters ranged from 0.51 to 4.83 milligrams per square meter per day. The maximum modeled P release rate for depths greater than 6 meters ranged from 1.1 to 8.4 milligrams per square meter per day. Inputs into the Barr Lake Model include the sediment fractionation data (Section 3.3) collected as part of this study, dissolved oxygen data measured in the lake, as well as the relationship between maximum potential P release and Fe-P concentration developed by Pilgrim et. al., 2007. Consistency between the microcosm and the modeling results strengthen confidence in the modeling results and the predicted benefits of an aluminum treatment.

3.3 Sediment Fractionation

3.3.1 Methods (Fractionation)

Phosphorus fractionation was performed following the methods described in Psenner (1988), with some modifications. Approximately 200 mg of sediment is subsampled and placed in a 15-mL centrifuge tube. Prior to subsampling, the sediment sample is homogenized by stirring with a stainless-steel spatula. The mass of sediment subsample is measured with an electronic balance. Extraction solutions are added sequentially to the centrifuge tube containing sediment. The tube is centrifuged before sampling and removal of the extraction removal, creating a sediment pellet at the bottom of the tube to avoid sediment loss when removing extraction solutions. After addition of the next extraction solution, the sediment pellet is mixed with a stainless-steel spatula. Centrifuge tubes are capped and regularly inverted to provide

further mixing of sediment and extraction solution. The sequential extraction solutions used for the phosphorus fractionation are as follows:

1. Loosely-sorbed P: 1 M ammonium chloride, two-hour duration
2. Iron-bound P: Buffered dithionite (17.4 g/L sodium dithionite and 9.2 g/L sodium bicarbonate), one-hour duration
3. Aluminum-bound P: 0.1 M sodium hydroxide (NaOH), 15 to 18-hour duration
4. Organic-P: Potassium persulfate digestion of 0.1 M sodium hydroxide
5. Calcium-bound P: 0.5 M hydrochloric acid (HCl), ~24-hour duration

A 2-mL aliquot of each extraction solution is transferred to a clean glass vial. NaOH extract solutions are brought to pH 7 with HCl, and HCl extract solutions are brought to pH 7 with NaOH. Double-deionized water is used to bring the total volume to 10 mL in each vial. The buffered dithionite vials are left to sit open to the air for 24-48 hours to allow oxygen diffusion and oxidation of the dithionite, which can interfere with the phosphorus color reagent reaction if not allowed first to oxidize and decompose. The organic-P fraction is measured by digesting 0.1 M NaOH extract with the addition of potassium persulfate and heating in an autoclave at 120°C for one hour.

Concentrations of phosphorus in aqueous solutions were measured using the ascorbic acid and ammonium molybdate colorimetric method (Standard Method 4500-P, modified). A cobalt-blue color forms from the reaction of orthophosphate with the molybdate ion. The color reagent was prepared fresh daily by combining solutions of ascorbic acid, ammonium molybdate, sulfuric acid, and potassium antimony tartrate. Phosphorus standards are prepared by diluting a stock solution of orthophosphate. Absorbance was measured at 880 nanometers (nm) on a Hach DR3900 spectrophotometer.

Buffered dithionite extracts were also analyzed for total iron, and 0.1 M NaOH extract solutions were analyzed for total aluminum. Iron and aluminum were analyzed by RMB Environmental Laboratories, Inc., using EPA Method 200.7.

3.3.2 Results

The full results of the sediment fractionation analysis are provided in Appendix D, and summaries are provided in Table 3-2 and Table 3-3. Figure 3-5 and Figure 3-6 show the spatial distribution of sediment phosphorus concentrations across Lake Carmi. The sediment P data are used to model internal P loading, as well as calculate aluminum doses (see Section 3.4). Overall, the concentration of Fe-P did not vary significantly across Lake Carmi. In general, deeper areas of the lake had incrementally higher concentrations of phosphorus compared to sediment collected closer to shore. However, sediment collected at the east side of the lake had the highest phosphorus. For aluminum dosing purposes, an average of 43.8 micrograms per cubic cm (0.0438 milligrams per cubic cm) was calculated using all sediment core data collected for the top four cms of sediment. Aluminum dosing calculations are based upon binding 43.8 micrograms per cubic cm Fe-P.

The contour data on Figure 3-5 and Figure 3-6 were used as inputs to the model to provide unique Fe-P and Org-P concentrations by lake depth. For example, in the model, the average Fe-P value for lake areas shallower than 6 meters was 21.8 micrograms per cubic cm, while areas deeper than 6 meters averaged

42.8 micrograms per cubic cm. There was little distinction by lake depth for Org-P. In general, Org-P concentrations in Lake Carmi were notably low. The average concentration of Org-P in the top 4 cm of sediment was 54 micrograms per cubic cm (0.054 milligrams per cubic cm). Over time, Org-P will decay and contribute to the Fe-P pool. Org-P decay will be one of the determinants of aluminum treatment longevity. Based upon the figures provided in Appendix E, it can be seen that Org-P, on a dry-weight basis, declines from the sediment surface and deeper into the sediment. It appears that there is an approximately 40 percent decline from the surface to 20 cms, suggesting that 40 percent of the Org-P decays over that depth.

Table 3-2 Average P concentration for the top 4 and 8 cm of lake bottom sediment

Location	0-4 cm				0-8 cm			
	Fe- P (mg P / cm^3)	Al-P (mg P / cm^3)	Org-P (mg P / cm^3)	Ca-P (mg P / cm^3)	Fe- P (mg P / cm^3)	Al-P (mg P / cm^3)	Org-P (mg P / cm^3)	Ca-P (mg P / cm^3)
SC1	0.033	0.003	0.061	0.058	0.054	0.063	0.137	1.123
SC2	0.055	0.003	0.058	0.055	0.050	0.059	0.163	0.888
SC3	0.037	0.002	0.057	0.031	0.034	0.057	0.104	1.123
SC4	0.031	0.001	0.049	0.048	0.027	0.050	0.140	0.803
SC5	0.067	0.003	0.059	0.060	0.066	0.064	0.080	1.110
SC6	0.039	0.001	0.047	0.046	0.030	0.049	0.113	0.638
SC7	0.045	0.001	0.053	0.051	0.046	0.055	0.071	0.655
SC8	0.036	0.002	0.055	0.053	0.027	0.054	0.042	0.668
SC9	0.031	0.001	0.049	0.048	0.026	0.049	0.046	0.668
SC10	0.034	0.001	0.050	0.049	0.031	0.049	0.034	0.661
Ex1	0.059	0.002	0.053	0.023	--	--	--	--
Ex2	0.057	0.002	0.053	0.024	--	--	--	--
Ex3	0.031	0.002	0.052	0.033	--	--	--	--
Ex4	0.055	0.006	0.057	0.035	--	--	--	--
Ex5	0.049	0.005	0.058	0.074	--	--	--	--
Ex6	0.042	0.006	0.053	0.052	--	--	--	--

Table 3-3 Average P concentration by depth for sediment cores SC1-10

Arithmetic Average of 10 Cores					
Depth (cm)	Fe-P (mg P / cm^3)	Fe-P (mg P / g dry)	Al-P (mg P / cm^3)	Org-P (mg P / cm^3)	Ca-P (mg P / cm^3)
1-2	0.041	0.577	0.002	0.049	0.030
3-4	0.041	0.427	0.002	0.056	0.041
5-6	0.039	0.324	0.003	0.057	0.049
7-8	0.037	0.269	0.006	0.058	0.057
9-10	0.034	0.232	0.008	0.059	0.067
11-15	0.034	0.171	0.009	0.056	0.084
16-20	0.014	0.078	0.003	0.049	0.091

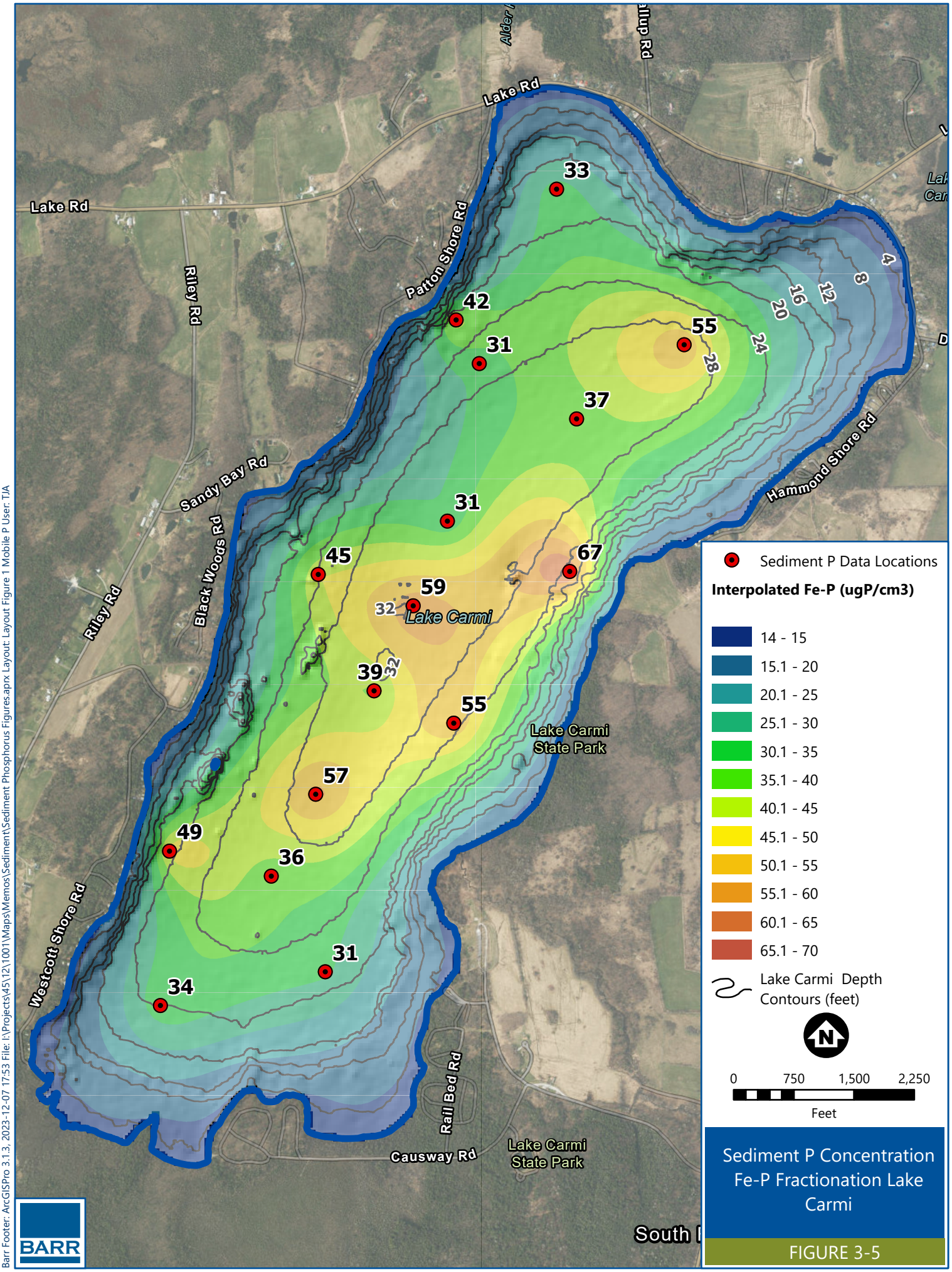

Sediment P Concentration Fe-P Fractionation Lake Carmi

FIGURE 3-5

BARR

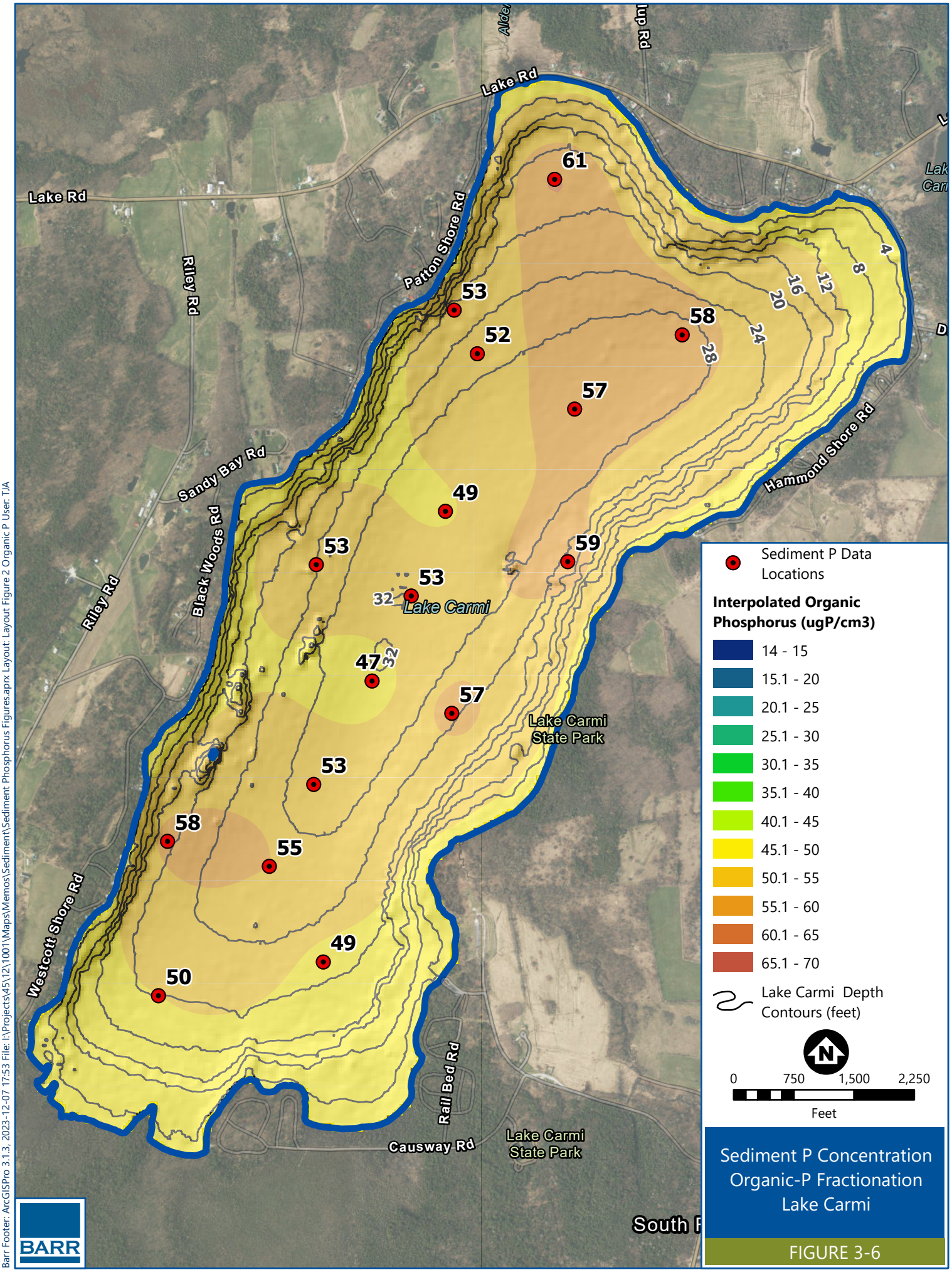

Sediment P Concentration Organic-P Fractionation Lake Carmi

FIGURE 3-6

BARR

3.4 Aluminum Dosing

When added to sediment, aluminum will replace iron bound to phosphate and form Al-P, the desired and stable product of this treatment. Aluminum must be added in excess to form the desired amount of Al-P. This excess is often described as the aluminum-to-phosphate ratio, which often ranges from 25 to 150 grams of Al to 1 gram of P. The relationship between how much Al-P is formed and how much aluminum is added (the dose) is not linear. Increased doses bind more phosphate and form more Al-P, but efficiency declines as the doses increase. However, the other goal is to reduce internal loading as much as possible. The primary task of dose determination is to identify the optimal dose where treatment will be most efficient from a P binding and cost perspective, as well as from an internal loading reduction perspective.

3.4.1 Methods

Equal volume subsamples of Lake Carmi sediment samples were composited and homogenized for the top 6 cm of cores SC4, SC5, and SC7 (i.e., 0-2 cm, 2-4 cm, and 4-6 cm intervals). Approximately 250 mg of composite sediment samples were transferred to separate 15-mL centrifuge tubes for a range of aluminum dose additions; the exact mass of sediment transferred to each tube was measured on an electronic balance and recorded. An aluminum hydroxide [$Al(OH)_3$] floc reagent was prepared by adding 4.4 mL aluminum sulfate and 2.2 mL sodium aluminate stock solutions to 485 mL deionized water, for a total volume of 500 mL. Aluminum is soluble in the low pH aluminum sulfate and high pH sodium aluminate products, until they are combined and the pH is neutralized and $Al(OH)_3$ precipitates as a floc. The $Al(OH)_3$ floc was mixed continuously with a magnetic stir bar to prevent floc settling while reagent volumes were measured out with a pipette and transferred to the centrifuge tubes. The concentration of aluminum in the $Al(OH)_3$ reagent was calculated to be 0.6 g Al/L, based on concentrations provided by the manufacturer for the aluminum sulfate and sodium aluminate products. A range of $Al(OH)_3$ floc reagent volumes were applied to each sediment composite sample, and the total volume was brought to 10 mL with the addition of deionized water in each tube. Each composite sediment sample was treated with five different aluminum doses, as well as a control of deionized water only. The centrifuge tubes were capped and inverted several times to thoroughly mix the sediment and $Al(OH)_3$ reagent. The centrifuge tubes with sediment and $Al(OH)_3$ reagent were stored in the dark at 20°C. After two weeks, the tubes were centrifuged to form a sediment and floc pellet in the bottom of the centrifuge tubes, and the overlying water was diskarded. Sediment phosphorus fractionation was performed on the sediment following methods described in Section 3.3.1 above; loosely-sorbed (combined with Fe-P/sodium dithionate extractant step) and calcium-bound phosphorus fractionation steps were excluded for the aluminum addition experiment.

3.4.2 Results

The P fractionation results for the aluminum-treated sediment are provided in Table 3-4. It can be seen that with increasing aluminum doses, Fe-P declines and Al-P increases. The mass of Al-P formed is a function of the aluminum dose, as well as the concentration of the starting Fe-P concentration. For a given aluminum dose, more Al-P is formed for sediments with higher Fe-P. Hence, the results from these

fractionations were used to create a relationship between aluminum dose and Fe-P concentration for the arithmetic mean Fe-P in the top 4 cm of Lake Carmi bottom sediment (0.0438 mg P/cm^3 wet sediment).

Table 3-4 P fractions for the aluminum-treated sediment

Core	[1]Dose (g Al/ m2*cm)	Moisture (%)	Loss On Ignition (%)	Density (g/cm^3)	Fe-P (mg P/g dry)	Al-P (mg P/g dry)	Org-P (mg P/g dry)	Fe-P (mg P/cm^3)	Al-P (mg P/cm^3)	Org-P (mg P/cm^3)
SC4	0	0.925	0.229	1.037	0.316	0.008	0.558	0.025	0.001	0.044
SC4	1.4	0.925	0.229	1.037	0.180	0.066	0.701	0.014	0.005	0.055
SC4	3.9	0.925	0.229	1.037	0.137	0.110	0.727	0.011	0.009	0.057
SC4	6.5	0.925	0.229	1.037	0.111	0.129	0.727	0.009	0.010	0.057
SC4	12.1	0.925	0.229	1.037	0.084	0.142	0.720	0.007	0.011	0.056
SC4	17.6	0.925	0.229	1.037	0.072	0.167	0.737	0.006	0.013	0.058
SC5	0	0.866	0.157	1.075	0.388	0.023	0.417	0.056	0.003	0.060
SC5	9.5	0.866	0.157	1.075	0.122	0.228	0.490	0.018	0.033	0.070
SC5	15.8	0.866	0.157	1.075	0.093	0.263	0.492	0.013	0.038	0.071
SC5	22.5	0.866	0.157	1.075	0.074	0.280	0.500	0.011	0.040	0.072
SC5	36.3	0.866	0.157	1.075	0.050	0.289	0.487	0.007	0.041	0.070
SC5	50.5	0.866	0.157	1.075	0.036	0.301	0.472	0.005	0.043	0.068
SC7	0	0.906	0.210	1.048	0.373	0.029	0.527	0.037	0.003	0.052
SC7	3.8	0.906	0.210	1.048	0.138	0.197	0.617	0.014	0.019	0.061
SC7	7.8	0.906	0.210	1.048	0.102	0.217	0.633	0.010	0.021	0.062
SC7	11.9	0.906	0.210	1.048	0.099	0.276	0.614	0.010	0.027	0.060
SC7	20.7	0.906	0.210	1.048	0.061	0.263	0.614	0.006	0.026	0.060
SC7	29.3	0.906	0.210	1.048	0.046	0.281	0.597	0.004	0.028	0.059

1. Dose is expressed as grams of aluminum over 1 square meter of lake bottom with a sediment depth of 1 cm. Total sediment volume is 10,000 cm^3

The relationship between aluminum dose and Fe-P lost developed for this study (using the data in Table 3-4) is shown in Figure 3-7. The figure shows that at a dose of 6.7, 16.6, 27.4, and 38.3 grams of aluminum applied over 1 meter of sediment depth and a mixing depth of 1 cm, it can be expected that available Fe-P would be bound by aluminum and reduced by 69, 85, 93, and 98 percent compared to the existing Fe-P in the sediment. This also means that the maximum potential rate of internal P loading would be reduced by 69 to 98 percent. Some additional considerations include:

- The total aluminum dose applied will depend on how deep in the sediment the aluminum can be expected to mix. For Lake Carmi, the mixing depth is expected to be 4 cms.
- There is clearly a loss of efficiency at the highest dose (38.3 g Al/m^2*1 cm depth), where very little additional Fe-P is lost (only 5% of total Fe-P) when the dose is increased from 27.4 g Al/m^2*1 cm depth.

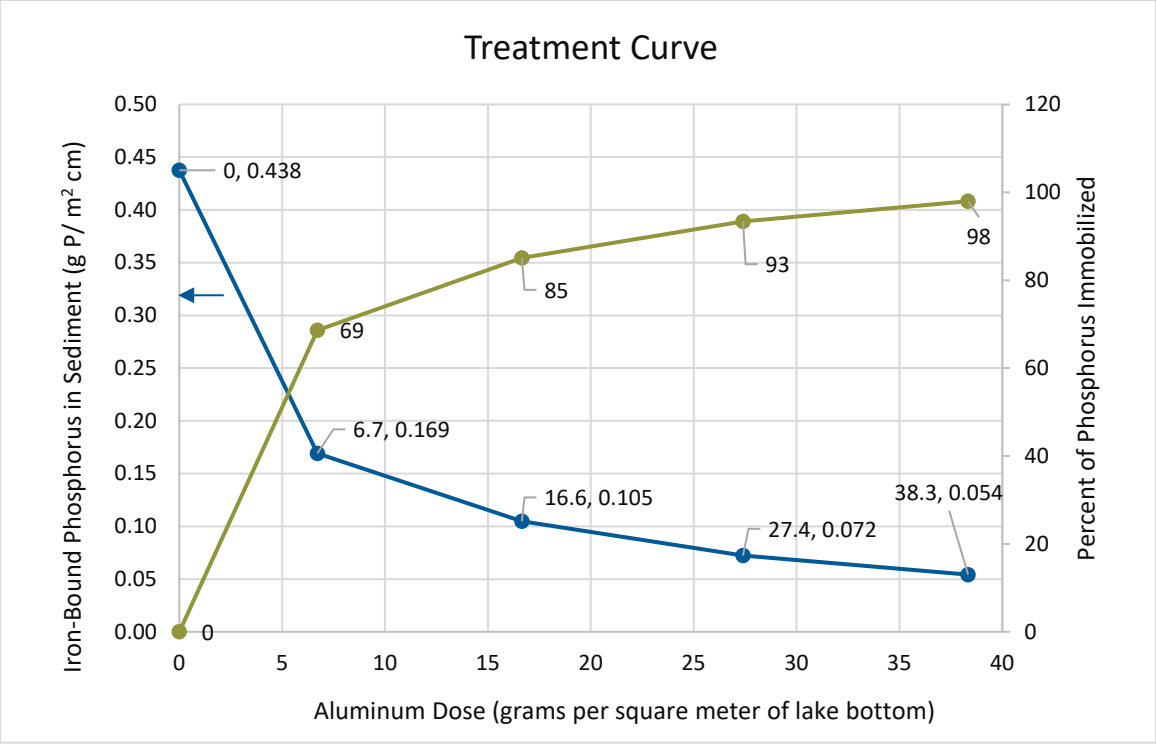

Figure 3-7 Relationship between aluminum dose and Fe-P reduction (as g P/m²*1 cm, and % reduction) with a Fe-P concentration in the sediment of 0.438 g P/m²*1 cm)

From the lake modeling work (Section 4), it was determined that 94 percent of internal loading occurs from the 20-foot (6.1 meters) contour and below (Figure 3-8). Hence, aluminum application should target the lake area under the 20-foot (6.1 meters) contour, which contains a total area of 775 acres. That target area will treat the sediment area responsible for 94 percent of the total internal P load.

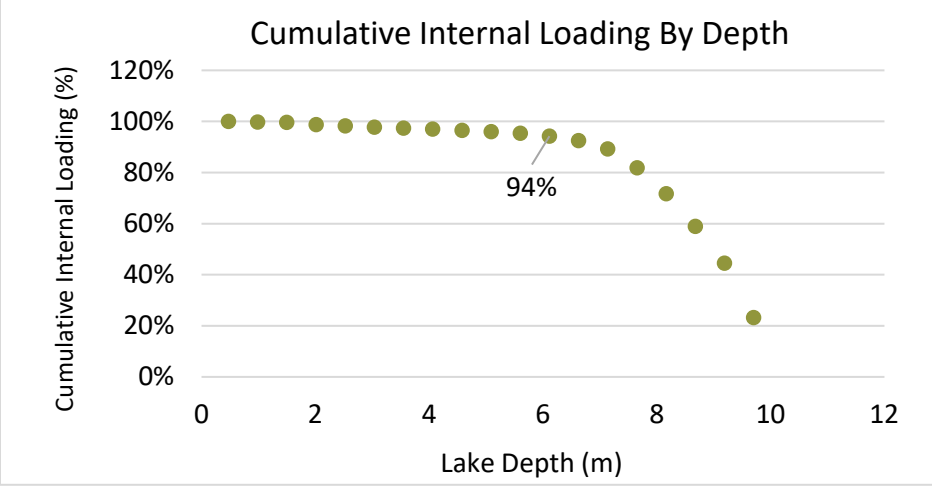

Figure 3-8 Cumulative internal loading by depth modeled from May 8 to October 2, 2018

A summary of low, middle (recommended) and high doses and the opinion of probable cost to conduct the treatment is provided in Table 2-1.

Table 3-5 Aluminum dosing and opinion of probable cost to achieve potential internal P loading reductions of (a) 69, (b) 85, and (c) 93%

(a) 69% internal P loading reduction (low dose)

Product	Ratio (by gallon)	Ratio (by mass)	Total Gallons Applied	Aluminum Mass (kg)	Estimated Unit Cost	Estimated Cost
Alum	2	0.437	166,140	36,833	2.68	$ 445,256
Sodium Aluminate	1	0.563	83,070	47,360	7.4	$ 614,719
			Total Al (kg)	**84,193**	**Total Cost**	**$ 1,059,975**

(b) 85% internal P loading reduction (recommended dosing)

Product	Ratio (by gallon)	Ratio by mass	Total Gallons Applied	Aluminum Mass (kg)	Estimated Unit Cost	Estimated Cost
Alum	2	0.437	412,183	91,380	2.68	$ 1104651
Sodium Aluminate	1	0.563	206,092	117,497	7.4	$ 1525077
			Total Al (kg)	**208,877**	**Total Cost**	**$ 2,629,728**

(c) 93% internal P loading reduction (high dose)

Product	Ratio (by gallon)	Ratio by mass	Total Gallons Applied	Aluminum Mass (kg)	Unit Cost	Cost
Alum	2	0.437	678,315	150,381	2.68	$ 1,817,884
Sodium Aluminate	1	0.563	339,157	193,361	7.4	$ 2,509,765
			Total Al (kg)	**343,742**	**Total Cost**	**$ 4,327,648**

4 Lake Response to Internal and External Controls

Computer modeling was used in this study to estimate stormwater runoff pollutant contributions from the watershed and internal loading contributions from the sediment and then link those loadings to observed nutrient concentrations in the lake water column (e.g., total phosphorus, total dissolved phosphorus, total Kjeldahl nitrogen (TKN), chlorophyll-*a*). Two types of models were used for this study: (1) a finite-difference model developed by Barr Engineering (herein referred to as the Barr Lake Model) and (2) BATHTUB models using the Canfield-Bachmann modeling framework. BATHTUB models were incorporated in this study to be consistent with the Lake Carmi TMDL modeling approach (Vermont Agency of Natural Resources, 2008). While BATHTUB models are useful for predicting lake responses to phosphorus inputs, additional error can be introduced for highly managed and more environmentally complex lakes, such as Lake Carmi. The Barr Lake Model was used to increase the understanding of Lake Carmi's environmental functions and increase confidence in predicting and assessing phytoplankton responses to nutrient loadings. The Barr Lake Model includes simulating dynamic internal lake processes such as phosphorus release from lake sediments by depth contour (variable internal sediment loads), phytoplankton nutrient uptake, and phytoplankton death and decay.

The Barr Models and BATHTUB models were used to simulate conditions in Lake Carmi in 2018 and 2022. These two years were selected to analyze lake processes before the aeration system was installed (2018) and after the aeration system was installed (2022). The sections below discuss how the models were calibrated for the different climate and environmental conditions of 2018 and 2022 and provide an overview of the nutrient-loading contributions from differing sources (e.g., watershed runoff, internal loading, atmospheric deposition). The sections below also discuss the predicted improvements to Lake Carmi water quality by implementing various BMPs.

4.1 Existing Conditions Calibration

4.1.1 Water Balance

The annual water loads to Lake Carmi under existing land use conditions were estimated for model years 2018 and 2022. Precipitation totals during model years 2018 and 2022 are summarized in Table 4-1 (source: NOAA precipitation gauge near Enosburg Falls, VT).

Table 4-1 Monitored precipitation for 2018 and 2022 model years

Model Year	Summer Season (June 1 – Sept 30) Precipitation (inches)	Annual Precipitation (inches)
2018	14.5	39.4
2022	18.5	45.0

The runoff water volume that reaches Lake Carmi from the tributary subwatersheds from precipitation events (termed the watershed runoff yield) will not be consistent throughout the year or from year-to-year. This is due to annual variability in climate, such as air temperature and solar radiation, and upland

environmental conditions, such as soil infiltration capacity (e.g., frozen vs. unfrozen, saturated vs. unsaturated) and vegetation evapotranspiration. As such, the watershed runoff yield for Lake Carmi was estimated using available monitoring data and a water balance approach.

Barr started with model year 2022 to inform the average watershed yield per month. Model year 2022 was used as a starting reference since there was monitoring data available that year, including flowrates for the Pike River (downstream of Lake Carmi) and relative water level data collected every 15 minutes for Lake Carmi. To estimate monthly watershed runoff yields, the changes in water volumes of the lake over time were calibrated by matching modeled surface elevations to the monitoring data. Calibrating known inflows (hourly precipitation) and outflows (hourly evaporation, Mill Pond Dam outflow rating curve; (Gomez and Sullivan Engineers, 2018)) to the observed lake levels allows for estimates of watershed yield. The estimated watershed runoff yield by month is presented in Table 4-2 for 2022 based on the calibrated water balance (Figure 4-1). The modeled hourly water levels, shown by the orange line on the plot, were calibrated to match as closely as possible to the observed water levels (plotted as average daily water levels), indicated by the black dashed line. The downstream Pike River flowrates are shown in yellow. Overall, the water balance calibrations for model year 2022 correlated well with the observed monitored data.

The watershed runoff yields developed for 2022 were used as a starting point for 2018. Water level data was not monitored in 2018 and, as such, the 2018 water balance could only be calibrated to one known water elevation, which was estimated from satellite imagery and LiDAR elevation data. This single data point indicated that the water yield in 2018 was higher from July – October to calibrate to this point, as shown in Table 4-2. The water balance for 2018 is presented in Figure 4-2.

Figure 4-3 provides a water balance volume comparison for the modeled periods of 2018 and 2022 (mid-May through early October).

Table 4-2 Estimated watershed runoff yield by month for model years 2018 and 2022

Month	2018	2022
May	0.4	0.4
June	0.5	0.5
July	0.2	0.1
August	0.2	0.1
September	0.2	0.1
October	0.2	0.1

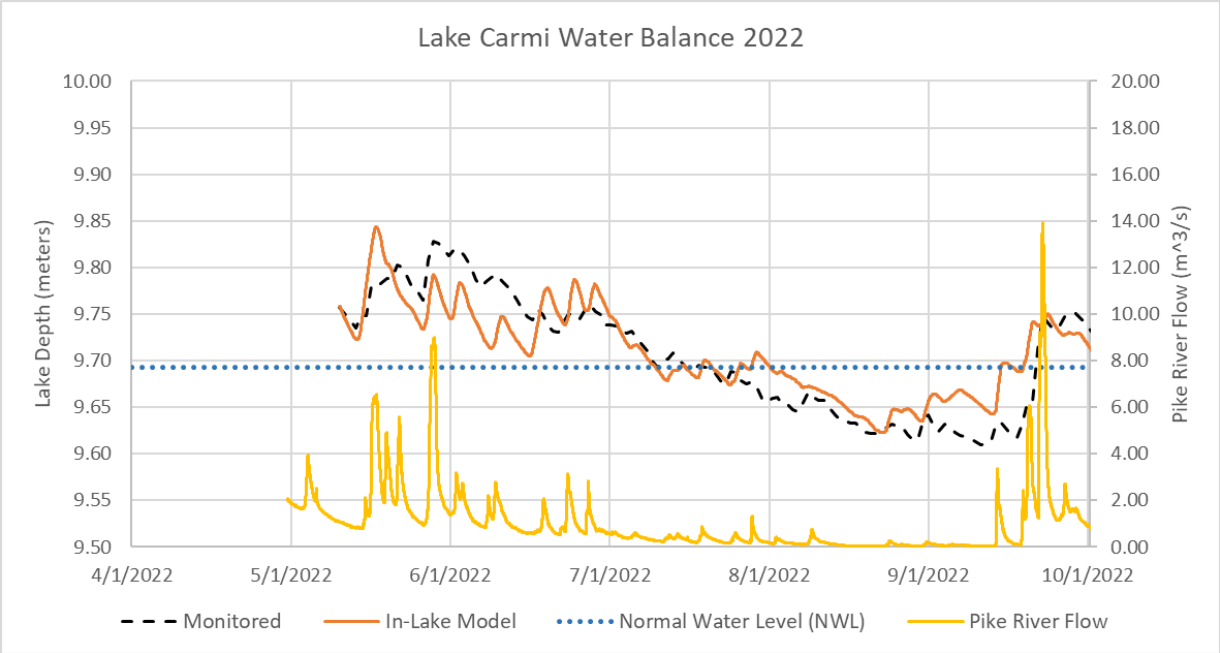

Figure 4-1 Lake Carmi 2022 water balance calibration

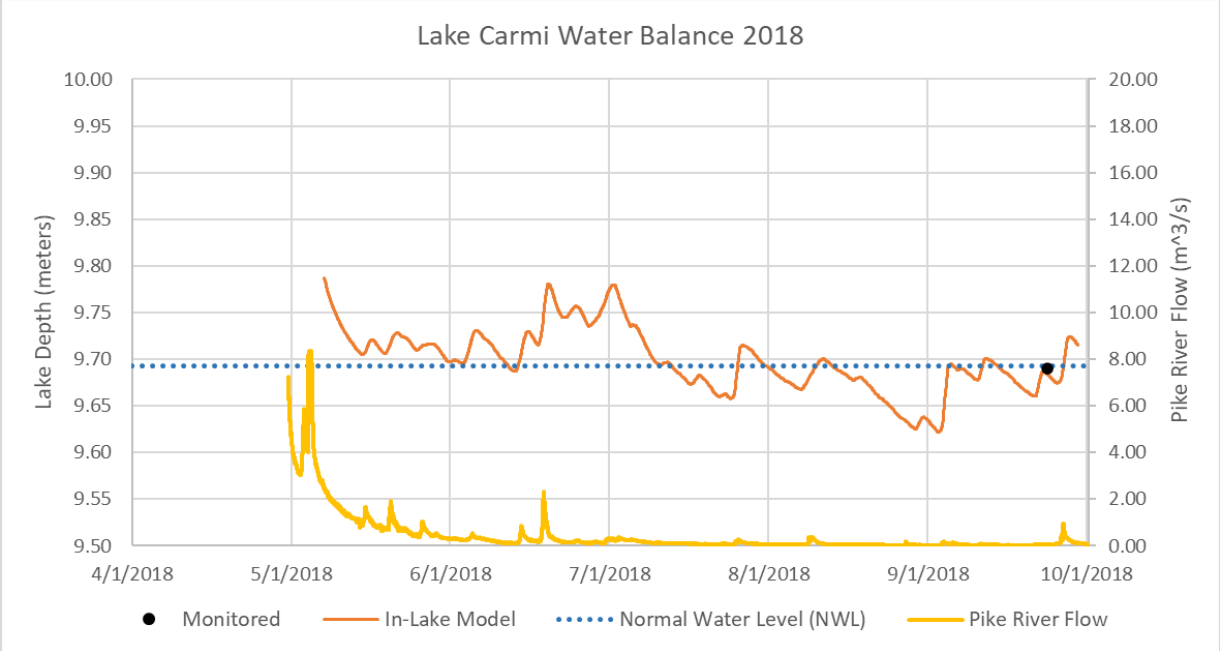

Figure 4-2 Lake Carmi 2018 water balance calibration

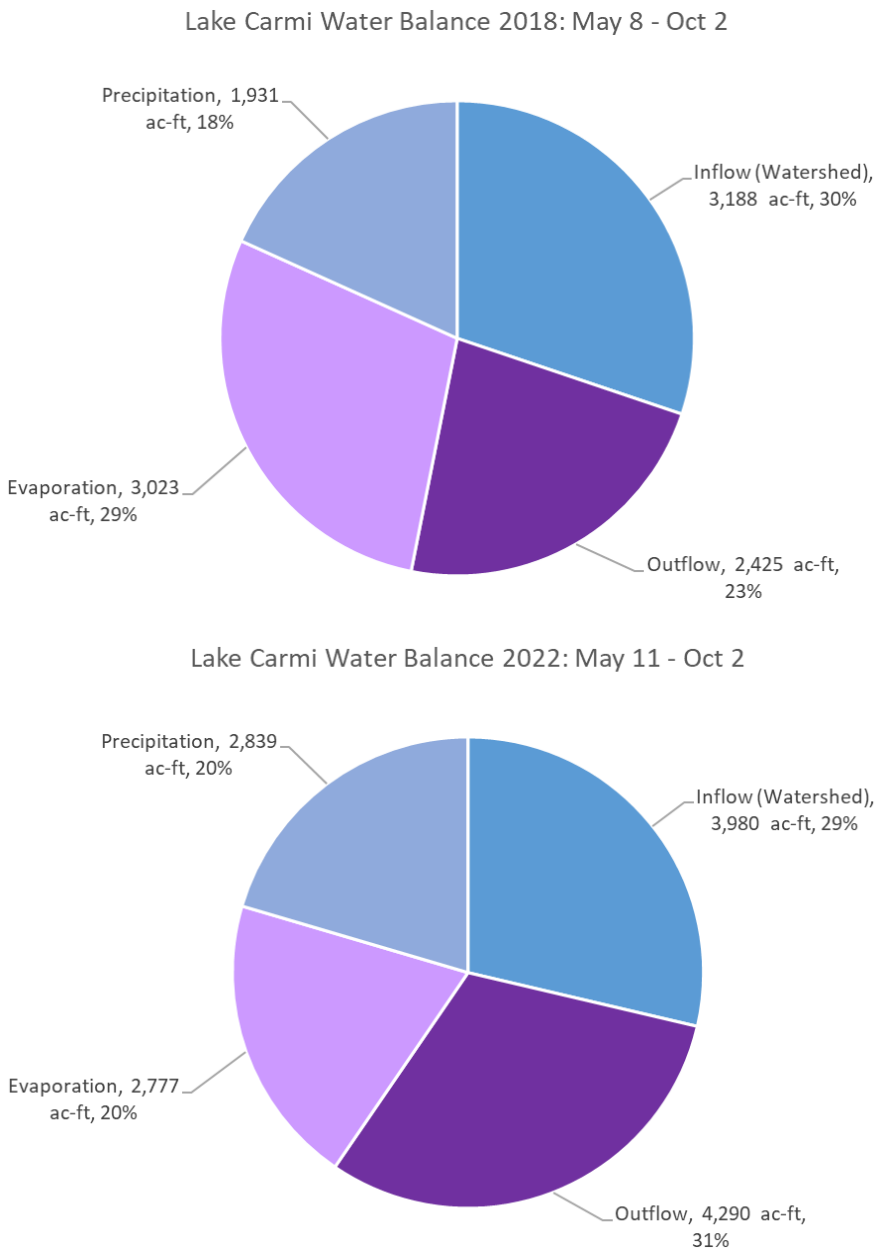

Figure 4-3 2018 and 2022 water balance summaries

It was assumed that the estimated watershed runoff yields presented in Table 4-2 were applicable to each subwatershed tributary to Lake Carmi. While each subwatershed has variable percentages of agriculture, forest, prairie, and impervious area (e.g., buildings, roads), the overall composite curve number (CN) for each subwatershed did not vary substantially. The calculated composite CNs ranged from 77 – 88, with the average composite CN equaling 83. Composite CNs were calculated using land cover and land use data available from the Vermont Open Geodata Portal (State of Vermont, 2023). Because the CNs were not notably variable, the watershed runoff volume per subwatershed was estimated by multiplying the total watershed area by the monitored precipitation depth and the corresponding watershed yield per month.

4.1.2 Watershed Nutrient Loading

The water quality monitoring data collected at various harge points throughout the Lake Carmi watershed in 2018 and 2022 were used to estimate the watershed nutrient loadings. The monitoring locations compared to the subwatershed divides developed for this study are shown in Figure 4-4. Not all of the subwatershed divides used for this study had accompanying monitoring data (i.e., watershed names starting with "NM" = "Not Monitored"). As such, the monitoring data from other subwatersheds were used to estimate nutrient loadings for the non-monitored subwatersheds. This includes watersheds that may have had water quality monitoring data in years other than model years 2018 and 2022.

In 2018, total phosphorus (TP) and total nitrogen (TN) were sampled at 14 monitoring locations. Of the 14 locations monitored, seven were located at creek and brook mouths near Lake Carmi; the other seven were located further upstream in the watershed. The number of samples collected at each monitoring location varied from two to seven samples between mid-April and early-October 2018. Average nutrient concentrations were applied for subwatersheds with no monitoring data in 2018.

In 2022, TP and total dissolved phosphorus (TDP) were sampled at 10 monitoring locations. Of the 10 locations monitored, six were located at creek and brook mouths near Lake Carmi; the other four were located further upstream in the watershed. The number of samples collected at each monitoring location varied from six to 13 samples between the end of April and mid-September 2022. Average nutrient concentrations were applied for subwatersheds with no monitoring data in 2022.

Because TDP monitoring data was absent in 2018, the phosphorus data collected in 2022 was used to inform 2018 TDP concentrations. The 2022 TDP:TP ratios were calculated for each storm event and then similar proportions were assumed for 2018. Similarly, because TN monitoring data was absent in 2022, the TN data collected in 2018 was used to inform 2022 TN concentrations. The 2018 TN:TP ratios were calculated for each storm event and then similar proportions were assumed for 2022.

The estimated summer growing period (June 1 – September 30) total phosphorus loads per subwatershed are presented in Table 4-3 for 2018 and 2022.

Table 4-3 Total phosphorus load estimate per subwatershed (pounds)

Subwatersheds	Subwatershed Model Number	Summer Total Phosphorus Load – lbs (June 1 – September 30)	
		Calibrated 2018 Existing Conditions	Calibrated 2022 Existing Conditions
DIR-WS (Direct)	1	34	28
LC1	2	8	5
LC10 + LC8.1 +LC8.2	3	140	152
LC12	4	5	5
LC13	5	21	22
LC15	6	6	6
LC16	7	1	1
LC2 + LC11	8	39	32
LC5 + LC3	9	42	27
LC6	10	26	22
NM-E1	11	26	24
NM-S1 & S2 & S3	12	62	58
NM-W1	13	9	8
NM-W2	14	8	8
NM-W3	15	10	9
Total		**437**	**408**

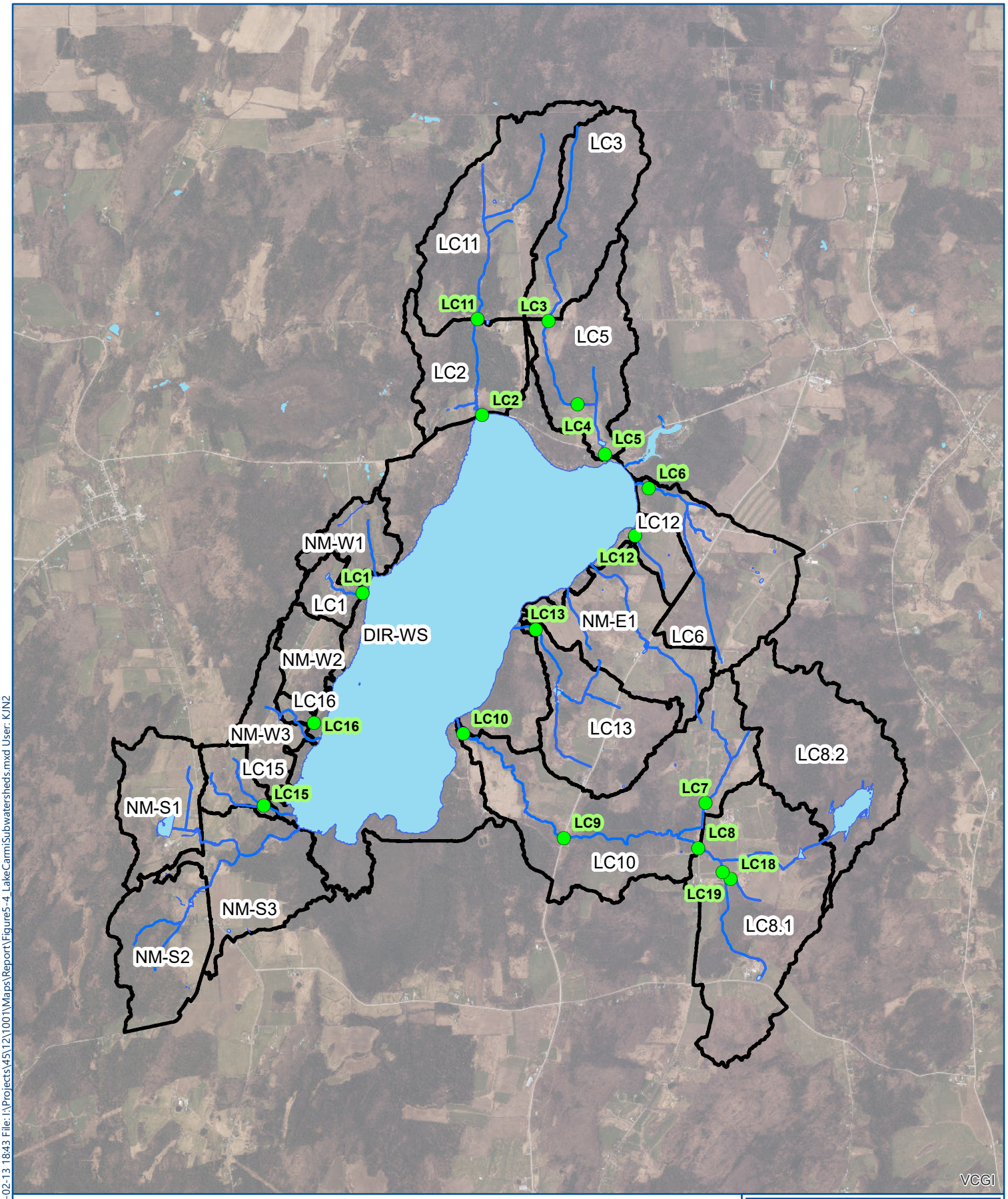
LC3
LC11
LC11
LC3
LC5
LC2
LC2
LC4
LC5
LC6
LC12
LC12
NM-W1
LC1
LC1
LC13
NM-E1
LC6
DIR-WS
NM-W2
LC16
LC16
LC10
LC13
LC8.2
NM-W3
LC15
LC15
LC7
NM-S1
LC9
LC8
LC10
LC18
LC19
NM-S3
LC8.1
NM-S2
VCGI
Subwatershed Divides
Watershed Monitoring Points
Open Water
Creeks & Brooks
N
0
4,000
Feet
BARR
LAKE CARMI
SUBWATERSHED
DIVIDES
FIGURE 4-4
Barr Footer: ArcGIS 10.9.1, 2024-02-13 18:43 File: I:\Projects\45\12\1001\Maps\Report\Figure5-4_LakeCarmiSubwatersheds.mxd User: KJN2

4.1.3 One-dimensional Lake Model

The purpose of in-lake modeling is to establish a relationship between the amount of nutrients that enter a lake and the concentration of these nutrients that remain in a lake. In recent years, it's becoming more widely acknowledged that in freshwater ecosystems, both in-lake phosphorus and nitrogen can limit algal growth and also select for the species present. As such, this study incorporated the effect of both phosphorus and nitrogen on phytoplankton growth in Lake Carmi.

The Barr Lake Model was the first in-lake model approach used for this study. The Barr Lake Model is one-dimensional, meaning the model is completely mixed horizontally but vertically splits the water column into defined layers to calculate mixing and transport as a result of wind-induced development of a surface mixed layer and advection-dispersion process below the mixed layer. The model integrates external and internal nutrient inputs and losses on an hourly timestep. Additionally, a major benefit of the model is that it incorporates phytoplankton (algae) growth, death, decay, and nutrient removal mechanisms (e.g., particulate organic phosphorus setting), which are often misrepresented in other model techniques. The model has been designed to model three major taxa of algae, including cyanobacteria, chlorophytes, and diatoms. Incorporating these three groups into the model is necessary as diatoms are dominant in the spring and settle out once a lake begins to stratify, cyanobacteria will dominate under nitrogen-limiting conditions, and chlorophytes are present in most lakes and can be affected by both phosphorus and nitrogen availability. Having a good understanding of algal growth dynamics is also important for good comprehension of the potential outcome of management recommendations (e.g., will P reduction also reduce cyanobacteria and begin to favor chlorophytes?).

The Barr Lake Model was calibrated for model years 2018 and 2022. Calibration is a process in which model parameters and coefficients are reasonably adjusted such that the model predictions are similar to in-lake measurements. The Lake Carmi models were calibrated to the following water quality parameters:

- Lake Temperature
- Total Phosphorus
- Total Dissolved Phosphorus
- Chlorophyll-*a* (Cyanobacteria, Chlorophytes, Diatoms)
- Total Nitrogen

Example in-lake model calibrations for Lake Carmi are provided below. Figure 4-5 and Figure 4-6 show the 2018 calibrations for surface TP and TDP concentrations, respectively. The orange line represents the modeled in-lake concentrations, and the blue circles represent the monitored concentrations. Plots showing all parameters used for calibration in 2018 and 2022 can be found in Appendix F. Both surface (TP, TDP, chlorophyll-*a*) and profile (temperature, TP, TN) monitoring data were used to calibrate the models.

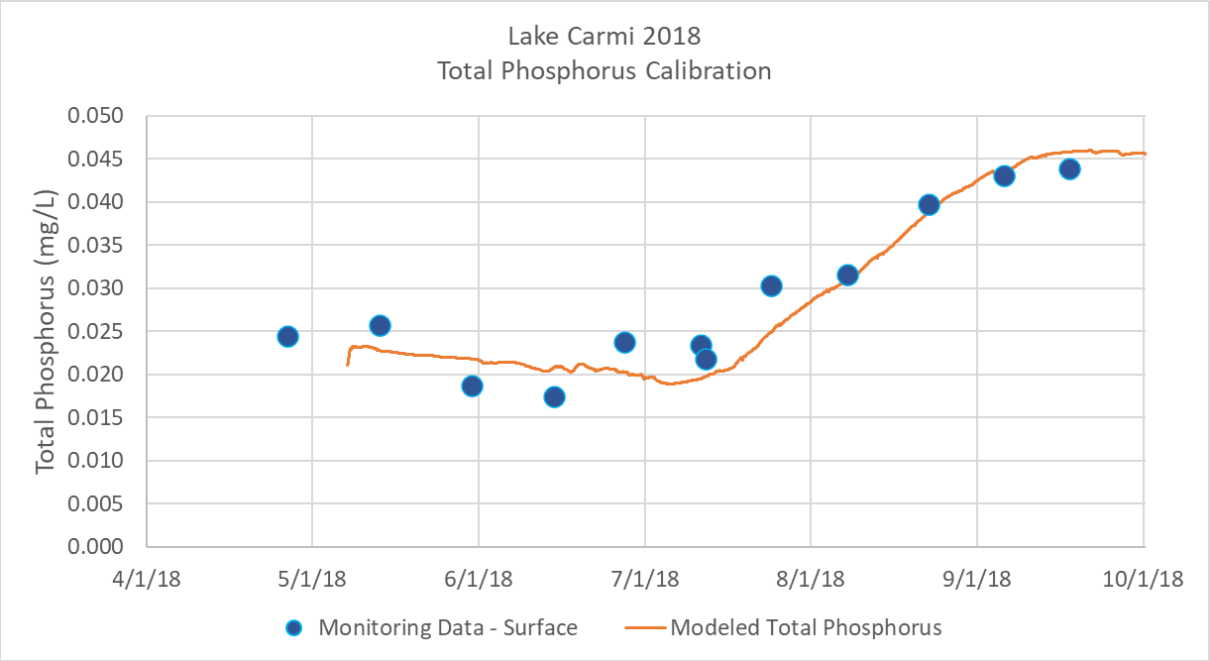

Figure 4-5 2018 in-lake calibration of total phosphorus concentrations

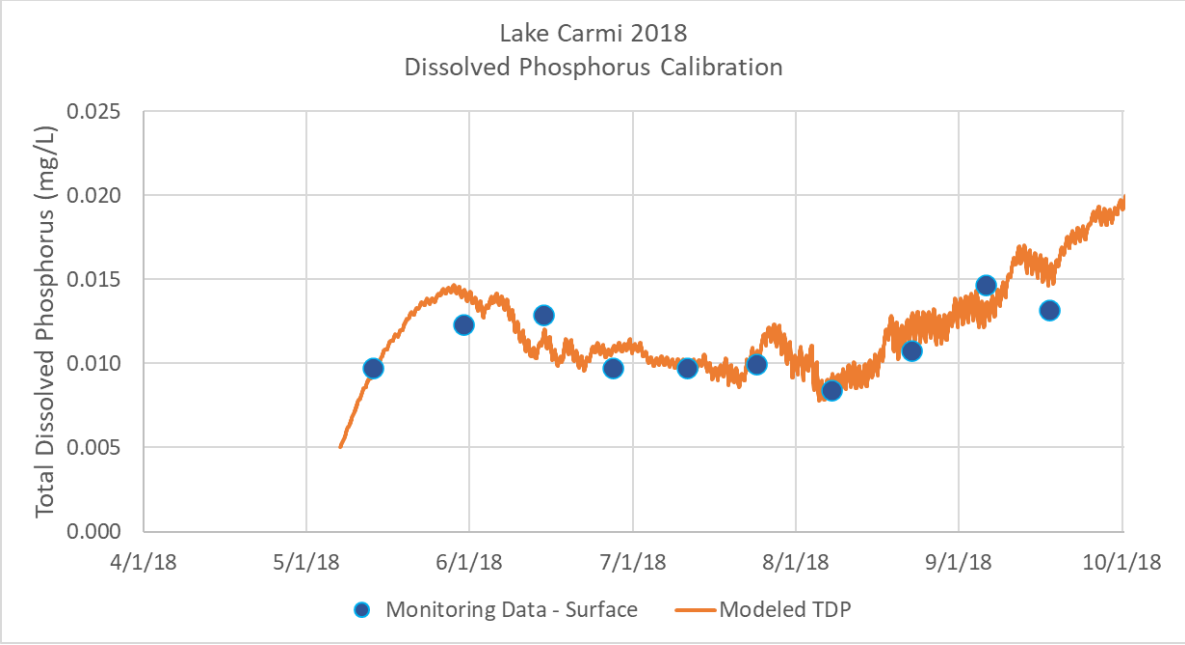

Figure 4-6 2018 in-lake calibration of total dissolved phosphorus concentrations

4.1.3.1 Barr Lake Model Calibration Phosphorus Loading Summaries

After the Barr Lake Model water quality calibrations were finalized, phosphorus loading summaries were developed. Figure 4-7 shows the total phosphorus loading summaries during the 2018 and 2022 summer growing periods (June 1 – September 30).

In 2018, the percentage of total phosphorus loading from lake bottom sediment was notably higher than the loading from watershed runoff or atmospheric deposition. The in-lake calibration shows that approximately 87% (3,073 pounds) of the total phosphorus load to Lake Carmi between June 1 – September 30, 2018, was from lake bottom sediment. The remaining 13% was contributed by watershed runoff (12%, 438 pounds) and atmospheric dry deposition (1%, 18 pounds). The total load of phosphorus to Lake Carmi during the 2018 summer growing period was estimated to be approximately 3,529 pounds.

In 2022, the percentage of total phosphorus loading from lake bottom sediment was also notably higher than the loading from watershed runoff or atmospheric deposition. The in-lake calibration shows that approximately 90% (3,638 pounds) of the total phosphorus load to Lake Carmi between June 1 – September 30, 2018, was from lake bottom sediment. The remaining 10% was contributed by watershed runoff (~10%, 408 pounds) and atmospheric dry deposition (<1%, 18 pounds). The total load of phosphorus to Lake Carmi during the 2022 summer growing period was estimated to be approximately 4,064 pounds.

The models indicate that phosphorus loading from lake bottom sediment is the primary source of phosphorus to Lake Carmi. Despite the installation of an aeration system in 2019, internal P loading has not been reduced compared to conditions without aeration. In addition to the evidence provided by the modeling results, the observed total phosphorus profile data show that the aeration system appears to be increasing the total phosphorus concentrations throughout the entire lake water. With mixing provided by the aeration system, higher total phosphorus concentrations from internal loading no longer remain in the hypolimnion. Instead, phosphorus released from lake bottom sediment is spread throughout the water column, becoming more bioavailable to algae near the surface and in the photic zone where growth can be greatest.

While phosphorus loading from lake bottom sediment is the primary source of phosphorus to Lake Carmi during the summer growing period of June through September, the watershed also contributes a notable phosphorus load (>400 pounds) during the summer growing period and should not be discounted. Implementing additional watershed BMPs could continue to reduce inflow concentrations and help prolong any sediment management practices employed.

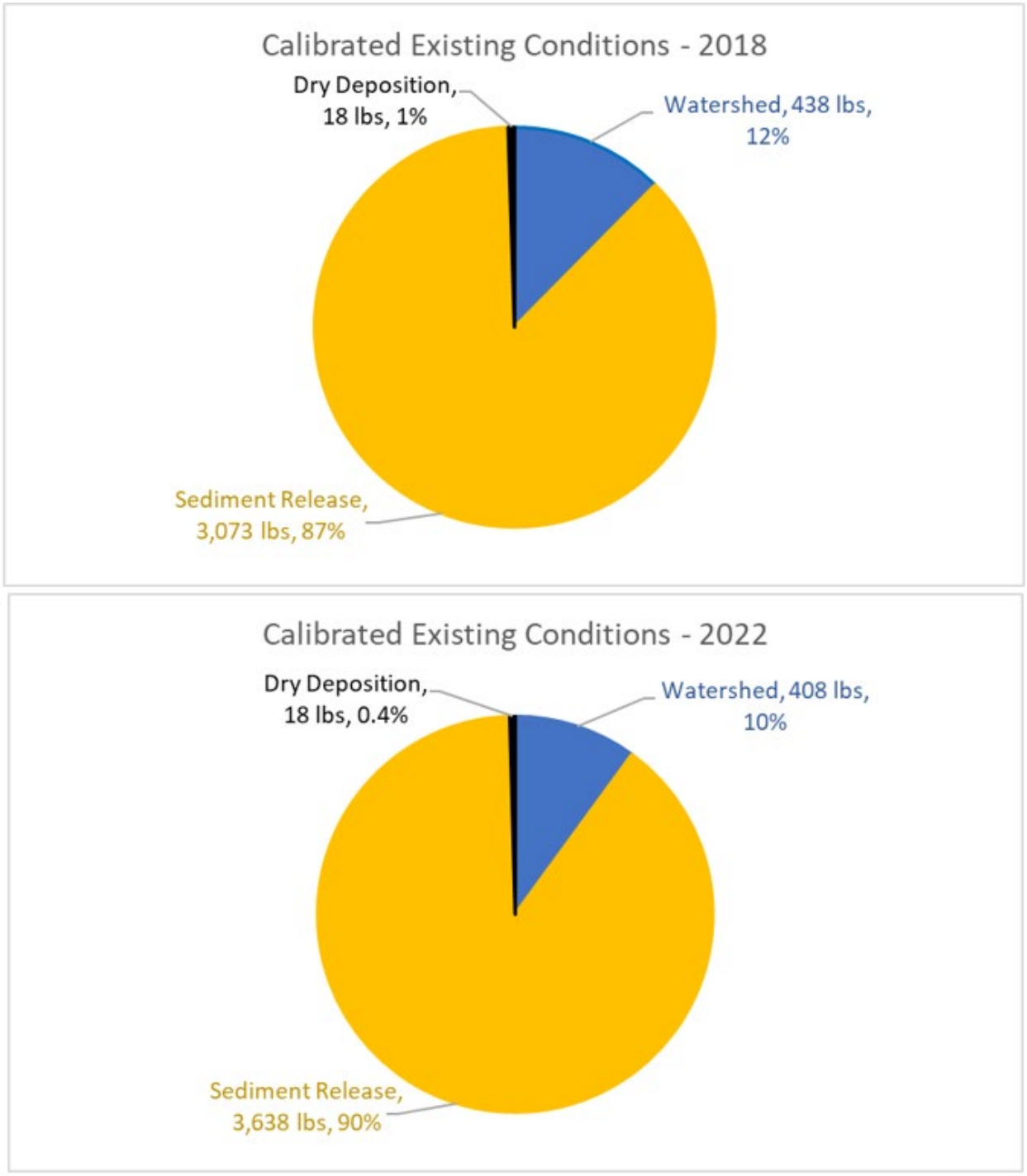

Figure 4-7 Barr Model total phosphorus loading summaries from June 1 – September 30

4.1.3.2 Additional Observations – Phytoplankton Growth Dynamics

Throughout the growing season, various factors can influence the rate and volume of phytoplankton growth, such as phosphorus and nitrogen concentrations, as well as light and temperature. The Barr Lake Model uses Michaelis Menten kinetics to determine which factor or combination of factors limit growth throughout the modeled time period. The model also incorporates taxa-level competitive advantages that can also notably influence growth rates and algal biomass. For example, the Barr Lake Model approximates the nitrogen-fixation and buoyancy regulation abilities that certain species of cyanobacteria exhibit. These cyanobacteria abilities create noteworthy competitive advantages because:

- Nitrogen fixation allows specific cyanobacteria species to convert atmospheric nitrogen (N_2) to usable forms when dissolved forms in the water column become too depleted. This allows cyanobacteria species to continue growing while other algal species do not have enough nitrogen for growth.
- Buoyancy regulation allows specific cyanobacteria species to travel vertically throughout the water column to access depths with more favorable nutrient, temperature, or light conditions.

The model calibration would not successfully predict the observed chlorophyll-*a* concentrations without incorporating these cyanobacteria abilities. An example from the 2018 model year is shown in Figure 4-8. The primary y-axis displays the three taxa of phytoplankton modeled as chlorophyll-*a*, including diatoms (Bacillariophyta) in green, cyanobacteria in cyan, and chlorophytes (Chlorophyta) in purple. The orange line is the combination of all three taxa. The dark blue points summarize the 2018 monitored chlorophyll-*a* concentrations. Comparing the orange line to the dark-blue points indicates that the modeled chlorophyll-*a* concentration represents the growth conditions in Lake Carmi fairly well. The modeled concentrations of nitrates and nitrites are shown in black on the secondary y-axis. We can see that at the start of June, nitrate/nitrite concentrations begin to decrease as the biomass of diatoms increases. The nitrate/nitrite concentrations drop so low at the start of July that nitrogen becomes a limiting factor for phytoplankton growth. While nitrogen limitation impacts the growth of diatoms and chlorophytes in July, the nitrogen fixation abilities of cyanobacteria species allow for continued growth. Without nitrogen fixation in the model, the modeled chlorophyll-*a* concentrations would not match the observed concentrations, as significant nitrogen limitation prevented growth without fixation.

The model findings are also supported by phytoplankton species data collected in 2018 by the University of Vermont (courtesy of Ana Morales) from July to the end of September and an increase in Chlorophyta abundance in the fall.

Additionally, of the four major genera of cyanobacteria observed in 2018, as shown in Figure 4-10, three genera contain species that have been observed to exhibit nitrogen fixation abilities (i.e., Aphanizomenon, Cuspidothrix, and Dolichospermum) further supporting the modeled nitrogen fixation assumptions.

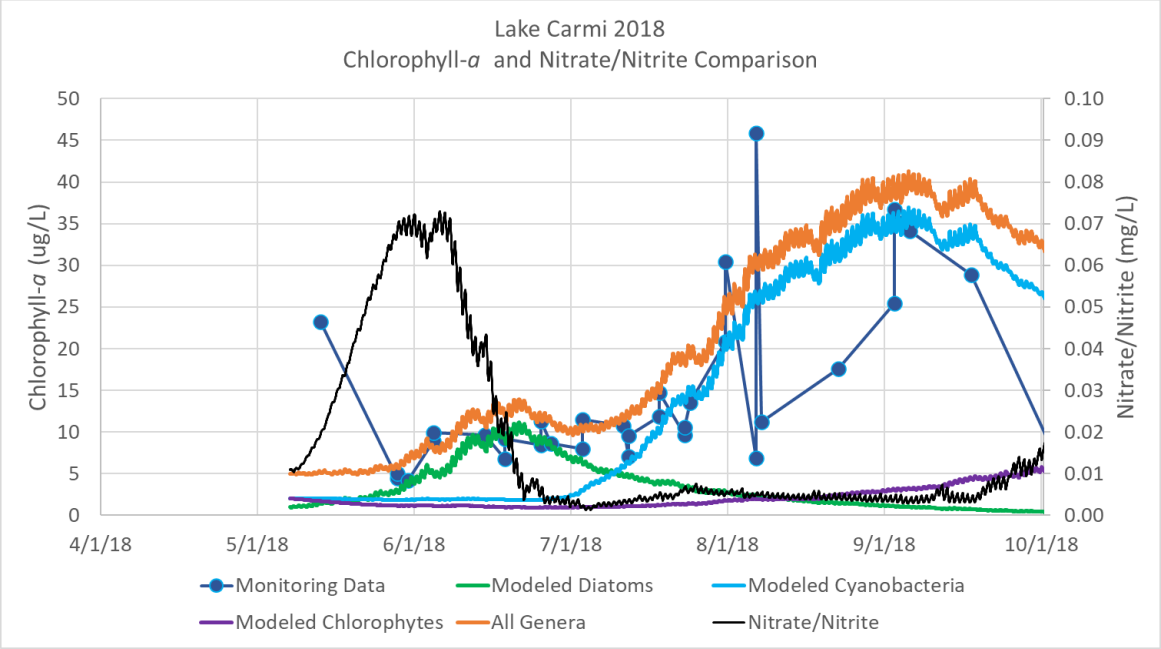

Figure 4-8 Comparison of 2018 chlorophyll-*a* and nitrate/nitrite concentrations[3]

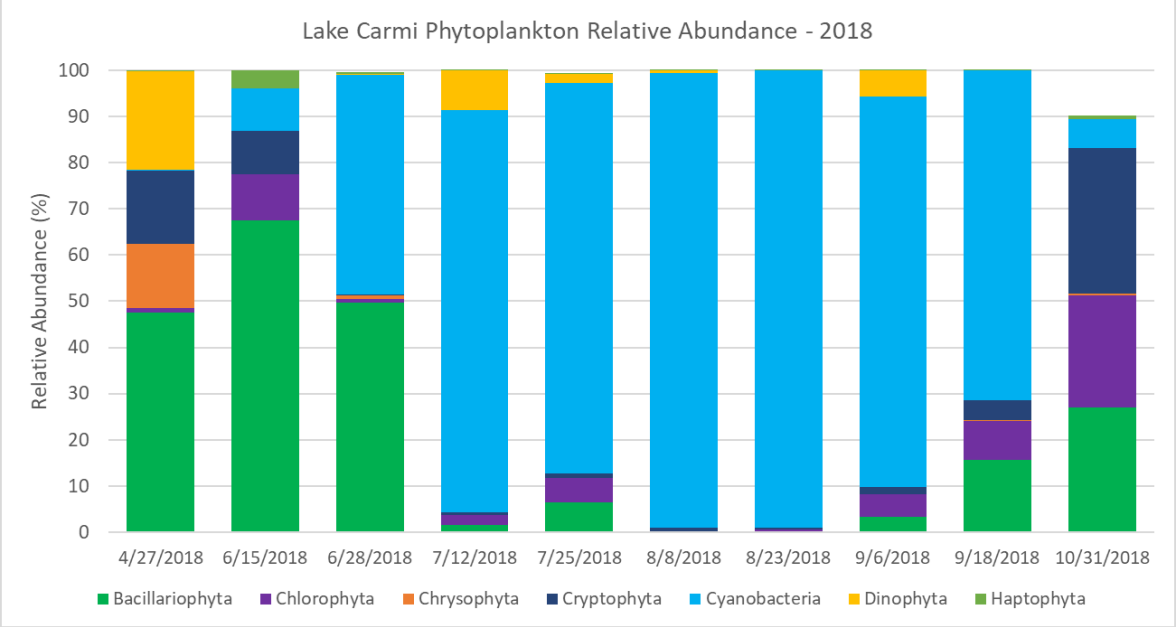

Figure 4-9 2018 observed phytoplankton relative abundance. Data courtesy of Ana Morales, University of Vermont.

[3] Note that samples were collected at variable depths in Lake Carmi based upon the thermocline depth, contributing to the high variability of the results.

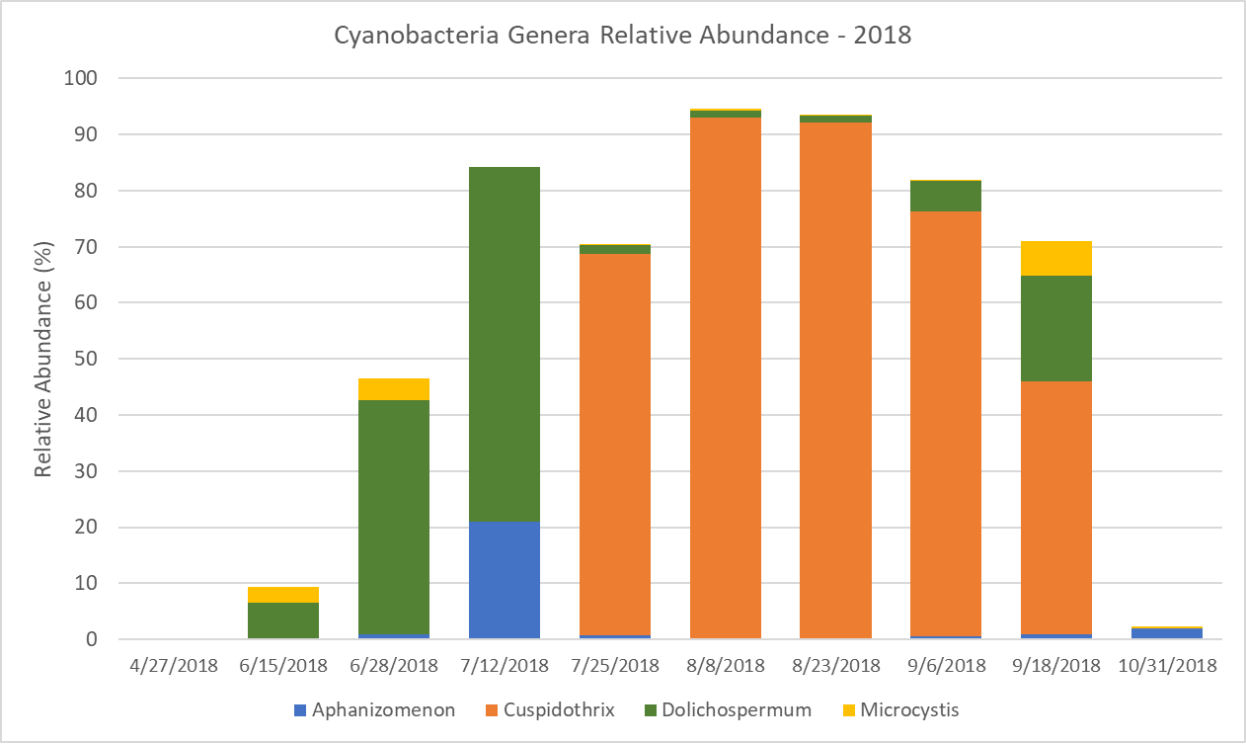

Figure 4-10 2018 observed cyanobacteria genera relative abundance. Data courtesy of Ana Morales, University of Vermont

The Barr Lake Model indicates that phosphorus is not the only nutrient that limits the growth of phytoplankton in Lake Carmi, with nitrogen limitation playing a role. Although low nitrate/nitrite concentrations can limit the growth of phytoplankton taxa, such as diatoms and chlorophytes, the nitrogen fixation ability of some cyanobacteria species can counterbalance this effect and still allow for higher algal growth. The phytoplankton growth limitations identified during model calibration reflect which parameters are currently limiting growth. As management is implemented, the phytoplankton growth limitations will likely change. For example, if phosphorus loading from lake bottom sediment is reduced, phosphorus limitation will become more dominant throughout the growing season, and the concentration of nitrogen increase as the lower phytoplankton population will not consume as much nitrogen.

4.1.4 TMDL Model (BATHUB)

In addition to the Barr Model, lake response to nutrient loading was modeled using BATHTUB to be consistent with the Lake Carmi TMDL (Vermont Agency of Natural Resources, 2008). BATHTUB is a series of empirical eutrophication models that predict the lake response to phosphorus inputs for lakes and reservoirs (Walker, 1996 (updated 1999)). Several models (subroutines) are available for use within the BATHTUB model, and the Canfield-Bachmann model was used in this study to predict the lake response to total phosphorus loads (to be consistent with the Lake Carmi TMDL model approach).

The Canfield-Bachmann model (Canfield & Bachmann, 1981) estimates the lake phosphorus sedimentation rate, which is needed to predict the relationship between in-lake phosphorus

concentrations and phosphorus load inputs. The phosphorus sedimentation rate is an estimate of net phosphorus loss from the water column to the lake bottom and is used alongside lake-specific characteristics, such as annual phosphorus loading (external and internal), mean depth, evaporative loss, and hydraulic flushing rate, to predict in-lake phosphorus concentrations. The model predictions are then compared to observed monitoring data to evaluate how well the model describes the lake system.

Estimated watershed, internal, and atmospheric phosphorus loads were used to predict in-lake concentrations for the 2018 and 2022 model years. An average year model was then developed using averages of the inputs from each of the model years and calibrated by adjusting the sedimentation term in the Canfield-Bachmann model.

Assumptions were needed to develop the watershed inputs since monitoring data (e.g., lake levels, in-lake water quality, tributary inflow water quality) has not been collected outside of April through October in any given year. The website, *Model My Watershed*, was used to estimate annual watershed runoff yield (Stroud Water Research Center). *Model My Watershed* is a part of Stroud Water Research Center's WikiWatershed initiative that enables users to analyze land use and soil data, model stormwater runoff and water-quality impacts, and compare how different conservation or development scenarios could modify runoff and water quality. Based on average monthly water fluxes from 30 years of daily water balance, the estimated average annual watershed runoff yield was 0.41. This watershed runoff yield of 0.41 was applied to the annual observed precipitation totals for model years 2018 and 2022 to develop an estimated annual runoff volume. The average total phosphorus concentrations monitored from the tributary watershed locations located at creek and brook mouths to Lake Carmi were used to estimate the annual total phosphorus load from the watershed. The average monitored TP concentrations in 2018 and 2022 were 56 and 64 µg/L, respectively.

Since in-lake water quality monitoring data has not been collected during the winter months to inform the magnitude of internal phosphorus loading under the ice, the internal phosphorus loads calculated using the Barr Lake Model were input directly in the BATHTUB model to be conservative (the BATHTUB model does not calculate internal loading). The total internal phosphorus load for the entire calibrated period (mid-May through early October) was as a BATHTUB model input.

Although much smaller in magnitude, phosphorus loads were estimated for atmospheric deposition and septic systems. The atmospheric deposition used the same aerial loading rate as the Barr Model, which was approximately 4.25 kg/km^2-year. The septic system loading rate used the same assumption as the Lake Carmi TMDL, estimated to be approximately 15 kg/year (Vermont Agency of Natural Resources, 2008).

4.1.4.1 BATHTUB Model Phosphorus Loading Summary

After the BATHTUB models were calibrated to the monitoring data, phosphorus loading summaries were developed. Table 4-4 and Table 4-5 show the estimated annual total phosphorus loads in 2018 and 2022 and compare the estimated loads to those predicted in the 2008 Lake Carmi TMDL (Vermont Agency of Natural Resources, 2008). The BATHTUB results in this study indicate that the internal phosphorus load from lake bottom sediment is the primary source of phosphorus in Lake Carmi, with over 1,400 kg (3,100

pounds) annually. Total phosphorus from watershed runoff is also a notable contribution, with over 600 kg (1,300 pounds) annually.

Table 4-4 BATHTUB model total phosphorus load summaries (kilograms)

Source of Phosphorus Load	Annual Phosphorus Load (kg/year)			
	2018	2022	Average	2008 TMDL
Watershed Tributaries[1]	605	775	690	1,421
Septic Loads	15	15	15	15
Internal Loads	1,451	1,971	1,711	97
Lake Carmi State Park WWTF[2]	0	0	0	2
Total	2,071	2,761	2,416	1,535

[1] Includes atmospheric deposition.

[2] The 2008 Lake Carmi TMDL estimated 2 kg/yr of indirect discharge through the WWTF leach field. This study assumes those indirect discharges have been addressed and are no longer contributing.

Table 4-5 BATHTUB model total phosphorus load summaries (pounds)

Source of phosphorus load	Annual Phosphorus Load (lbs/year)			
	2018	2022	Average	2008 TMDL
Watershed Tributaries[1]	1,334	1,708	1,521	3,133
Septic Loads	33	33	33	33
Internal Loads	3,199	4,345	3,772	214
Lake Carmi State Park WWTF[2]	0	0	0	4
Total	4,566	6,087	5,326	3,384

[1] Includes atmospheric deposition.

[2] The 2008 Lake Carmi TMDL estimated 2 kg/yr of indirect discharge through the WWTF leach field. This study assumes those indirect discharges have been addressed and are no longer contributing.

4.2 Lake Response to Internal and External Phosphorus Loading Reductions (Treatment)

The calibrated Barr Lake Models were used to predict the effects of implementing various BMPs to improve the water quality of Lake Carmi. The following BMPs were assessed:

1. Alum sediment treatment to reduce internal phosphorus loading from lake bottom sediment
2. Reducing entire watershed TP load by 10%, 25%, and 50% (by implementing multiple BMPs)
3. Installing an alum treatment facility to treat watershed TP loads near monitoring location LC10 (Marsh Brook near the mouth of Lake Carmi)

Figure 4-11 and Figure 4-12 summarize the estimated pounds of phosphorus removed during the 2018 and 2022 summer growing periods, respectively, assuming the implementation of the BMPs described

above. The application of a sediment alum treatment is expected to decrease the TP load to Lake Carmi by 62% to 70% over one summer growing period (June – September). Comparatively, the implementation of watershed BMPs has less of an impact over one summer growing period with less than a 10% reduction in TP load. However, the implementation of watershed BMPs can have a positive long-term impact by continuing to reduce nutrient loads reaching Lake Carmi and prolonging any internal BMPs implemented.

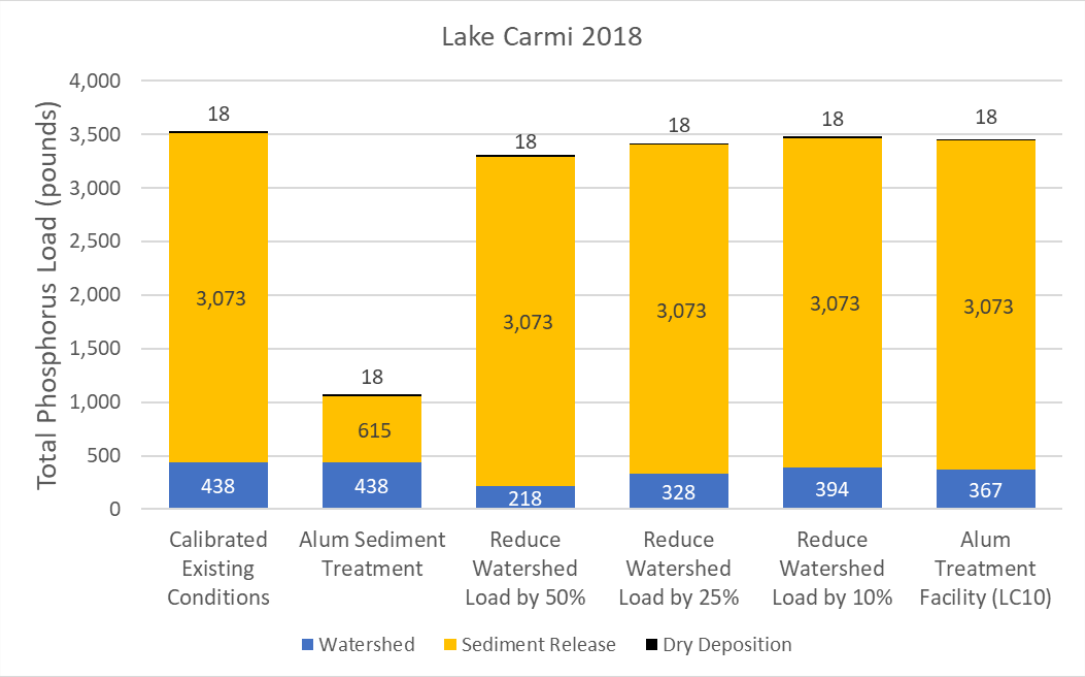

Figure 4-11 2018 estimated reduction in total phosphorus load to Lake Carmi with implementation of BMPs (June 1 – September 30)

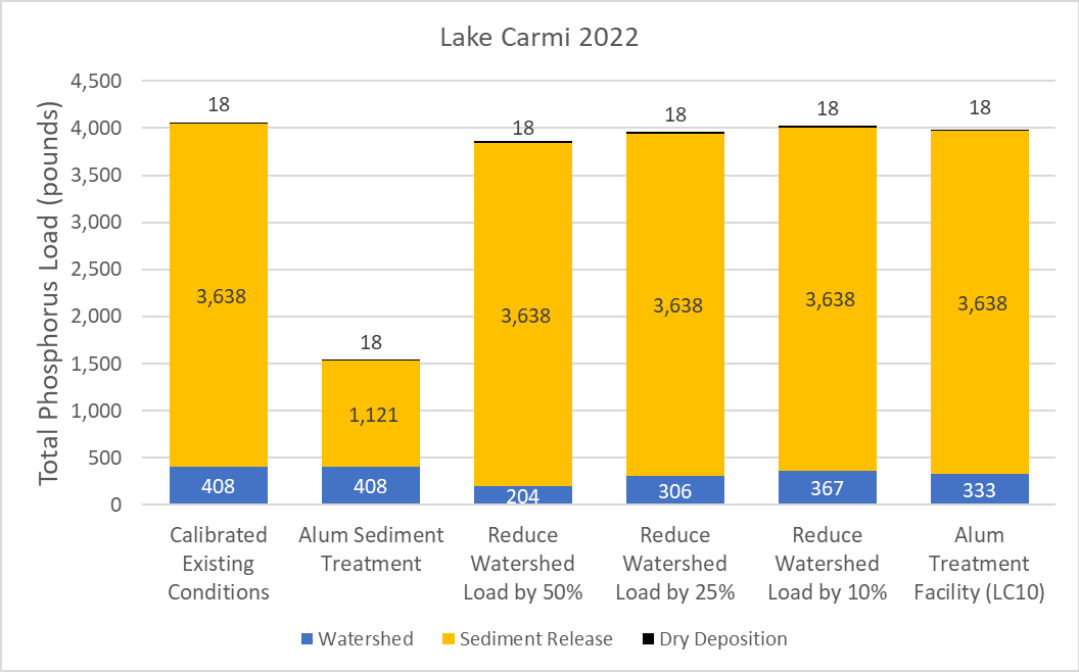

Figure 4-12 2022 estimated reduction in total phosphorus load to Lake Carmi with implementation of BMPs (June 1 – September 30)

Reductions in phosphorus load translate to reductions in the phosphorus concentrations in the lake and, consequently, reductions in chlorophyll-*a* concentrations and improvements in Secchi disc depth. Table 4-6 and Table 4-7 summarize the 2018 and 2022 Barr Lake Model estimated reductions in summer average total phosphorus and chlorophyll-*a* concentrations for the modeled internal and watershed BMPs, respectively. The improvements to Secchi disk depth were estimated by developing a relationship between observed chlorophyll-*a* and Secchi disk depth monitored in Lake Carmi between the mid-1970s to 2022. Plots summarizing the changes in modeled TP and chlorophyll-*a* concentrations can be seen in Appendix G.

Table 4-6 2018 Barr Lake Model predicted changes for total phosphorus, chlorophyll-*a*, and Secchi disk depth with implementation of BMPs

Modeled Summer Average Concentrations - µg/L (June 1 - Sept 30)			Estimated Secchi Disk (m)
Scenario	Total Phosphorus	Chlorophyll-a	
Calibrated Existing Conditions	31	24	1.5
Sediment Treatment, Aluminum	15	7	2.6
Reduce Watershed Load by 50%	29	22	1.6
Reduce Watershed Load by 25%	30	23	1.5
Reduce Watershed Load by 10%	30	24	1.5
Alum Treatment Facility (LC10)	30	23	1.5

Table 4-7 2022 Barr Lake Model predicted changes for total phosphorus, chlorophyll-a, and Secchi disk depth with implementation of BMPs

Modeled Summer Average Concentrations - µg/L (June 1 - Sept 30)			Estimated Secchi Disk (m)
Scenario	Total Phosphorus	Chlorophyll-a	
Calibrated Existing Conditions	42	33	1.3
Sediment Treatment, Aluminum	18	12	2.0
Reduce Watershed Load by 50%	39	31	1.4
Reduce Watershed Load by 25%	40	32	1.3
Reduce Watershed Load by 10%	41	32	1.3
Alum Treatment Facility (LC10)	41	32	1.3

Model results indicate that treatment of lake bottom sediments with aluminum will reduce total phosphorus in Lake Carmi to below the lake eutrophication standard of 22 µg/L.

It should be noted that the predictions in Table 4-6 and Table 4-7 are a result of reduced total phosphorus loads. All other variables that may affect growth (e.g., watershed nitrogen loads, temperature, solar radiation) were not changed.

5 Sediment Inactivation Treatment Design and Cost Analysis

This report section provides a comprehensive assessment of (1) treatment options (e.g., doses), (2) a dosing plan, (3) an assessment of treatment with respect to the aluminum criterion, (4) estimated treatment longevity, and (5) a cost-benefit analysis.

A synopsis of treatment options and the outcome of calculations to support this assessment is provided in Table 5-1. The treatment area is 775 acres and the basis of this decision was identified in Section 2 and 3 of this report. The recommended dose is the middle dose (67 g Al/m^2), which provides an 85% reduction in the maximum potential internal P loading rate. This dose can either be applied as a single application or split in half and applied in separate years with a gap between the treatments of one to five years. Splitting the dose further (e.g., thirds) is not recommended as pin floc may develop and reduce settling rates, resulting in higher in-lake total aluminum concentrations, as well as higher residual dissolved or colloidal aluminum (further discussion is provided below). Both approaches, the application of the full dose or split dosing, are viable. The full dose will result in a greater reduction in internal P loading over the short term. A split dose can be expected to be more efficient, and over the long term, the overall internal P load reduction should be greater.

Table 5-1 Aluminum treatment options

Treatment Options	Dose (g Al/m^2)	Alum (gallons)	Sodium Aluminate (gallons)	Mass of Aluminum Applied (kg)	Estimated Treatment Days	Daily Treatment Zone		Average over Full 775 Acre Treatment Zone	
						Maximum Al During Treatment (mg/L)	Average 24 Hour Al (mg/L)	Maximum Al (mg/L)	Average 24 Hour Al (mg/)
Option 1: Low Dose	27	166,140	83,070	84,193	12	1.7	0.56	0.14	0.05
Option 2: Middle Dose	67	412,183	206,092	208,877	29	4.2	1.4	0.14	0.05
Option 3: High Dose	110	678,315	339,157	343,742	48	6.8	2.3	0.14	0.05

Notes:

Treatment area is 775 acres.

Volume of lake in treatment area is 5,926,404 cubic meters.

Treatment zone includes lake areas at 20 feet and deeper.

Daily application rate estimated to be 14,000 gallons alum and 7,000 gallons sodium aluminate.

Aluminum floc settling rate is 0.07 cm/s.

Average depth of treatment area is 26.2 feet.

Time for floc to settle 26.2 feet is 3.2 hours.

Effect of Treatment on In-lake Aluminum

For this analysis, the area and volume of lake water treated in one day is considered to be the treatment zone for that day. For each dose, the calculated number of days to apply the dose is provided in Table 5-1. Based upon a literature-reported aluminum floc settling rate (Gorczyca, B. and J. Ganczarczyk, 2001), it can be expected that the aluminum floc ($Al(OH)_3$) will settle to the bottom of Lake Carmi in just over three hours. Conceptually, as the barge travels across the lake and applies alum and sodium aluminate, floc will settle. During an 8-hour treatment day, the floc will be at different stages of settling within the treatment zone. Using the application and settling rate, lake volume for the area being treated, and dose, the average concentration in the treatment zone water column was calculated for each hour of a 24-hour period. The estimated average in-lake total aluminum concentration for the treatment zone can be seen for each hour in Figure 5-1 for the recommended dose (middle dose (67 g Al/m^2)),. Three hours after treatment is complete for a given day, all aluminum floc will have settled to the bottom of the lake. In essence, the entire lake will have "reset" after each treatment day with respect to in-lake total aluminum. The average total aluminum concentration in the treatment zone for a treatment day is estimated to be 1.4 mg/L (this value should be reduced accordingly (e.g., 0.7 mg/L for a half dose) if the treatment is split). On an average basis for the entire 775-acre treatment area, the maximum total aluminum concentration is 0.14 mg/L, and the average is 0.05 mg/L.

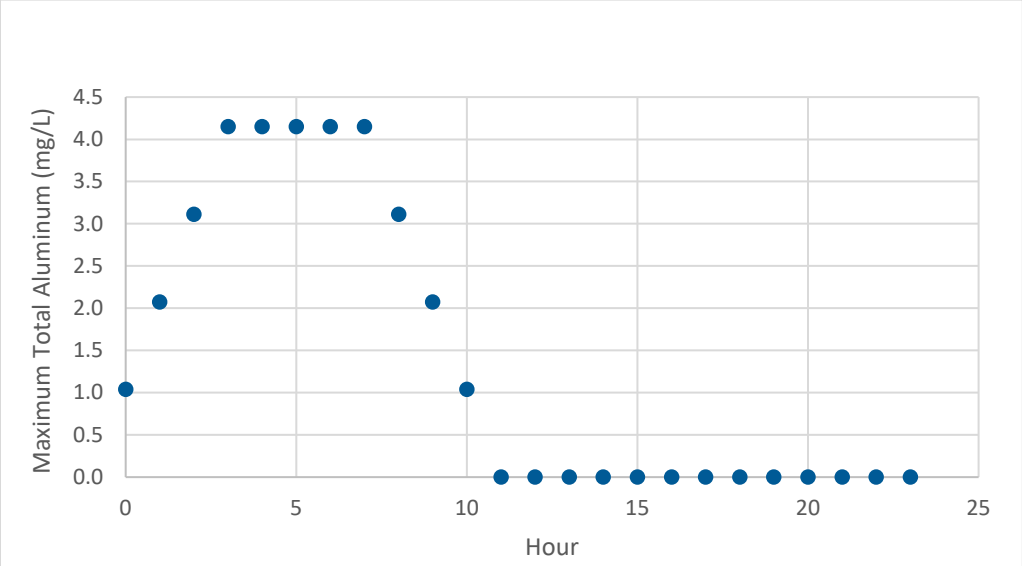

Figure 5-1 Estimated change in-lake total aluminum concentration within the daily treatment zone for the recommended full dose

Using pH of 7.85 (most recent 10-year monitoring period and surface to lake bottom), hardness of 44.6 mg/L (2019 through 2023), and DOC of 4.05 mg/L (from 2018 and 2019), the applicable CMC (acute criteria) is 2.7 mg Al/L and the CCC (chronic criteria) is 1.1 mg Al/L. Given the identified applicable criteria, to avoid exceeding the CMC, it may be necessary to: (1) Conduct a "double pass" where half of the alum dose is applied on one day and the other half of the dose is applied that following day in the same area. This will effectively reduce the maximum (from 4.2 to 2.1 mg/L) and average (from 1.1 to 0.55 mg/L) total aluminum concentration experienced across the treatment zone to concentrations below the CMC and

CCC, and (2) Apply half the dose in one year and the other half a year or more later. This will also effectively reduce the maximum (from 4.2 to 2.1 mg/L) and average (from 1.1 to 0.55 mg/L) total aluminum concentration experienced across the treatment zone to concentrations below the CMC and CCC.

5.1 Longevity Estimate

The longevity of the alum treatment will be largely determined by: (1) external P loads and the fraction of those loads that will be deposited on the lake bottom sediment, and (2) decay of existing Org-P in lake bottom sediments. Based upon modeling (Section 4), it is expected that 76 percent of external P loads to Lake Carmi will be deposited in the lake bottom sediment after the aluminum treatment. Over time, this deposition will feed the Fe-P pool and eventually Fe-P will return to pre-treatment concentrations. Some of the P that deposits into the lake will form Ca-P and Org-P. Based upon the fractionation data collected for Lake Carmi, 49 percent of the phosphorus in the sediments is Fe-P and this is the best estimate of future partitioning. Organic P decay is estimated at 60 percent and is based upon the change in Org-P from the sediment surface to a depth of 20 cm. From a study by Kaleb, 2022, it is estimated that the age of sediments 20 cm deep is 127 years, and using this an annual estimate of Org-P decay is 56 kilograms per year for a 4 cm depth over the total area of Lake Carmi. The longevity estimate is (1) the difference between the initial and treated Fe-P concentration in the top 4 cm of sediment times the total sediment volume in the top 4 cm, and (2) this value divided by the annual mass of P loading to the sediment. The result of this analysis is a longevity of 31 years based upon new Fe-P formation in Lake Carmi sediment back to pre-treatment conditions. It is more likely, however, that longevity will be limited by the long-term mixing of the aluminum-treated layer by biota. This will cause the aluminum-treated layer to migrate deeper into the sediment while high P sediment will accumulate on the sediment surface. Longevity of properly dosed lakes is consistently approximately 10 years. Although admittedly a wide-ranged longevity estimate, longevity of 10 to 30 years can be expected for the Lake Carmi treatment.

Table 5-2 Inputs used to calculate estimated aluminum treatment longevity.

Condition	Value
Fraction of Inflows Captured by Settling	76
2018 External Loading (kg)	580
Mass P Settling to Sediment In One Year (kg)	441
Mass P Contributed to Fe-P by Org-P Decay in One Year (kg)-4 cm Sediment Depth	56
Org-P Concentration (g P/m^2*1 cm) to 4 cm	0.525
Org-P Estimated Decay (%)	60
Annual Estimated Org-P Contribution to the Fe-P Pool (g P/m^2*1 cm)	0.002
Lake Area (ac)	1,402
Lake Area (m^2)	5,673,894
Volume of 4 cm of sediment (m^2)	226,956
Untreated Fe-P Concentration (g P/m2*1 cm)	0.438
Untreated Fe-P Concentration (g P/m^3)	43.8
Treated Fe-P Concentration (g P/m^3)	10.5
Fraction of Fe-P to TP (sum of fractions) in Sediment	0.49
Mass P (g) to Return to Pre-treatment Concentrations	15,423,728
Time (yrs) to return to pre-treatment conditions	31

5.2 Cost Benefit Analysis

The inputs into the cost benefit analysis are provided in the previous sections (see summary in Table 3-5) but are reproduced here as well as the calculation of cost benefit with aluminum treatment of bottom sediment:

- Estimated Treatment Cost ($)
    - High: $4,327,648
    - Mid (recommended): $2,629,728
    - Low: $4,327,648
- Current Internal P Load (lb):
    - Average of 2018 and 2022: 3,355 (spring to fall)
- Average Internal P Load Removed (lb): 2,369
- Annualized Estimated Treatment Cost ($/year) for Recommended Dose:
    - 10-year longevity: $262,972
    - 20-year longevity: $131,486
    - 30-year longevity: $76,576
- Annualized Cost per Pound of TP Removed ($/lb) for the Recommended Dose:
    - 10-year longevity: $111
    - 20-year longevity: $55
    - 30-year longevity: $37
      44
- Current In-Lake Summer-Average Phosphorus Concentration (µg/L): 34.5 (average of 2018, 2022)
- In-Lake Phosphorus (µg/L) Reduction
    - Average of 2018 and 2022 after treatment: 17.5
    - Change: 34.5-17.5 = 17.0
- Cost Benefit ($/µg/L P Reduction): $154,698

6 Evaluation of Potential Concerns with Inactivation Treatment

There are often several questions that arise prior to the use of aluminum to control internal P loading. There is substantial evidence that aluminum treatments (often called alum treatments) are safe with respect to the protection of aquatic life and human heath (NALMS, 2024), they are effective for a large number of lake systems, and the benefits of the treatments outweigh potential effects thereby resulting in an overall positive ecological outcome. However, it is reasonable and prudent to review and address these concerns. The Vermont Department of Conservation staff identified the concerns below to be addressed as part of this study.

6.1 Potential Impacts on Fish Populations in Lake Carmi

Potential toxicological impacts are being addressed in this section, and potential trophic impacts (i.e., the effect of reduced nutrients on the overall ecological productivity and, hence, reduced food abundance for fish) are evaluated in the subsequent section. It is important to be very deliberate when evaluating and making conclusions about toxicity because toxicity is measured and presented in many ways. There is acute and chronic toxicity. Effects are considered to be acute when the exposure to the toxic chemical is measured in days, typically one to four days. Chronic toxicity has an exposure period of weeks and upwards of two months. Acute is measured by survival. Chronic toxicity can be measured by survival, as well as reproduction, weight gain, and an extensive range of sub-lethal biochemical indicators. With respect to aluminum treatments, acute effects are applicable during the period that the alum floc passes through the water column during treatment. Chronic effects are applicable to the residual amount of aluminum (e.g., colloidal aluminum) that may reside in the water column for a few weeks after treatment.

The U.S. EPA criteria document for aluminum (U.S. EPA, 2018) is the most comprehensive source of aluminum toxicological data for a wide range of aquatic species. The values for acute and chronic criteria provided in this document are driven by the test species most sensitive to aluminum and, hence, the criteria may not be a good indicator of potential risks to fish species. Hence, to evaluate fish species relevant to Lake Carmi, a summary is provided below derived from Table 3 and Table 4 of the U.S. EPA criteria document. The chemical conditions for the Table 3 and Table 4 data are a pH of 7, dissolved organic carbon of 1 mg/L, and hardness of 100 mg/L. It can be expected that with the buffered alum and sodium aluminate treatment, the pH in Lake Carmi will not drop below 7 during treatment. Dissolved organic carbon in Lake Carmi is greater than 1 mg/L, while hardness is less than 100. Hence, the toxicological endpoints in Table 6-1 are relevant to Lake Carmi. For acute toxicity, the mean acute value for the most sensitive species, Atlantic salmon, is 8,642 µg/L (8.642 mg/L). This value is greater than the maximum total aluminum concentration of 4.2 mg/L (Figure 5-1) expected to occur (see discussion regarding these calculations in Section 5) as an instantaneous one-hour average aluminum concentration within the daily treatment area (recommended dosing, no splitting). The average exposure concentration in the daily treatment area is expected to be 1.4 mg/L during the daily treatment period. It should be noted that acute toxicity tests have an exposure period of two to four days, with four days being most typical with fish. The longer the exposure period, the lower the toxicological endpoint (e.g., acute

endpoint such as LC50). Hence, the low exposure period of fish to the alum floc in Lake Carmi during treatment relative to the exposure period used to calculate toxicological thresholds for the toxicity tests provides another level of safety. It can be concluded that there is very low risk of acute toxicity to fish with the proposed aluminum treatment.

Table 6-1 Acute and chronic toxicity endpoints for aluminum and fish provided by the US EPA criteria document for pH 7, dissolved organic carbon of 1 mg/L, and hardness of 100 mg/L

Acute Toxicity		
Genus	**Species**	**Mean Acute Value (µg Al/L)**
Lepomis	Green sunfish, *Lepomis cyanellus*	>31,087
Pimephales	Fathead minnow, *Pimephales promelas*	>22,095
Hybognathus	Rio Grande silvery minnow, *Hybognathus amarus*	>21,779
Salvelinus	Brook trout, *Salvelinus fontinalis*	18,913
Poecilia	Guppy, *Poecilia reticulata*	9,061
Salmo	Atlantic salmon, *Salmo salar*	8,642
Chronic Toxicity		
Genus	**Species**	**Mean Chronic Value (µg Al/L)**
Pimephales	Fathead minnow, *Pimephales promelas*	2,407
Danio	Zebrafish, *Danio rerio*	1,342
Salvelinus	Brook trout, *Salvelinus fontinalis*	638.2
Salmo	Atlantic salmon, *Salmo salar*	434.4

Chronic toxicity values provided in Table 6-1 are relevant to the longer-term exposure period that may occur during the weeks of active treatment and for a few weeks after treatment. Although aluminum is highly insoluble in the pH range 6.3 to just over 7, it can be expected that there will be some residual concentration of colloidal aluminum that will settle out slowly over time (a net apparent settling rate of 74 meters/year has been provided by Pilgrim and Brezonik (2005)). Hence, the residual aluminum may take over a month to settle out. In the same work by Pilgrim and Brezonik (2005), the residual total

aluminum after 16 hours in a settling column dosed with 8 mg/L total aluminum (from liquid alum) ranged from 0.312 mg/L to 0.860 mg/L. Assuming that these concentrations may represent the aluminum residual after treatment, it can be expected that these concentrations will continue to decline, and in approximately four to six weeks, aluminum concentrations will decline to the limits of aluminum solubility given prevailing pH. It is possible that residual aluminum concentrations may approach or be within the range of chronic endpoints for the fish identified in Table 6-1 and Figure 6-5 for a week or two after treatment but will be well below these thresholds within a month after treatment.

It is important to note that chronic toxicity tests for fish are typically conducted on juveniles or younger life stages, which are: (1) notably more sensitive than adults, and (2) found predominately in the spring as spawning predominantly occurs in the spring. Treatment during the fall will reduce risks to fish as the fish will be adults during that period. Finally, even if treatment is conducted in the spring, treatment will occur at depths of 6 meters and greater which is deeper than typical spawning depths.

6.2 Impact of Potential Change in Trophic Status on Fisheries

The intent of this exercise is to assess to what degree the proposed aluminum treatment, which will reduce phosphorus and phytoplankton concentrations, may impact the trophic state of the fishery in Lake Carmi. This analysis was conducted by comparing the trophic state and fisheries conditions for a set of Vermont Lakes and also comparing aluminum-treated lakes for changes in fish populations.

6.2.1 All Lakes

Initially, lakes were selected that had a similar lake surface area to Lake Carmi (1,402 acres). This list was compiled by using the Vermont Official State website Inland Lake Scorecard system (Lake Score Card | Department of Environmental Conservation (vermont.gov)). This website was also used to determine whether walleye, perch, and/or largemouth bass were present in the lakes that were closest in surface area to Lake Carmi. According to this selected dataset, only six lakes have walleye and perch in the state of Vermont. This was too small of a sample size for a statistical analysis. However, the dataset for largemouth bass was acceptable for this analysis given that 12 lakes of similar size had comparable datasets.

The lake score cards were reviewed to summarize available water quality data, as well as lake characteristics. Table 6-2 summarizes the summer average Secchi disk depths and total phosphorus concentrations for the 12 study lakes. It should be noted that the number of sample years varied by waterbody. disk

Table 6-2 Summary of summer average water quality data for the 12 lakes included in the study

Lake Name	Surface Area (acres)	Average Summer Secchi Depth (m)	Average Summer TP (µg/L)
Fairlee	461.8	6.1	16.6
Nivenah	175.6	2.8	11.6
Parker	253.1	3.5	17.8
Hortonia	500.9	5.3	18.8
St. Catherine	885.4	5	15.1
Raponda	123.8	3.4	11.4
Lowell	93.4	4	12.2
Bomoseen	2415.1	7.4	13.2
Morey	549.8	6.6	20
Halls	85.2	4.4	19
Shadow	131.6	5.8	NA
Derby	211.6	3.1	NA

Twelve lakes with bass were found to have fisheries data with similar metrics. Two electrofishing metrics, relative weight and catch per hour, were used for this analysis as there was not enough data on average length or weight for largemouth bass or any other species provided on the Vermont Fish and Wildlife website. Relative weight was used to determine if the fish was in good condition and is calculated by taking the weight of the individual fish and dividing it by the expected or standard weight of a fish with the same length and then multiplying that by 100. Generally, if the weight is above 80%, the fish is healthy, and if it is below 80%, it is considered to be thin. Catch per hour is an indirect way to determine relative species abundance. It is calculated by dividing the total catch by the number of hours fished. This is a metric that is typically examined over time to determine how a population is performing. Therefore, the strongest metric for a correlation study is the relative weight.

Table 6-3 Relative largemouth bass weight and catch per hour for the selected Vermont lake dataset

Lake Name	Relative Weight (Wr)	Catch Per Hour (CPH)
Fairlee	96	35
Nivenah	98.9	4.1
Parker	100	2.7
Hortonia	98.28	86.77
St. Catherine	100.84	29.48
Raponda	99.2	4.3
Lowell	88.8	20.5
Bomoseen	91.7	77.6
Morey	93	45.9
Halls	100	27.9
Shadow	95	NA
Derby	94	56.7

Regression analysis was used to find a correlation between Secchi disk depth and relative weight, Secchi disk depth and catch per hour (CPH), TP and relative weight, and TP and CPH. The linear regression analysis did not show strong correlations (R^2 values) for any of these relationships, with values ranging from 0.03 to 0.4. Based on the data available, the largemouth bass population did not appear to be linearly dependent on Secchi depth or TP concentration (Figure 6-1 and Figure 6-2). However, it can be seen that there was a breakpoint between Secchi depth and relative weight percent at a Secchi disk depth of 5 meters, with a notable decline in relative weight percent thereafter. However, the relative weight percent was stable between approximately 3 meters and 5 meters, suggesting that weights may not be sensitive for Secchi disk depths below 5 meters. It is also notable that with greater Secchi disk depth, greater CPH (Figure 6-2) can be expected.

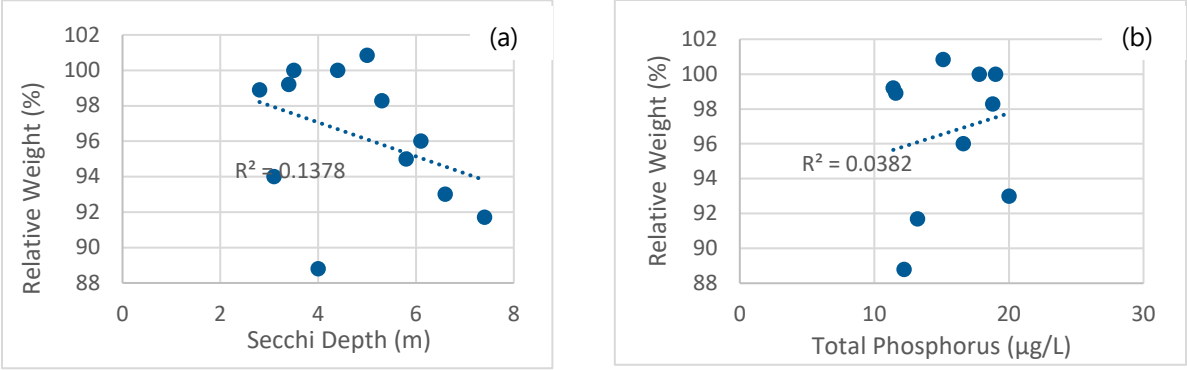

Figure 6-1 Correlation between relative weight and Secchi depth (a) and total phosphorus (b)

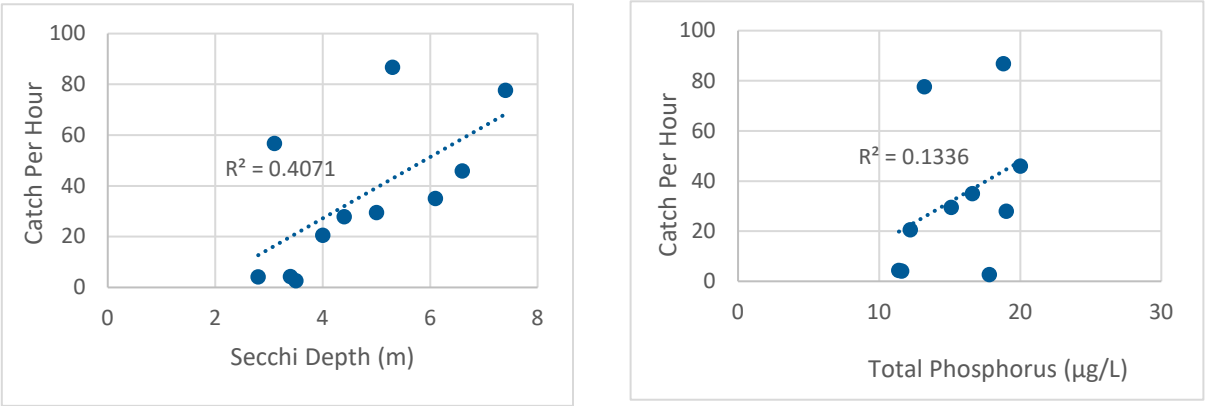

Figure 6-2 Correlation between catch per hour and Secchi depth (a) and total phosphorus (b)

It can be concluded that based upon available bass data for Vermont lakes, the expected changes in Secchi disk depth for Lake Carmi with the proposed aluminum treatment will not affect the trophic condition of fish in the lake. It may, however, improve fishing success by anglers.

6.2.2 Aluminum-treated Lakes

This study focused on three Minnesota lakes that received aluminum treatments: Bde Maka Ska, Lake Harriet, and Bald Eagle Lake (Table 6-4). Bde Maka Ska and Lake Harriet received an aluminum treatment in 2001. Bald Eagle Lake received two aluminum treatments, one in the spring of 2014 and another in the spring of 2016. Bde Maka Ska and Lake Harriet are urban waterbodies, while Bald Eagle Lake is a suburban waterbody.

Table 6-4 Summary of lake characteristics

Lake Name	Surface Area (acres)	Mean Depth (ft)	Maximum Depth (ft)
Bde Maka Ska	419	30	82
Harriet	341	29	87
Bald Eagle	1049	13.3	36

Fisheries data was collected from the Minnesota Department of Natural Resource LakeFinder database (LakeFinder | Minnesota DNR (state.mn.us)). The analysis focused on two fish species, walleye and largemouth bass (LMB). Fisheries data included average weight, average length, and count. Average weight provided the most complete data set. Count was excluded due to potential bias in population numbers because of stocking events that included walleye and LMB in all lakes.

Regression Analysis: Average Weight and Pre- and Post-Aluminum Treatment

Linear regression was used to examine the relationship between average fish weights for both walleye and LMB over a span of years that included equal pre-aluminum treatment years and post-aluminum treatment years. Depending on the available data, the pre- and post-treatment years were selected as close to the aluminum application as possible. Using R-Studio, a Mann-Kendall test was used to determine if there was a significant trend in the fisheries data, and a Welch Two Sample t-test was performed to determine if the average weights were significantly different for pre and post-aluminum treatment.

Regression Analysis: Average Weight and Water Quality

Linear regression was used to examine the relationship between the average fish weight and average total P and Secchi disk depth water quality measurements. Water quality data was obtained from the Minnesota Pollution Control Agency website (Surface Water (state.mn.us)). Regressions compared pre- and post-treatment years and the water quality data. In R-Studio, a Mann-Kendall test was used to determine if there were any trends in water quality data over time, and a Welch Two Sample t-test was performed to determine if the water quality averages were different pre-treatment vs. post-treatment.

Results

Bde Maka Ska results showed no relationship between the average weight of walleye or LMB over a period of 10 years (pre-treatment: 1982, 1987, 1992, 1996, 2000; post-treatment: 2003, 2005, 2009, 2014, 2019). There were no significant trends in average weights of either fish species (Mann-Kendall p-values > 0.050), and there were no differences in average weights between the pre-treatment years and post-treatment years (Table 6-5).

Lake Harriet results showed no relationship between the average weight of the walleye or LMB over a period of six years (pre-treatment: 1984, 1994, 2000; post-treatment: 2003, 2005, 2009). There were no significant trends in average weights of either fish species (Mann-Kendall p-values > 0.050), and there

were no differences in average weights between the pre-treatment years and post-treatment years (T-test p-values > 0.05).

Bald Eagle results showed there was no relationship between the average weight of the walleye or LMB over a period of 12 years (pre-treatment: 2002, 2006, 2008, 2010, 2011, 2012; post-treatment: 2014, 2016, 2017, 2018, 2020, 2022). There were no significant trends in average weights of either fish species (Mann-Kendall p-values >0.05), and there were no differences in average weights between the pre-treatment years and post-treatment years (T-test p-values >0.05).

Table 6-5 Results from average weight of fish species and pre- and post-alum treatment years

Lake	Fish Species	Pre Treatment Mean Weight	Post Treatment Mean Weight	R^2 Value	Mann-Kendall p-value (1)	Welch Two Sample T-test p-value(1)
Bde Maka Ska	Walleye	1.65	2.36	0.1085	0.28	0.18
	LMB	0.55	1.82	0.4626	0.07	0.55
Harriet	Walleye	2.6	2.0	0.114	0.71	0.52
	LMB	0.64	0.51	0.0036	1	0.83
Bald Eagle	Walleye	3.1	2.54	0.0001	1	0.44
	LMB	0.63	0.48	0.015	1	0.55

(1) P-value significance <0.05, *denotes significant value

Bde Maka Ska years were different for the regression analysis between fish weight and water quality due to a gap in water quality data. Walleye analysis was examined for eight years (pre-treatment: 1982, 1992, 200; post-treatment: 2003, 2005, 2009, 2014). Results showed that the average walleye weight was not dependent on average TP or Secchi depth measurements (p-values >0.05). LMB analysis was examined for a different set of eight years (pre-treatment: 1982, 1992, 1996, 2000; post-treatment: 2003, 2005, 2009, 2014). LMB weight varied significantly with a change in TP measurements (p-value < 0.05). As the TP measurements decreased, the weight of the LMB population increased.

Lake Harriet's results showed that the average walleye weight and average LMB weights were not dependent on average TP or Secchi depth measurements (p-values >0.05). The years in this data set were not changed; there were no gaps in water quality data.

Bald Eagle Lake years were different for the regression analysis between fish weight and water quality due to a gap in water quality data, and this study included 10 years (pre-treatment: 2006, 2008, 2010, 2011, 2012, post-treatment: 2014, 2016, 2018, 2020, 2022). Walleye weight and average LMB weights were not dependent on average TP or Secchi depth measurements (p-values >0.05). See Table 6-6 and Table 6-7 for a summary of all results.

Table 6-6 Regression results from average weight of fish species and average total phosphorus (µg/L)

Lake	Fish Species	R^2 Value	Regression p-value [1]
Bde Maka Ska	Walleye	0.33	0.13
	LMB	0.5338	0.04*
Harriet	Walleye	0.3509	0.21
	LMB	0.0783	0.59
Bald Eagle	Walleye	0.3013	0.10
	LMB	0.157	0.26

[1] P-value significance < 0.05, *denotes significant value

Table 6-7 Regression results from average weight of fish species and Secchi depth (m)

Lake	Fish Species	R^2 Value	Regression p-value [1]
Bde Maka Ska	Walleye	0.2918	0.27
	LMB	0.4907	0.12
Harriet	Walleye	0.0283	0.77
	LMB	0.1207	0.49
Bald Eagle	Walleye	0.0000	0.94
	LMB	0.0606	0.49

[1] P-value significance <0.05, *denotes significant value

The same years were used in the regression analysis between the water quality parameters and pre and post treatment years that were used in the average fish weight and water quality parameter regressions. Bde Maka Ska showed a significant difference in TP concentration (T-test p-value < 0.05) but not in Secchi Depth (T-test p-value > 0.05). Lake Harriet did not have any significant changes in water quality parameters between pretreatment and post treatment years (T-test p-values > 0.05). Lake Harriet did not show any statistically significant trends in water quality data (p-value > 0.05). In Bald Eagle Lake, Secchi depth had a significant increasing trend (Mann-Kendall p-value < 0.05). Additionally in Bald Eagle Lake, there were statistically significant differences between pretreatment and post treatment years for both Secchi depth and TP averages (T-test p-values <0.05). All statistical results are displayed in Table 6-8.

Table 6-8 Regression results from water average water quality measurements and pre- and post-alum treatments

Lake	Water Quality Parameter	Pre Treatment Mean	Post Treatment Mean	R^2 Value	Mann-Kendall p-value [(1)]	Welch Two Sample T-test p-value[(1)]
Bde Maka Ska	TP	65.5	31.5	0.0666	0.53	0.05*
	Secchi Depth	2.9	4.7	0.6749	0.06	0.09
Harriet	TP	88.3	71.6	0.0441	0.71	0.47
	Secchi Depth	2.9	4.1	0.3065	0.16	0.11
Bald Eagle	TP	72.6	35.1	0.6001	0.1	0.00*
	Secchi Depth	1.42	2.36	0.6305	0.01*	0.00*

(1) P-value significance <0.05, *denotes significant value

Conclusions

For the lakes evaluated, there is no statistical evidence that the average weight of the walleye or the LMB was changed by an aluminum treatment. Also, there is no statistical evidence that either the walleye or the LMB responds to changes in total phosphorus or Secchi depth water quality measurements. The one statistically significant exception is the LMB population in response to TP. However, the response was favorable to the health of the fish. As TP concentration decreased, the weight of the LMB population increased.

6.3 Effectiveness of Alum Treatment in the Presence of Benthivorous Fish Communities

It is well known that carp dig in lake sediment in search of food, sometimes to depths of up to 25 cm. This can have several effects on nutrient cycling and measures to manage nutrients in lakes. Research has shown that carp can increase the rate of export of nutrients from sediment and that their removal can drastically improve water quality, especially in shallow lakes (Huser et al., 2021). Measures to reduce sediment release can be affected by sediment mixing by carp in several ways. First, the sediment mixing depth increases from approximately 4-6 cm to 15-20 cm, depending on factors like sediment density and the size of carp (Huser et al., 2015). This will not affect an aluminum treatment directly, but it will increase the amount of sediment P that would need to be permanently bound by the aluminum mineral due to increased sediment mixing depth and nutrient availability. On the other hand, the study results above suggest that carp may improve binding efficiency between aluminum and P. This is mainly due to the aging of the aluminum mineral. If the aging (crystallization) process happens before most of the P is bound, the number of binding sites on the mineral decrease, limiting the amount of P that is permanently inactivated by the mineral. Carp can increase the probability that the aluminum mineral contacts P quickly and before aging occurs. This may increase the binding efficiency of the treatment. Overall, carp may facilitate P binding but may also require a higher aluminum dose if it is expected that carp will be active in aluminum-treated zone of the lake sediments. Split dosing is likely a good strategy to assess and compensate for the effects of carp. Aluminum can be applied with follow-up coring to assess the degree

that the carp are dispersing the aluminum in the treated sediment. If there is significant dispersion in the sediment, then a second dose can be targeted to compensate for the observed dispersion and increases in Fe-P in surficial sediments.

6.4 Post-treatment Relationship between Water Clarity and Macrophyte (Aquatic Plant) Growth

Sediment treatment will reduce internal P loading, total phosphorus concentrations, and phytoplankton growth, as well as increase lake clarity (measured as Secchi disk depth). According to the modeling work (Table 4-6 and Table 4-7), Secchi disk depth would have been 2.6 meters in 2018 (increasing from 1.5 meters) and 2.0 meters in 2022 (increasing from 1.3 meters) with aluminum treatment. The effect of increased Secchi disk depth can be assessed using data from a study report by Ray Newman at the University of Minnesota (Newman, R.M., 2018) and data from the Ramsey-Washington Metro Watershed District in Minnesota. These studies reported maximum depth of aquatic plant growth (from point intercept surveys) and Secchi disk depth. Using these data, a relationship was developed between lake clarity as Secchi disk depth and the maximum depth to which aquatic plants can be expected to grow (Figure 6-3).

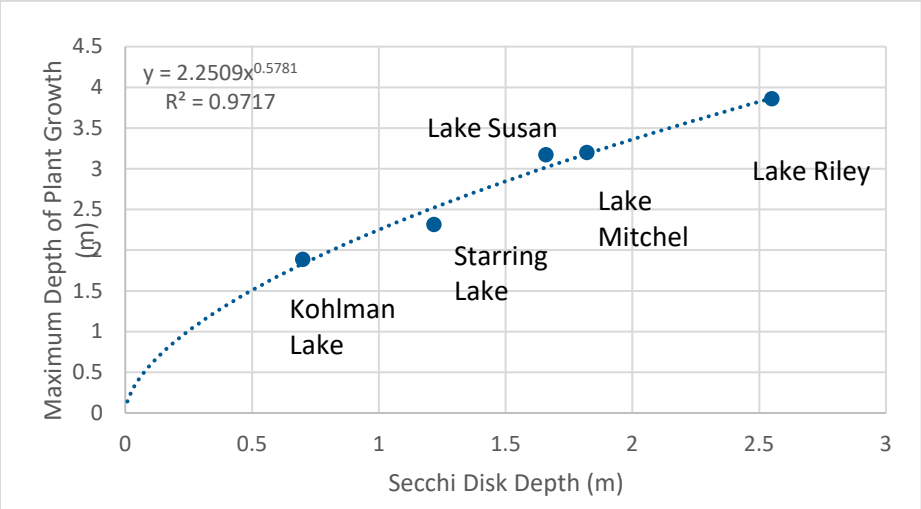

Figure 6-3 Relationship between measured maximum depth of aquatic plant growth and lake clarity measured as Secchi disk depth

Using the relationship provided in Figure 6-5, it can be expected that the maximum depth of aquatic plant growth in Lake Carmi will extend from the current regression estimated depth range of 2.6 to 2.8 meters to upwards of 3.9 meters with internal P load reductions predicted with the recommended aluminum dose. It should be noted that diminished cyanobacteria growth (resulting from reduced phosphorus concentrations) is the primary reason that Secchi disk depths will increase in Lake Carmi. Increased aquatic plant growth will also have additional benefits as the plants will take up phosphorus and nitrogen from the water column, potentially further reducing phytoplankton growth.

6.5 Potential Impacts on Benthic Invertebrate Populations in Lake Carmi

If there are effects on benthic invertebrates with the deposition of aluminum floc on sediments, the effect is physical in nature rather than toxicological. The author of this document has first-hand knowledge of the relative effect of sediments enriched by aluminum compared to sediments covered by a physical barrier of aluminum floc (Pilgrim and Brezonik, 2005). For a wetland that received aluminum floc and aluminum was enriched from approximately 5 milligrams per dry gram of benthic sediment to 20 to 30 milligrams per dry gram of benthic sediment, there was no effect on the benthic invertebrate population compared to the relative population size of the control and the population measured pre-treatment (Pilgrim and Brezonik, 2005). When aluminum floc was enriched for this same system one year later with a pure aluminum floc layer of approximately 30 cm depth there were significant effects on invertebrate populations. The physical effect was apparent with significant gas production, hydrogen sulfide smell, and aquatic invertebrates physically struggling with 30 cm of floc. In contrast, an aluminum treatment at Lake Carmi will be similar to the condition where aluminum enriches sediment rather than creates a physical barrier.

Initially with an aluminum treatment, it can be expected that aluminum floc will accumulate to approximately one to two cm in depth above the sediment surface. This floc will be unconsolidated ("fluffy") and then benthic activity will mix the floc into the sediment. Observation of aquatic invertebrate behavior in microcosm experiments suggests that benthic invertebrates will be responsible for some of the mixing of aluminum floc and sediment. Fish may also enhance mixing. A study by Narf (1990) is one of the most comprehensive studies to evaluate the effect of alum treatments on benthic invertebrates. Benthic invertebrate samples were collected before and after treatment in four alum-treated Wisconsin lakes. In two of the treated lakes (Snake Lake and Horseshoe Lake) there was a clear and notable increase in chironomids and or chaoborus after treatment. In Pickeral Lake, the benthic population a few years after treatment was no different than the pre-treatment population. A number of years after treatment there appeared to have been a significant increase in benthic populations and an increase in diversity. For the fourth lake, Long Lake, the post-treatment benthic population was unchanged compared to pre-treatment. A laboratory study was also conducted as part of the Narf study and at an equivalent aluminum dose of 80 mg/L (greater than 10 times the dose recommended for LakeCarmi), there was an impact on benthic invertebrates likely from trapped gasses such as hydrogen sulfide. Other more recent research appears to also support the conclusion that alum treatments do not affect benthic invertebrates.

6.6 Other Non-target Impacts

We do not expect any non-target impacts. Alum and sodium aluminate will be added at the 6 meter contour and below and the floc will settle to the lake bottom very rapidly. There will not be an opportunity for the chemical to affect riparian aquatic or terrestrial life. Once the floc reaches the lake bottom it will incorporate readily into the sediment and will remain in the sediment.

7 Additional Treatment Considerations

7.1 Site Access Issues

We do not anticipate any site access issues. The boat launch and associated parking lot in the Lake Carmi State Park provides a good location for deploying the barge, staging chemical tanks and re-filling chemical tanks from tanker trucks. It is recognized that this site may not be appropriate during the operating season of the park. If the treatment is in October after the park in closed, this site is likely preferred. Access along highway 120 on the north-west corner of the lake also provides a good site for chemical tank staging. There would be some disturbance to traffic during chemical tank filling but this can be managed with appropriate traffic management. The barge would be deployed at the boat dock for both options.

7.2 Permitting

It is expected that an NPDES permit with aluminum limits and monitoring requirements will be issued for the aluminum treatment. If limits are established from the CMC and CCC, then it will be necessary to either split the dose and apply alum and sodium aluminate in two passes or in subsequent years.

7.3 Lake Size Interaction with Treatment

We do not expect lake size to affect the proposed aluminum treatment. The recommended treatment depth is below the lake surface by 6 meters and greater and propagation of wave effects below this depth is not likely. Furthermore, sediment core data show that Fe-P is enriched in the top four to six cm of lake sediment indicating that disturbance of the sediment at the planned depths is not significant (if there was significant disturbance, the Fe-P profile would be equal (mixed) from the sediment surface and deeper).

7.4 Alternatives Analysis

Alternatives such as dredging and hydrogen peroxide treatment are not feasible or practical for Lake Carmi. Dredging is prohibitively expensive and the benefits unproven. For example, for the Shell Rock Watershed District in Minnesota, the plan is to spend 17 million dollars to dredge 1.2 million cubic yards of sediment in Fountain Lake (Factsheet-2020_Senate_Bonding_Tour.pdf (shellrock.org)). Given the depth of phosphorus enrichment in Lake Carmi, a dredging depth of at least 20 cm or greater would be required. The dredging volume would be at a minimum 0.8 million cubic yards (dredging area of 775 acres) and using the cost for Fountain Lake, the minimal cost to dredge Lake Carmi would be 11 million dollars. It would very likely be much more as the actual dredging depth to prevent internal P loading could be as deep as a meter or more (Proceedings of the 2017 Dredging Summit and Expo (westerndredging.org). Besides the cost, multiple years may be needed to dredge the large sediment volume required and there would be an ongoing disturbance to recreational users during dredging. Given the even distribution of phosphorus across the Lake Carmi bottom, selective dredging would have no perceivable benefit to the lake as internal loading would only be proportionately reduced (if successful) by a fraction of the area dredged compared to the total area releasing P.

An attempt to time a whole lake hydrogen peroxide treatment for a lake the size of Lake Cami would be impractical (see lake size recommendations in https://hcb-1.itrcweb.org/peroxide-application/). Several tanker trucks of chemical would be required to conduct the treatment and mobilizing a large volume of chemical requires planning, and a quick mobilization to capture a bloom seems unlikely. Several simultaneously operating treatment barges would be needed to execute the treatment in a timely manner. After treatment the dead algae would sink to the sediments, further enriching the sediment. The problem is not solved with hydrogen peroxide treatment but rather is perpetuated. The cost to conduct such a large treatment is not known and it is not clear if there is a contractor capable of executing such a large treatment.

7.5 Post project monitoring

The following post-project monitoring and analysis is recommended at the surface, mid-depth, and near bottom (1 meter off the bottom) at one location in the lake: (1) total aluminum, total phosphorus, dissolved organic carbon, hardness, and pH, (2) standard profile measurements (1-meter increment) of dissolved oxygen, temperature, and specific conductance, (3) 2-meter surface composite sample for chlorophyll *a* sample and for phytoplankton species (can be fluoroprobe to identify groups rather than genus and species), and (4) Secchi disk depth.

Sediment coring 1, 3 ,and 5 years after treatment is recommended. Each event should include a total of 10 cores with sediment slices collected at 1 cm increments up to 10 cms depth and 2 cm increments up to 20 cms depth. Analysis should include Fe-P, Al-P, and NaOH extractable aluminum.

7.6 Impact of Sulfur Dynamics

The application of alum will add sulfate to the water column. The lake-wide sulfate concentration after treatment will be 20 mg/L with the recommended dose if the dose is not split. Because sulfate is instantly soluble upon application of alum, sulfate will be predominantly in the completely mixed layer. Sulfate will be lost as the lake flushes out and the surface waters with higher sulfate will flush out first. Eventually the lake will mix completely with fall or spring turnover and sulfate will be in contact with bottom sediments. Reducing conditions in bottom sediments will transform sulfate to sulfide. Fortunately, the Lake Carmi bottom sediments are enriched with iron and it can be expected that the ultimate repository for sulfate will be as an iron sulfide mineral in the bottom sediments.

7.7 Future Use of Aeration System

The aeration system will not be needed after the aluminum treatment (it should be removed prior to treatment to avoid disturbing the treatment with removal of the tubing and aerations heads). The aluminum treatment will increase lake clarity and as such light will penetrate to greater depths. This will have two effects: (1) the mixed layer will become deeper, and (2) photosynthesis will occur at greater depths. These effects have been demonstrated for several aluminum-treated lakes. The outcome is that oxygen will increase throughout the water column. Over time, the reduction in the phytoplankton population will also reduce the deposition of organic carbon (dead phytoplankton) onto the lake bottom sediments. This will reduce sediment oxygen demand over time.

7.8 Tributary Phosphorus Inactivation Application Effectiveness and Cost

The potential benefit and cost of installing an inflow alum treatment facility at the terminus of watershed LC10 was evaluated. Watershed LC10 (see Figure 4-4) is the largest subwatershed to Lake Carmi and likely the best location to site a treatment facility as there is access and potentially available state land. Based upon monitoring data at the Tanner's Lake alum treatment facility (https://rwmwd.org/projects/tanners-lake-alum-treatment-facility), it is expected that 50 percent of the phosphorus loads can be removed by such a facility given the prevailing total phosphorus concentrations of LC10. These systems need to be operated during the warm weather months (flocculation is poor in cold weather and concentrated alum can crystalize under cold conditions) and hence the load reduction was assumed to occur during the period that the Barr Lake Model was run (May 11 to October 2). This is also when tributary data were available for the analysis. The basis for the cost estimate is a proposed treatment system in Prior Lake, Minnesota (FINAL-Buck-Lake-Feasibility-Study-Report-Barr-Engineering.pdf (plslwd.org)). This system consists of a diversion weir, pumps, a treatment building, chemical holding tanks, and chemical feed pump, and a floc pond. The cost includes annual operating and maintenance cost. A significant cost of the facility is disposal of accumulated alum floc in the floc pond.

The results of the cost benefit analysis are provided in Table 7-1. It can be seen that the cost per pound of P removed at $6,300 is high for a BMP. This is largely a function of the generally low concentration of phosphorus in Marsh Brook. The low concentration reduces treatment efficiency and also the mass of P removed with treatment. These types of systems are generally more cost effective when the treated water has high P.

Table 7-1 Cost benefit of the inflow alum treatment system located at watershed LC10

Location	BMP Average GS TP Removal (lbs/GS)	Concept Design Construction/ Engineering Cost Estimate	Planning Level Cost Estimate Range (-30% to +50%)	Estimated Annual Maintenance Cost	Estimated Annualized Cost	Annualized Cost per Pound TP Removed during GS	Estimated Project Life (years)
Alum Treatment Facility	73	$1,821,000	$1275000 - $2732000	$341,000	$463,000.00	$6,300.00	20

8 Findings, Conclusions and Recommendations

There are several findings, conclusions and recommendations that have been developed as part of this study:

Findings

- Operation of the aerator has not reduced the mass of internal P loading to Lake Carmi.
    - Without Aeration: Internal P loading in 2018 from May 8 to October 2 was 3,073 pounds
    - With Aeration: Internal P loading in 2022 from May 8 to October 2 was 3,638 pounds
- Current cyanobacteria blooms are largely a consequence of internal P loading and nitrogen limiting conditions. Nitrogen fixing cyanobacteria are contributing significantly to the nitrogen pool in Lake Carmi.
- From modeling and experimental data, internal P loading is 71 percent of the total P loads to Lake Carmi.

Conclusions

- Internal P loading control is the most cost-effective method to improve Lake Carmi clarity and significantly reduce cyanobacteria blooms.
- Additional watershed controls alone will not result in measurable improvements in lake water quality. Continued watershed control will extend the life of the aluminum treatment.
- Dredging and construction and operation of an inflow alum treatment facility are not cost effective approaches to improve Lake Carmi clarity and water quality. Hydrogen peroxide treatment would be impractical for a lake the size of Lake Carmi.
- Implementation of an aluminum treatment for internal load control will result in the following estimated water quality improvements:

Modeled Summer Average Concentrations - µg/L (June 1 - Sept 30)			Estimated Secchi Disk (m)
Scenario	Total Phosphorus	Chlorophyll-a	
Calibrated Existing Conditions (2018)	31	24	1.5
Sediment Treatment, Aluminum (2018)	15	7	2.6

- Implementation of an aluminum treatment will also result in a more balanced population of diatoms, green algae, and cyanobacteria.
- Macrophytes (natives and invasives) can be expected to grow deeper (estimated maximum depth of growth of 3.9 meters) with the application.
- It is expected that the aluminum treatment will last from 10 to 30 years.

Recommendations

- The recommended aluminum dose is 67 g/m^2
- Treatment should be conducted for the lake area corresponding to 6 meters depth and greater. The total treatment area is 775 acres.
- Treatment should occur as a volumetric 2 to 1 mixture of alum and sodium aluminate.
- There may be some marginal benefits of splitting the dose into two different treatment years but splitting the dose is not a recommendation.
- A "double pass" approach may be necessary to meet applicable in-lake acute and chronic water quality criteria for aluminum.
- The opinion of probable cost to conduct the treatment is $2,629,728. However, this cost will be greater if "double pass" treatment approach is required to comply with permit conditions.

9 References

Canfield, D., & Bachmann, R. W. (1981). Prediction of Total Phosphorus Concentrations, Chlorophyll a, and Secchi Depths in Natural and Artificial Lakes. *Canadian Journal of Fisheries and Aquatic Sciences 38(4)*, 414-423.

Gomez and Sullivan Engineers. (2018). *Lake Carmi Dam - Hydrologic, Hydraulic, and Alternative Analyses*. Prepared for Vermont Department of Environmental Conservation.

Gorczyca, B. and J. Ganczarczyk. (2001). Fractal Analysis of Pore Distributions in Alum Coagulation and Activated Sludge Flocs. *Water Quality Research Journal of Canada, 36*(10.2166/wqrj.2001.036.).

Huser, B.J., Bajer, P.G., Kittelson, S., Christenson, S. and Menken, K., 2021. Changes to water quality and sediment phosphorus forms in a shallow, eutrophic lake after removal of common carp (Cyprinus carpio). Inland Waters, pp.1-14.

Huser, B. J., P. G. Bajer, C. J. Chizinski, P. W. Sorensen. (2015). Effects of common carp (Cyprinus carpio) on sediment mixing depth and phosphorus availability in a shallow lake. Hydrobiologia. 763: 23-33

Jones, Kaleb, "A paleolimnological analysis of lake sediments in northern and central Vermont" (2022). Graduate College Dissertations and Theses. 1581.

NALMS. (2024). *The Use of Alum for Lake Management*. Retrieved March 23, 2024, from North American Lake Management Society: https://www.nalms.org/nalms-position-papers/the-use-of-alum-for-lake-management/#:~:text=NALMS%20Positions,with%20toxicity%20to%20aquatic%20life

Narf, Richard P. (1990). Interactions of Chironomidae and Chaoboridae (Diptera) with Aluminum Sulfate Treated Lake Sediments. *Lake and Reservoir Management* 6 (1990): 33-42.

Newman, R.M. (2018). *Aquatic Plant Community of Lakes Lucy, Mitchell, Susan, Riley and Staring within the Riley Purgatory Bluff Creek Watershed: Final Report for 2015-2017.* Retrieved March 23, 2024, from https://rpbcwd.org/application/files/5516/3105/5141/2017_RPBCWDPlantFinalReport.pdf

Pilgrim, K.M. and P.L. Brezonik. (2005). Evaluation of the potential adverse impacts of lake inflow treatment with alum. *Lake and Reservoir Management, 21(1):78-88*.

Pilgrim, Keith & Huser, Brian & Brezonik, Patrick. (2007). A method for comparative evaluation of whole-lake and inflow alum treatment. Water research. 41. 1215-24. 10.1016/j.watres.2006.12.025.

Psenner, Roland & Boström, Bengt & Dinka, M. & Pettersson, Kurt & Puckso, R.. (1988). Fractionation of phosphorus in suspended matter and sediment. Arch Hydrobiol Beih Ergeb Limnol. 30. 98-103.

State of Vermont. (2023). *Vermont Open Geodata Portal*. Retrieved from https://geodata.vermont.gov/

Steinman AD, Ogdahl ME. (2012) Macroinvertebrate response and internal phosphorus loading in a Michigan Lake after alum treatment. J Environ Qual. 2012 Sep-Oct;41(5):1540-8.

Stroud Water Research Center. (n.d.). *Model My Watershed*. Retrieved from https://modelmywatershed.org/

U.S. EPA. (2018). *Final Aquatic Life Ambient Water Quality Criteria For Aluminum 2018, EPA-822-R-18-001*.

Vermont Agency of Natural Resources. (2008). Phosphorus Total Maximum Daily Load (TMDL) for Lake Carmi (Waterbody VT05-02L01).

Walker, W. W. (1996 (updated 1999)). Simplified Procedures for Eutrophication Assessment & Prediction: User Manual Instruction Report W-96-2. *USAE Waterways Experiment Station*.

White, David & Miller, MF. (2010). Benthic invertebrate activity in lakes: Linking present and historical bioturbation patterns. Aquatic Biology - AQUAT BIOL. 2. 269-277. 10.3354/ab00056.

Appendix A

Wind Rose Plots

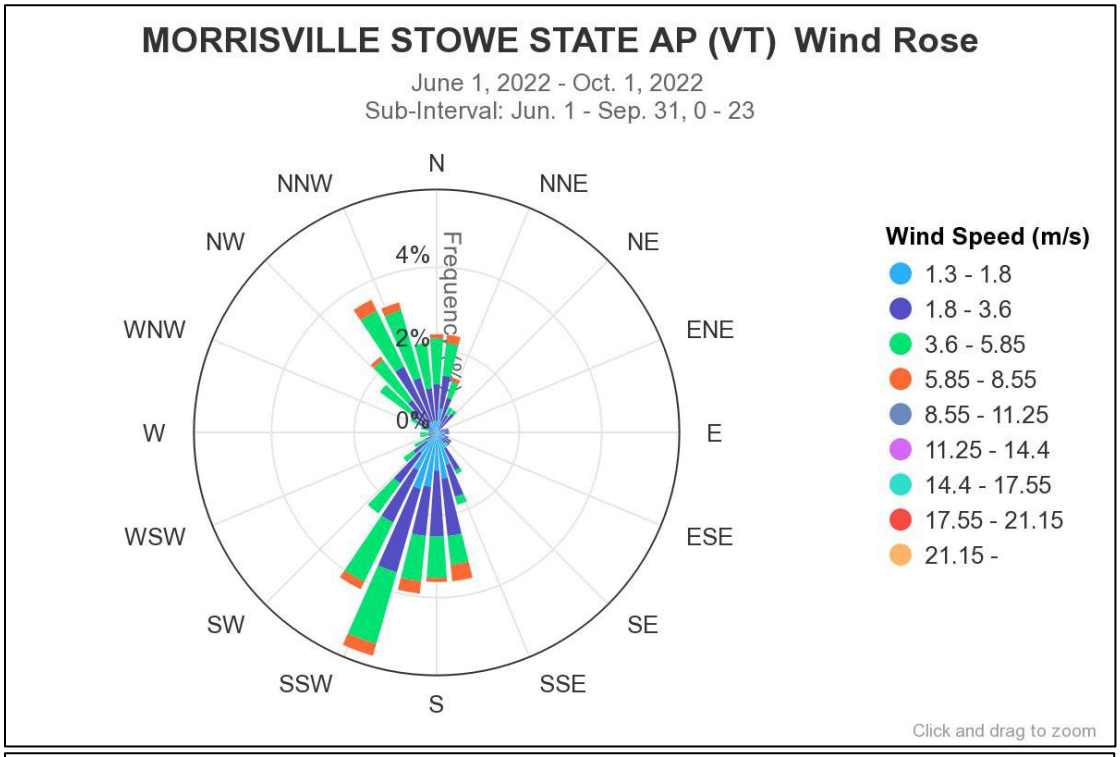
MORRISVILLE STOWE STATE AP (VT) Wind Rose
June 1, 2022 - Oct. 1, 2022
Sub-Interval: Jun. 1 - Sep. 31, 0 - 23
N
NNE
NE
ENE
E
ESE
SE
SSE
S
SSW
SW
WSW
W
WNW
NW
NNW
4%
2%
0%
Frequency (%)
Wind Speed (m/s)
1.3 - 1.8
1.8 - 3.6
3.6 - 5.85
5.85 - 8.55
8.55 - 11.25
11.25 - 14.4
14.4 - 17.55
17.55 - 21.15
21.15 -
Click and drag to zoom

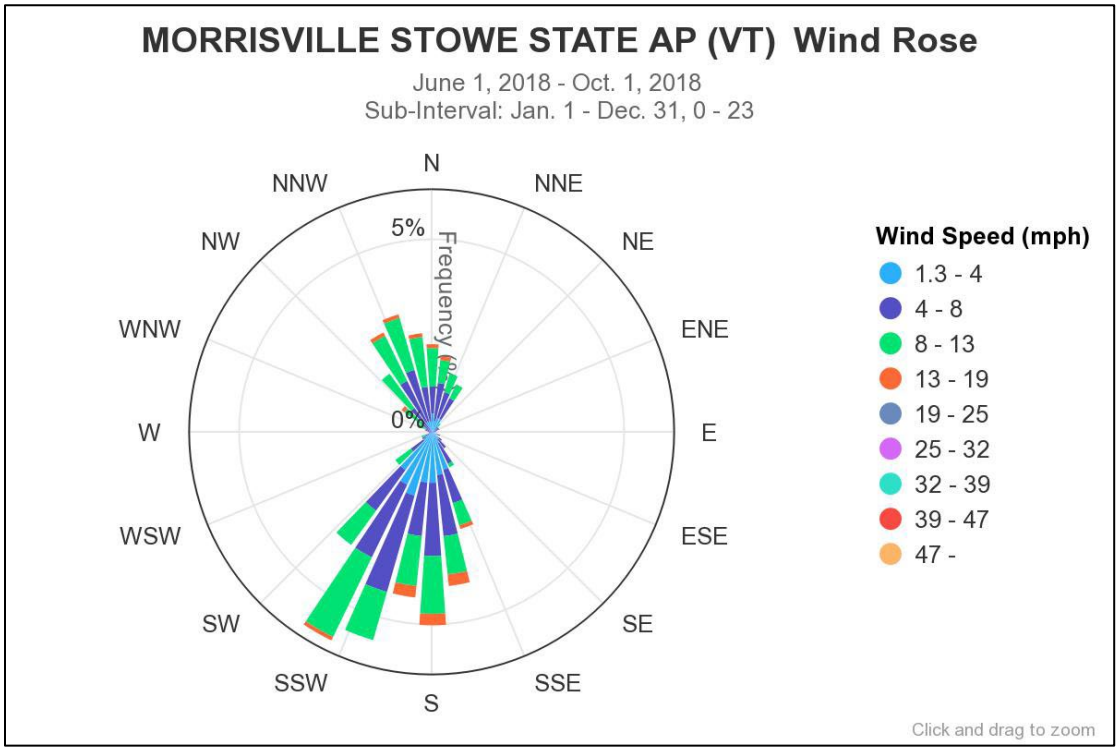
MORRISVILLE STOWE STATE AP (VT) Wind Rose
June 1, 2018 - Oct. 1, 2018
Sub-Interval: Jan. 1 - Dec. 31, 0 - 23
N
NNE
NE
ENE
E
ESE
SE
SSE
S
SSW
SW
WSW
W
WNW
NW
NNW
5%
0%
Frequency (%)
Wind Speed (mph)
1.3 - 4
4 - 8
8 - 13
13 - 19
19 - 25
25 - 32
32 - 39
39 - 47
47 -
Click and drag to zoom

Appendix B

Temperature Profiles

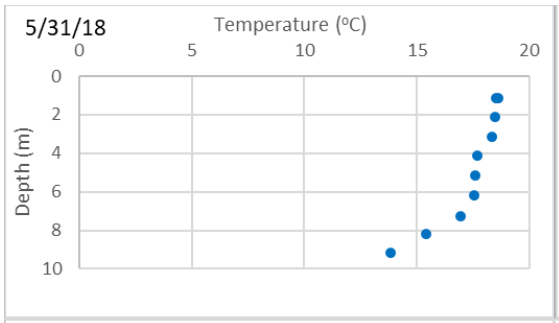
5/31/18
Temperature (°C)
0 5 10 15 20
Depth (m)
0 2 4 6 8 10

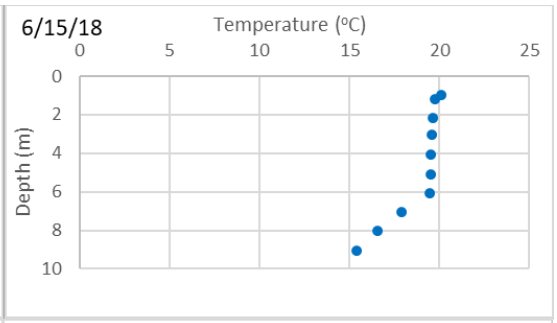
6/15/18
Temperature (°C)
0 5 10 15 20 25
Depth (m)
0 2 4 6 8 10

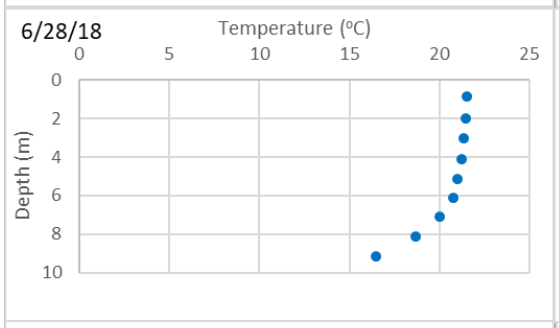
6/28/18
Temperature (°C)
0 5 10 15 20 25
Depth (m)
0 2 4 6 8 10

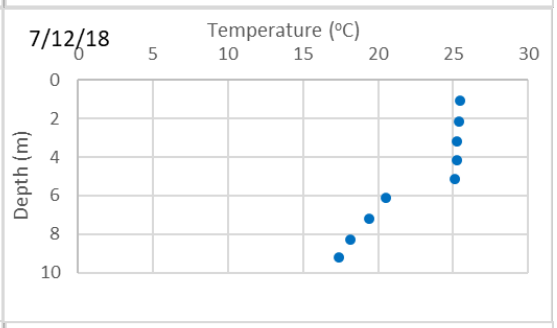
7/12/18
Temperature (°C)
0 5 10 15 20 25 30
Depth (m)
0 2 4 6 8 10

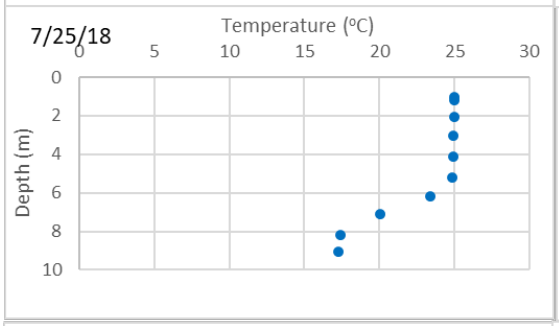
7/25/18
Temperature (°C)
0 5 10 15 20 25 30
Depth (m)
0 2 4 6 8 10

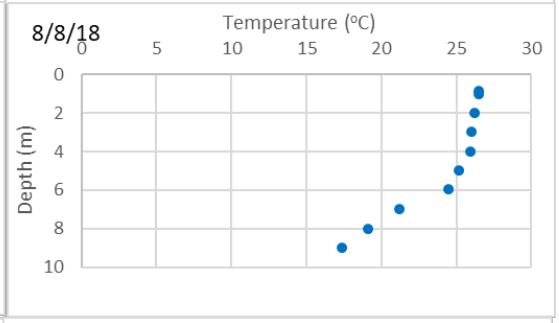
8/8/18
Temperature (°C)
0 5 10 15 20 25 30
Depth (m)
0 2 4 6 8 10

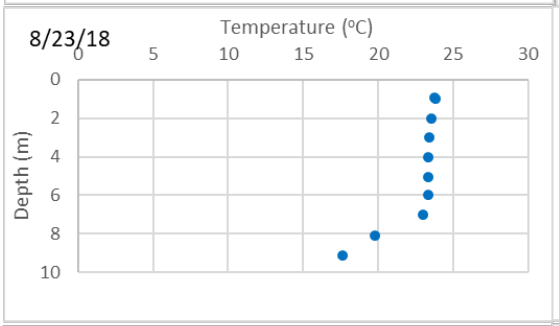
8/23/18
Temperature (°C)
0 5 10 15 20 25 30
Depth (m)
0 2 4 6 8 10

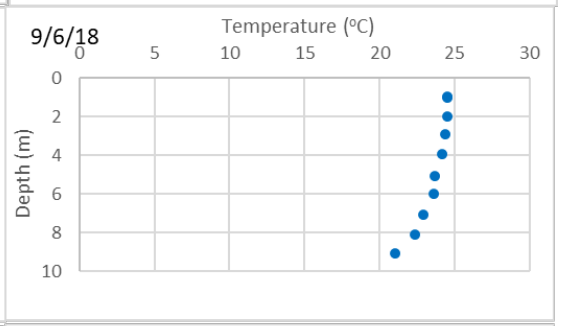
9/6/18
Temperature (°C)
0 5 10 15 20 25 30
Depth (m)
0 2 4 6 8 10

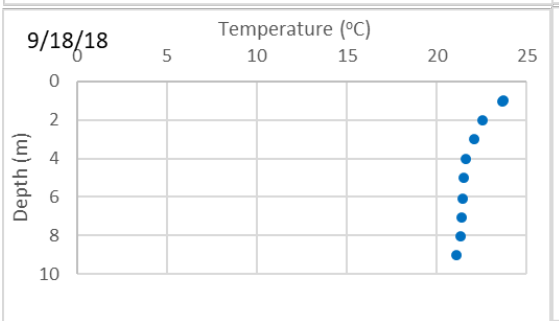
9/18/18
Temperature (°C)
0 5 10 15 20 25
Depth (m)
0 2 4 6 8 10

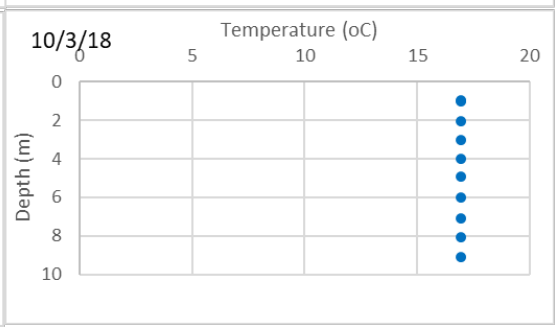
10/3/18
Temperature (oC)
0 5 10 15 20
Depth (m)
0 2 4 6 8 10

Appendix C

Temperature Profiles

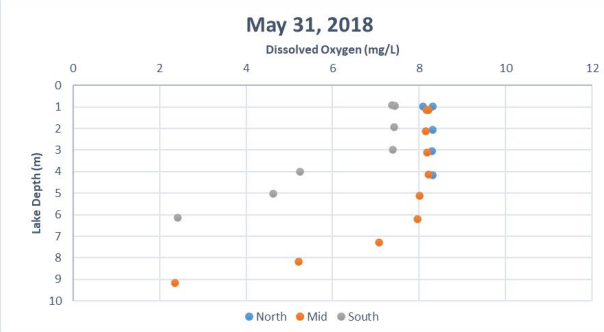
May 31, 2018
Dissolved Oxygen (mg/L)
Lake Depth (m)
North Mid South

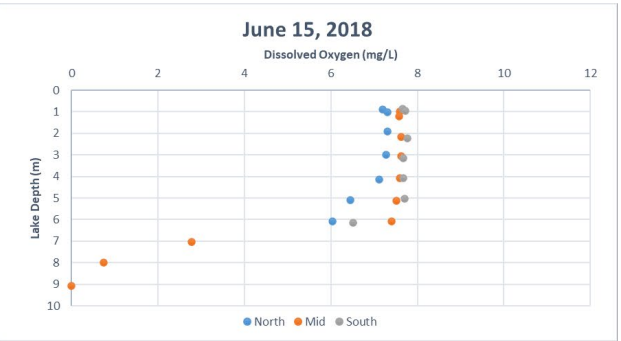
June 15, 2018
Dissolved Oxygen (mg/L)
Lake Depth (m)
North Mid South

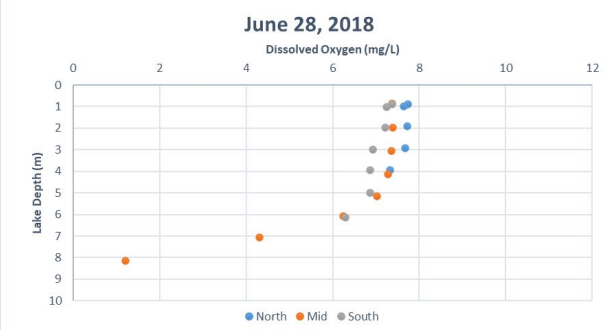
June 28, 2018
Dissolved Oxygen (mg/L)
Lake Depth (m)
North Mid South

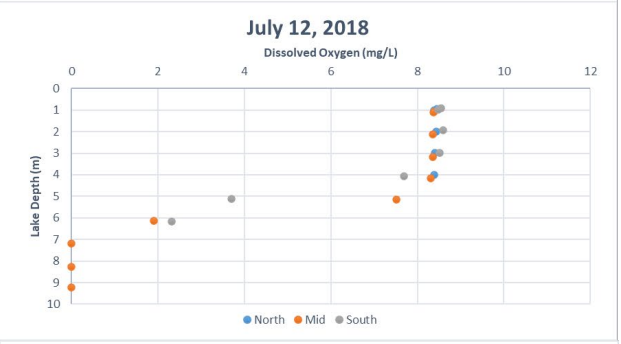
July 12, 2018
Dissolved Oxygen (mg/L)
Lake Depth (m)
North Mid South

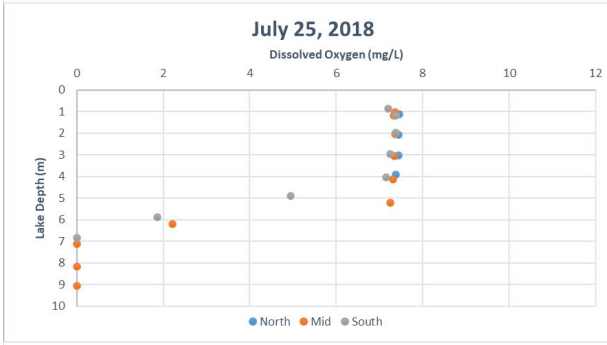
July 25, 2018
Dissolved Oxygen (mg/L)
Lake Depth (m)
North Mid South

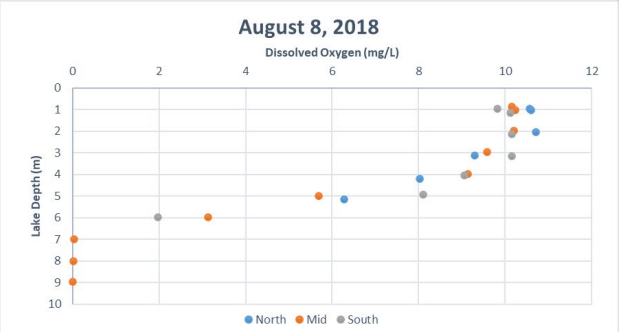
August 8, 2018
Dissolved Oxygen (mg/L)
Lake Depth (m)
North Mid South

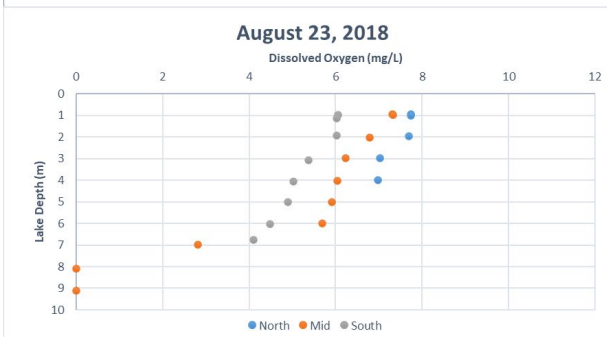
August 23, 2018
Dissolved Oxygen (mg/L)
Lake Depth (m)
North Mid South

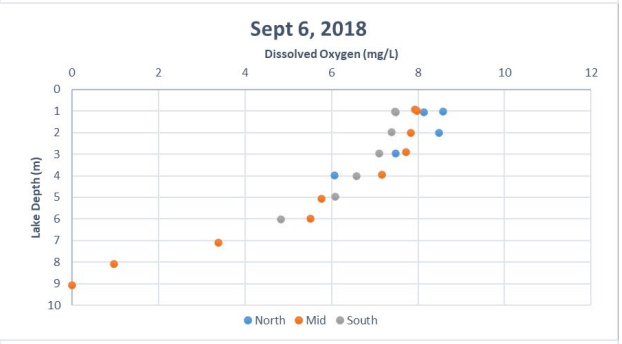
Sept 6, 2018
Dissolved Oxygen (mg/L)
Lake Depth (m)
North Mid South

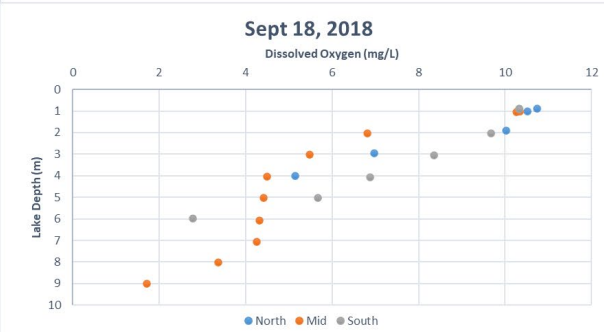
Sept 18, 2018
Dissolved Oxygen (mg/L)
Lake Depth (m)
North Mid South


Oct 3, 2018
Dissolved Oxygen (mg/L)
Lake Depth (m)
North Mid South

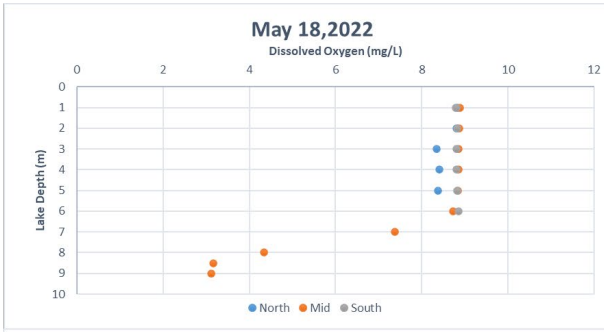
May 18,2022
Dissolved Oxygen (mg/L)
Lake Depth (m)
North Mid South

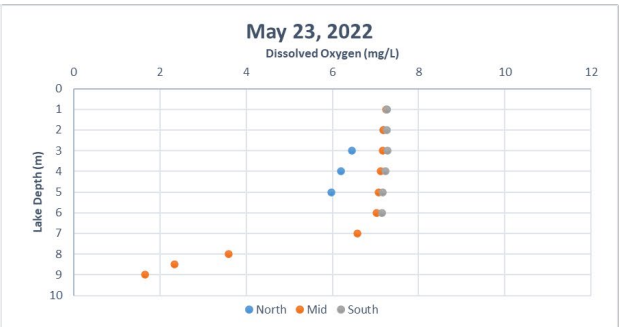
May 23, 2022
Dissolved Oxygen (mg/L)
Lake Depth (m)
North Mid South

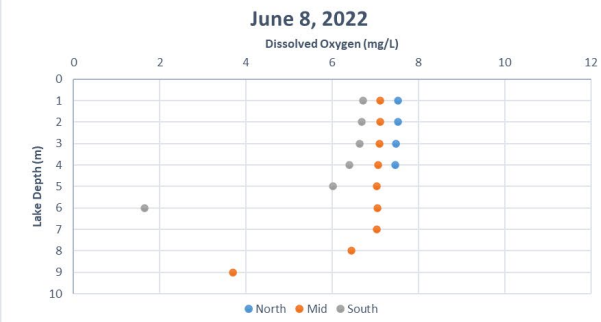
June 8, 2022
Dissolved Oxygen (mg/L)
Lake Depth (m)
North Mid South

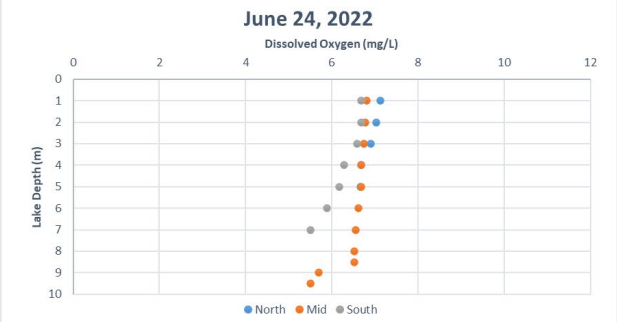
June 24, 2022
Dissolved Oxygen (mg/L)
Lake Depth (m)
North Mid South


July 6, 2022
Dissolved Oxygen (mg/L)
Lake Depth (m)
North Mid South

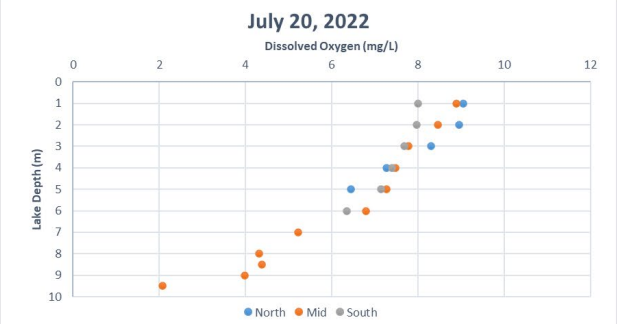
July 20, 2022
Dissolved Oxygen (mg/L)
Lake Depth (m)
North Mid South

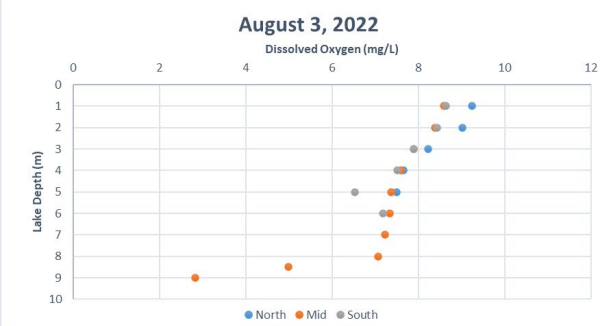
August 3, 2022
Dissolved Oxygen (mg/L)
Lake Depth (m)
North Mid South

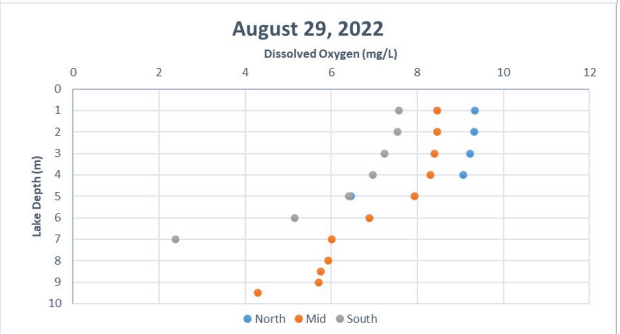
August 29, 2022
Dissolved Oxygen (mg/L)
Lake Depth (m)
North Mid South

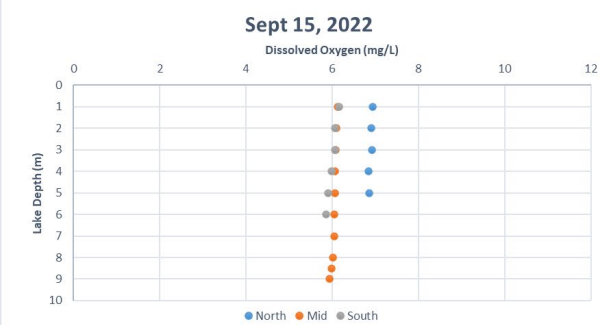
Sept 15, 2022
Dissolved Oxygen (mg/L)
Lake Depth (m)
North Mid South


Sept 29, 2022
Dissolved Oxygen (mg/L)
Lake Depth (m)
North Mid South

Appendix D

Phosphorus Fractionation Results

Core	Interval (cm)		mg P or metal / g wet sediment							mg P / g dry sediment						
			Lossely Sorbed-P	Fe-P	Al-P	Org-P	Ca-P	Total Fe Extract	Total Al Extract	Lossely Sorbed-P	Fe-P	Al-P	Org-P	Ca-P	Total Fe Extract	Total Al Extract
Ex1	0	4	---	0.0570	0.0023	0.0512	0.0226	---	---	---	0.911	0.037	0.819	0.361	---	---
Ex2	0	4	---	0.0548	0.0023	0.0511	0.0232	---	---	---	0.850	0.036	0.792	0.360	---	---
Ex3	0	4	---	0.0296	0.0017	0.0499	0.0313	---	---	---	0.357	0.020	0.603	0.379	---	---
Ex4	0	4	---	0.0526	0.0054	0.0551	0.0340	---	---	---	0.620	0.063	0.650	0.401	---	---
Ex5	0	4	---	0.0453	0.0047	0.0537	0.0684	---	---	---	0.303	0.031	0.359	0.456	---	---
Ex6	0	4	---	0.0389	0.0058	0.0502	0.0715	---	---	---	0.282	0.042	0.365	0.519	---	---
SC1	0	2	0.0000	0.0282	0.0020	0.0509	0.0483	0.8905	0.1349	0.000	0.279	0.020	0.503	0.477	8.801	1.333
SC1	2	4	0.0000	0.0327	0.0038	0.0571	0.0749	---	---	0.000	0.231	0.026	0.403	0.529	---	---
SC1	4	6	0.0000	0.0690	0.0141	0.0568	0.0857	1.5121	0.1879	0.000	0.407	0.083	0.335	0.505	8.912	1.108
SC1	6	8	0.0000	0.0666	0.0304	0.0612	0.0995	---	---	0.000	0.361	0.165	0.332	0.539	---	---
SC1	8	10	0.0000	0.0671	0.0369	0.0594	0.1157	1.5137	0.1905	0.000	0.358	0.197	0.317	0.617	8.069	1.016
SC1	13	15	---	0.0251	0.0234	0.0533	0.1443	---	---	---	0.108	0.100	0.229	0.620	---	---
SC1	18	20	---	0.0172	0.0060	0.0346	0.1511	0.7868	0.2522	---	0.065	0.023	0.131	0.572	2.978	0.955
SC1 DUP	0	2	---	0.0312	0.0026	0.0506	0.0493	---	---	---	0.309	0.025	0.500	0.488	---	---
SC2	0	2	0.0052	0.0547	0.0027	0.0520	0.0288	0.8415	0.1258	0.074	0.789	0.039	0.751	0.415	12.142	1.815
SC2	2	4	0.0035	0.0511	0.0024	0.0541	0.0350	---	---	0.041	0.597	0.028	0.632	0.409	---	---
SC2	4	6	0.0023	0.0467	0.0027	0.0605	0.0434	0.8155	0.1958	0.023	0.460	0.026	0.596	0.427	8.031	1.929
SC2	6	8	0.0000	0.0392	0.0030	0.0595	0.0477	---	---	0.000	0.354	0.027	0.538	0.431	---	---
SC2	8	10	0.0000	0.0424	0.0106	0.0702	0.0516	0.8393	0.2214	0.000	0.349	0.087	0.577	0.424	6.896	1.820
SC2	13	15	---	0.0215	0.0028	0.0559	0.0718	---	---	---	0.157	0.020	0.407	0.524	---	---
SC2	18	20	---	0.0111	0.0030	0.0551	0.0776	0.4573	0.2667	---	0.067	0.018	0.332	0.467	2.753	1.605
SC3	0	2	0.0018	0.0300	0.0017	0.0455	0.0218	0.6140	0.1056	0.028	0.476	0.026	0.721	0.346	9.730	1.674
SC3	2	4	0.0023	0.0420	0.0022	0.0632	0.0374	---	---	0.025	0.460	0.024	0.692	0.409	---	---
SC3	4	6	0.0035	0.0395	0.0017	0.0538	0.0327	0.6601	0.1549	0.041	0.462	0.019	0.630	0.383	7.729	1.814
SC3	6	8	0.0000	0.0206	0.0015	0.0565	0.0401	---	---	0.000	0.219	0.015	0.598	0.425	---	---
SC3	8	10	0.0000	0.0178	0.0021	0.0666	0.0487	0.6139	0.2350	0.000	0.166	0.020	0.624	0.456	5.751	2.201
SC3	13	15	---	0.0116	0.0019	0.0562	0.0518	---	---	---	0.098	0.016	0.472	0.435	---	---
SC3	18	20	---	0.0087	0.0018	0.0505	0.0576	0.4138	0.2482	---	0.067	0.014	0.388	0.442	3.178	1.906
SC4	0	2	0.0030	0.0255	0.0009	0.0409	0.0215	0.5259	0.1129	0.050	0.431	0.015	0.691	0.363	8.884	1.906
SC4	2	4	0.0034	0.0345	0.0009	0.0520	0.0258	---	---	0.046	0.469	0.013	0.708	0.351	---	---
SC4	4	6	0.0040	0.0238	0.0011	0.0498	0.0316	0.5230	0.1745	0.043	0.257	0.012	0.537	0.341	5.645	1.883
SC4	6	8	0.0000	0.0205	0.0007	0.0482	0.0402	---	---	0.000	0.188	0.007	0.442	0.369	---	---
SC4	8	10	0.0000	0.0155	0.0008	0.0480	0.0465	0.5222	0.2122	0.000	0.135	0.007	0.417	0.404	4.537	1.844
SC4	13	15	---	0.0100	0.0007	0.0477	0.0500	---	---	---	0.077	0.005	0.365	0.383	---	---
SC4	18	20	---	0.0085	0.0013	0.0470	0.0573	0.3054	0.2600	---	0.059	0.009	0.326	0.397	2.118	1.803

Core	Interval (cm)		mg P or metal / g wet sediment							mg P / g dry sediment						
			Lossely Sorbed-P	Fe-P	Al-P	Org-P	Ca-P	Total Fe Extract	Total Al Extract	Lossely Sorbed-P	Fe-P	Al-P	Org-P	Ca-P	Total Fe Extract	Total Al Extract
SC5	0	2	0.0022	0.0583	0.0021	0.0504	0.0490	1.0455	0.1506	0.020	0.534	0.019	0.462	0.448	9.573	1.379
SC5	2	4	0.0000	0.0667	0.0031	0.0600	0.0641	---	---	0.000	0.534	0.025	0.480	0.513	---	---
SC5	4	6	0.0000	0.0537	0.0031	0.0587	0.0769	1.0072	0.1814	0.000	0.301	0.017	0.329	0.430	5.635	1.015
SC5	6	8	0.0000	0.0622	0.0082	0.0633	0.0998	---	---	0.000	0.288	0.038	0.293	0.461	---	---
SC5	8	10	0.0000	0.0455	0.0148	0.0611	0.1279	0.9822	0.2142	0.000	0.188	0.061	0.252	0.529	4.060	0.885
SC5	13	15	---	0.1024	0.0367	0.0590	0.1617	---	---	---	0.280	0.100	0.161	0.442	---	---
SC5	18	20	---	0.0128	0.0029	0.0331	0.1580	0.5459	0.2935	---	0.047	0.010	0.120	0.574	1.983	1.066
SC6	0	2	0.0045	0.0398	0.0009	0.0428	0.0212	0.5650	0.1122	0.076	0.679	0.016	0.729	0.362	9.636	1.914
SC6	2	4	0.0034	0.0348	0.0014	0.0456	0.0273	---	---	0.043	0.438	0.018	0.573	0.344	---	---
SC6	4	6	0.0115	0.0227	0.0009	0.0516	0.0342	0.5449	0.1973	0.128	0.252	0.010	0.575	0.381	6.071	2.198
SC6	6	8	0.0023	0.0183	0.0009	0.0502	0.0353	---	---	0.024	0.193	0.010	0.530	0.373	---	---
SC6	8	10	0.0024	0.0155	0.0010	0.0514	0.0371	0.5078	0.2157	0.024	0.154	0.010	0.512	0.369	5.056	2.147
SC6	13	15	---	0.0144	0.0013	0.0480	0.0459	---	---	---	0.120	0.011	0.401	0.383	---	---
SC6	18	20	---	0.0107	0.0020	0.0505	0.0518	0.4867	0.3613	---	0.081	0.015	0.383	0.393	3.699	2.746
SC7	0	2	0.0014	0.0451	0.0012	0.0474	0.0336	0.8080	0.1071	0.019	0.593	0.015	0.623	0.442	10.618	1.408
SC7	2	4	0.0017	0.0416	0.0017	0.0509	0.0411	---	---	0.017	0.438	0.018	0.536	0.433	---	---
SC7	4	6	0.0000	0.0459	0.0022	0.0531	0.0531	0.9568	0.1618	0.000	0.403	0.019	0.466	0.466	8.408	1.422
SC7	6	8	0.0000	0.0428	0.0021	0.0562	0.0551	---	---	0.000	0.353	0.017	0.463	0.454	---	---
SC7	8	10	0.0000	0.0332	0.0025	0.0518	0.0617	0.9443	0.1807	0.000	0.255	0.019	0.398	0.474	7.256	1.389
SC7	13	15	---	0.0426	0.0036	0.0533	0.0664	---	---	---	0.288	0.024	0.360	0.448	---	---
SC7	18	20	---	0.0176	0.0024	0.0496	0.0798	0.7485	0.2138	---	0.105	0.014	0.294	0.474	4.443	1.269
SC8	0	2	0.0017	0.0422	0.0017	0.0498	0.0212	0.6881	0.1125	0.029	0.722	0.030	0.851	0.363	11.763	1.923
SC8	2	4	0.0017	0.0284	0.0017	0.0535	0.0259	---	---	0.022	0.381	0.023	0.718	0.347	---	---
SC8	4	6	0.0000	0.0143	0.0014	0.0513	0.0311	0.5027	0.1582	0.000	0.170	0.017	0.610	0.370	5.976	1.881
SC8	6	8	0.0000	0.0206	0.0017	0.0521	0.0342	---	---	0.000	0.226	0.019	0.570	0.374	---	---
SC8	8	10	0.0000	0.0286	0.0023	0.0535	0.0393	0.6857	0.2033	0.000	0.279	0.022	0.522	0.383	6.690	1.984
SC8	13	15	---	0.0228	0.0011	0.0479	0.0435	---	---	---	0.194	0.009	0.409	0.371	---	---
SC8	18	20	---	0.0093	0.0013	0.0440	0.0523	0.4048	0.2403	---	0.070	0.009	0.331	0.394	3.048	1.809
SC9	0	2	0.0035	0.0345	0.0014	0.0432	0.0223	0.7367	0.0970	0.061	0.604	0.025	0.757	0.391	12.895	1.698
SC9	2	4	0.0017	0.0258	0.0010	0.0496	0.0325	---	---	0.020	0.312	0.012	0.600	0.393	---	---
SC9	4	6	0.0000	0.0185	0.0016	0.0491	0.0372	0.7729	0.1683	0.000	0.202	0.018	0.536	0.407	8.437	1.837
SC9	6	8	0.0000	0.0220	0.0015	0.0460	0.0411	---	---	0.000	0.211	0.014	0.442	0.395	---	---
SC9	8	10	0.0000	0.0179	0.0017	0.0457	0.0474	0.7246	0.1852	0.000	0.159	0.015	0.405	0.420	6.418	1.640
SC9	13	15	---	0.0217	0.0016	0.0408	0.0632	---	---	---	0.145	0.011	0.273	0.423	---	---
SC9	18	20	---	0.0157	0.0018	0.0373	0.0781	0.6298	0.2272	---	0.089	0.010	0.210	0.441	3.556	1.283

Core	Interval (cm)		mg P or metal / g wet sediment							mg P / g dry sediment						
			Lossely Sorbed-P	Fe-P	Al-P	Org-P	Ca-P	Total Fe Extract	Total Al Extract	Lossely Sorbed-P	Fe-P	Al-P	Org-P	Ca-P	Total Fe Extract	Total Al Extract
SC10	0	2	0.0068	0.0352	0.0010	0.0486	0.0193	0.6853	0.1008	0.126	0.658	0.019	0.907	0.360	12.799	1.883
SC10	2	4	0.0034	0.0311	0.0010	0.0470	0.0275	---	---	0.046	0.415	0.014	0.627	0.367	---	---
SC10	4	6	0.0024	0.0276	0.0015	0.0495	0.0314	0.7334	0.1653	0.028	0.323	0.017	0.579	0.367	8.569	1.932
SC10	6	8	0.0022	0.0266	0.0013	0.0461	0.0336	---	---	0.025	0.297	0.015	0.516	0.376	---	---
SC10	8	10	0.0000	0.0272	0.0015	0.0442	0.0366	0.7005	0.1671	0.000	0.277	0.016	0.450	0.373	7.135	1.703
SC10	13	15	---	0.0289	0.0014	0.0432	0.0441	---	---	---	0.248	0.012	0.369	0.377	---	---
SC10	18	20	---	0.0182	0.0017	0.0423	0.0545	0.5768	0.2542	---	0.132	0.013	0.307	0.396	4.186	1.845
SC6 DUP	0	2	---	0.0399	0.0015	0.0422	0.0219	---	---	---	---	---	---	---	---	---
SC8 DUP	2	4	---	0.0293	0.0014	0.0541	0.0274	---	---	---	---	---	---	---	---	---
SC9 DUP	5	6	---	0.0187	0.0014	0.0621	0.0362	---	---	---	---	---	---	---	---	---

Core	Interval (cm)		mg P / cm^3 wet sediment							g P / m^2 x cm wet sediment				
			Lossely Sorbed-P	Fe-P	Al-P	Org-P	Ca-P	Total Fe Extract	Total Al Extract	Lossely Sorbed-P	Fe-P	Al-P	Org-P	Ca-P
SC1	0	2	0.000	0.030	0.002	0.054	0.051	0.939	0.142	0.000	0.298	0.021	0.537	0.510
SC1	2	4	0.000	0.035	0.004	0.062	0.081	---	---	0.000	0.353	0.041	0.617	0.809
SC1	4	6	0.000	0.076	0.016	0.062	0.094	1.662	0.207	0.000	0.758	0.155	0.625	0.942
SC1	6	8	0.000	0.074	0.034	0.068	0.110			0.000	0.739	0.337	0.679	1.103
SC1	8	10	0.000	0.075	0.041	0.066	0.129	1.683	0.212	0.000	0.746	0.410	0.660	1.287
SC1	13	15	---	0.029	0.027	0.061	0.165	---	---	---	0.288	0.267	0.610	1.652
SC1	18	20	---	0.020	0.007	0.040	0.176	0.919	0.295	---	0.201	0.071	0.404	1.765
SC2	0	2	0.005	0.057	0.003	0.054	0.030	0.871	0.130	0.053	0.566	0.028	0.538	0.298
SC2	2	4	0.004	0.053	0.002	0.057	0.037	---	---	0.037	0.534	0.025	0.565	0.366
SC2	4	6	0.002	0.049	0.003	0.064	0.046	0.859	0.206	0.024	0.492	0.028	0.637	0.457
SC2	6	8	0.000	0.042	0.003	0.063	0.050	---	---	0.000	0.415	0.032	0.630	0.505
SC2	8	10	0.000	0.045	0.011	0.075	0.055	0.894	0.236	0.000	0.452	0.113	0.748	0.550
SC2	13	15	---	0.023	0.003	0.060	0.077	---	---	---	0.231	0.030	0.601	0.772
SC2	18	20	---	0.012	0.003	0.060	0.085	0.500	0.292	---	0.121	0.033	0.603	0.849
SC3	0	2	0.002	0.031	0.002	0.047	0.022	0.633	0.109	0.018	0.310	0.017	0.469	0.225
SC3	2	4	0.002	0.044	0.002	0.066	0.039	---	---	0.024	0.440	0.023	0.662	0.391
SC3	4	6	0.004	0.041	0.002	0.056	0.034	0.689	0.162	0.036	0.412	0.017	0.562	0.341
SC3	6	8	0.000	0.022	0.002	0.059	0.042	---	---	0.000	0.216	0.015	0.592	0.420

Core	Interval (cm)		mg P / cm^3 wet sediment							g P / m^2 x cm wet sediment				
			Lossely Sorbed-P	Fe-P	Al-P	Org-P	Ca-P	Total Fe Extract	Total Al Extract	Lossely Sorbed-P	Fe-P	Al-P	Org-P	Ca-P
SC3	8	10	0.000	0.019	0.002	0.070	0.051	0.648	0.248	0.000	0.187	0.022	0.703	0.514
SC3	13	15	---	0.012	0.002	0.060	0.055	---	---	---	0.124	0.021	0.597	0.550
SC3	18	20	---	0.009	0.002	0.054	0.062	0.443	0.265	---	0.093	0.019	0.540	0.616
SC4	0	2	0.003	0.026	0.001	0.042	0.022	0.541	0.116	0.031	0.263	0.009	0.421	0.221
SC4	2	4	0.004	0.036	0.001	0.054	0.027	---	---	0.035	0.358	0.010	0.539	0.267
SC4	4	6	0.004	0.025	0.001	0.052	0.033	0.547	0.183	0.042	0.249	0.011	0.521	0.330
SC4	6	8	0.000	0.022	0.001	0.051	0.042	---	---	0.000	0.217	0.008	0.509	0.424
SC4	8	10	0.000	0.016	0.001	0.051	0.049	0.553	0.225	0.000	0.164	0.008	0.509	0.492
SC4	13	15	---	0.011	0.001	0.051	0.053	---	---	---	0.107	0.007	0.509	0.534
SC4	18	20	---	0.009	0.001	0.051	0.062	0.329	0.280	---	0.092	0.014	0.506	0.617
SC5	0	2	0.002	0.062	0.002	0.053	0.052	1.108	0.160	0.023	0.618	0.022	0.534	0.519
SC5	2	4	0.000	0.071	0.003	0.064	0.069	---	---	0.000	0.713	0.034	0.641	0.685
SC5	4	6	0.000	0.059	0.003	0.065	0.085	1.113	0.200	0.000	0.594	0.034	0.649	0.850
SC5	6	8	0.000	0.070	0.009	0.072	0.113	---	---	0.000	0.705	0.093	0.717	1.131
SC5	8	10	0.000	0.052	0.017	0.070	0.147	1.133	0.247	0.000	0.524	0.171	0.704	1.475
SC5	13	15	---	0.129	0.046	0.074	0.204	---	---	---	1.294	0.463	0.745	2.042
SC5	18	20	---	0.015	0.003	0.039	0.186	0.644	0.346	---	0.151	0.034	0.390	1.863
SC6	0	2	0.005	0.041	0.001	0.044	0.022	0.581	0.115	0.046	0.410	0.009	0.440	0.218
SC6	2	4	0.004	0.036	0.001	0.047	0.028	---	---	0.036	0.362	0.015	0.474	0.284
SC6	4	6	0.012	0.024	0.001	0.054	0.036	0.569	0.206	0.120	0.237	0.010	0.539	0.358
SC6	6	8	0.002	0.019	0.001	0.053	0.037	---	---	0.024	0.191	0.010	0.526	0.370
SC6	8	10	0.003	0.016	0.001	0.054	0.039	0.534	0.227	0.026	0.163	0.010	0.541	0.390
SC6	13	15	---	0.015	0.001	0.051	0.049	---	---	---	0.153	0.014	0.510	0.487
SC6	18	20	---	0.011	0.002	0.054	0.055	0.520	0.386	---	0.114	0.021	0.539	0.553
Ex1	0	4	0.000	0.059	0.002	0.053	0.023	---	---	---	0.588	0.024	0.528	0.233
Ex2	0	4	0.000	0.057	0.002	0.053	0.024	---	---	---	0.565	0.024	0.527	0.240
Ex3	0	4	0.000	0.031	0.002	0.052	0.033	---	---	---	0.308	0.017	0.520	0.326
Ex4	0	4	0.000	0.055	0.006	0.057	0.035	---	---	---	0.548	0.056	0.575	0.355
Ex5	0	4	0.000	0.049	0.005	0.058	0.074	---	---	---	0.493	0.051	0.583	0.743
Ex6	0	4	---	0.042	0.006	0.054	0.077	---	---	---	0.419	0.063	0.541	0.771
SC1 DUP	0	2	0.000	0.033	0.003	0.053	0.052	---	---	---	0.329	0.027	0.534	0.521
SC2 DUP	4	6	---	0.053	0.003	0.062	0.048	---	---	---	0.534	0.032	0.618	0.476

Core	Interval (cm)		mg P / cm^3 wet sediment							g P / m^2 x cm wet sediment				
			Lossely Sorbed-P	Fe-P	Al-P	Org-P	Ca-P	Total Fe Extract	Total Al Extract	Lossely Sorbed-P	Fe-P	Al-P	Org-P	Ca-P
SC7	0	2	0.001	0.047	0.001	0.049	0.035	0.839	0.111	0.015	0.469	0.012	0.492	0.349
SC7	2	4	0.002	0.044	0.002	0.053	0.043	---	---	0.017	0.436	0.018	0.534	0.431
SC7	4	6	0.000	0.049	0.002	0.056	0.056	1.013	0.171	0.000	0.486	0.023	0.562	0.562
SC7	6	8	0.000	0.046	0.002	0.060	0.059	---	---	0.000	0.455	0.022	0.597	0.586
SC7	8	10	0.000	0.036	0.003	0.055	0.066	1.009	0.193	0.000	0.355	0.026	0.554	0.659
SC7	13	15	---	0.046	0.004	0.058	0.072	---	---	---	0.460	0.039	0.575	0.717
SC7	18	20	---	0.019	0.003	0.054	0.087	0.818	0.233	---	0.193	0.026	0.542	0.872
SC8	0	2	0.002	0.043	0.002	0.051	0.022	0.707	0.116	0.018	0.434	0.018	0.511	0.218
SC8	2	4	0.002	0.029	0.002	0.055	0.027	---	---	0.017	0.294	0.018	0.554	0.268
SC8	4	6	0.000	0.015	0.001	0.053	0.032	0.524	0.165	0.000	0.149	0.015	0.535	0.324
SC8	6	8	0.000	0.022	0.002	0.054	0.036	---	---	0.000	0.216	0.018	0.545	0.357
SC8	8	10	0.000	0.030	0.002	0.056	0.041	0.721	0.214	0.000	0.301	0.024	0.562	0.413
SC8	13	15	---	0.024	0.001	0.051	0.046	---	---	---	0.242	0.012	0.508	0.461
SC8	18	20	---	0.010	0.001	0.047	0.056	0.433	0.257	---	0.100	0.013	0.470	0.560
SC9	0	2	0.004	0.035	0.001	0.044	0.023	0.757	0.100	0.036	0.354	0.015	0.444	0.229
SC9	2	4	0.002	0.027	0.001	0.052	0.034	---	---	0.018	0.268	0.011	0.516	0.338
SC9	4	6	0.000	0.019	0.002	0.051	0.039	0.808	0.176	0.000	0.194	0.017	0.514	0.390
SC9	6	8	0.000	0.023	0.002	0.048	0.043	---	---	0.000	0.232	0.016	0.484	0.433
SC9	8	10	0.000	0.019	0.002	0.048	0.050	0.767	0.196	0.000	0.190	0.018	0.484	0.502
SC9	13	15	---	0.023	0.002	0.044	0.068	---	---	---	0.235	0.017	0.441	0.683
SC9	18	20	---	0.017	0.002	0.041	0.086	0.691	0.249	---	0.173	0.019	0.409	0.857
SC10	0	2	0.007	0.036	0.001	0.050	0.020	0.702	0.103	0.069	0.361	0.011	0.497	0.197
SC10	2	4	0.004	0.032	0.001	0.049	0.028	---	---	0.035	0.322	0.011	0.486	0.284
SC10	4	6	0.003	0.029	0.002	0.052	0.033	0.763	0.172	0.025	0.287	0.015	0.515	0.327
SC10	6	8	0.002	0.028	0.001	0.048	0.035	---	---	0.023	0.277	0.014	0.481	0.350
SC10	8	10	0.000	0.028	0.002	0.046	0.038	0.734	0.175	0.000	0.285	0.016	0.463	0.383
SC10	13	15	---	0.031	0.001	0.046	0.047	---	---	---	0.306	0.015	0.457	0.467
SC10	18	20	---	0.019	0.002	0.045	0.058	0.617	0.272	---	0.194	0.019	0.453	0.583
SC6 DUP	0	2	---	---	---	---	---	---	---	---	---	---	---	---
SC8 DUP	2	4	---	---	---	---	---	---	---	---	---	---	---	---
SC9 DUP	5	6	---	---	---	---	---	---	---	---	---	---	---	---

Appendix E

Phosphorus Fractionation Profiles

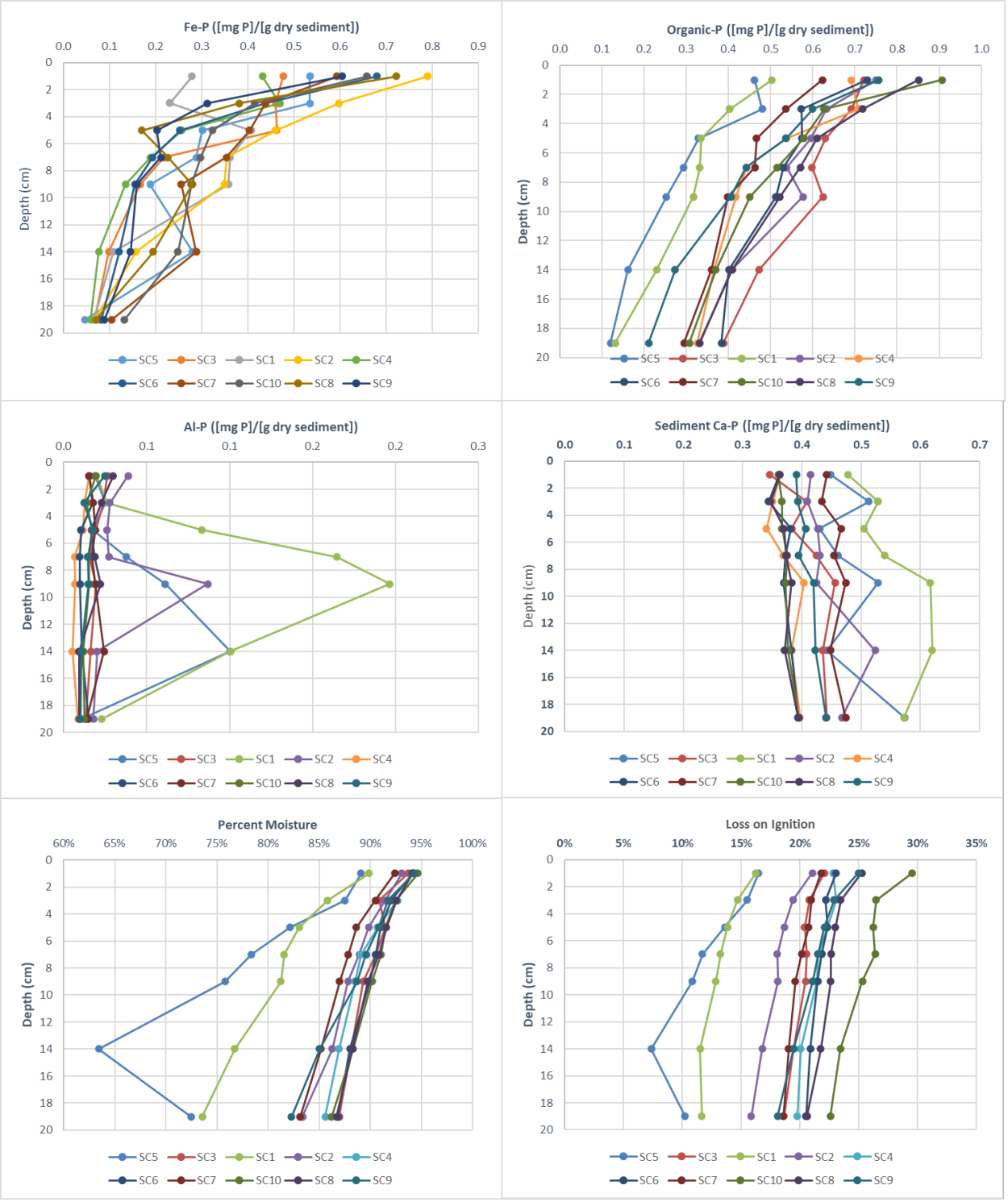
Fe-P ([mg P]/[g dry sediment])
Organic-P ([mg P]/[g dry sediment])
Al-P ([mg P]/[g dry sediment])
Sediment Ca-P ([mg P]/[g dry sediment])
Percent Moisture
Loss on Ignition
Depth (cm)
SC5 SC3 SC1 SC2 SC4
SC6 SC7 SC10 SC8 SC9

Appendix F

Calibration Figures

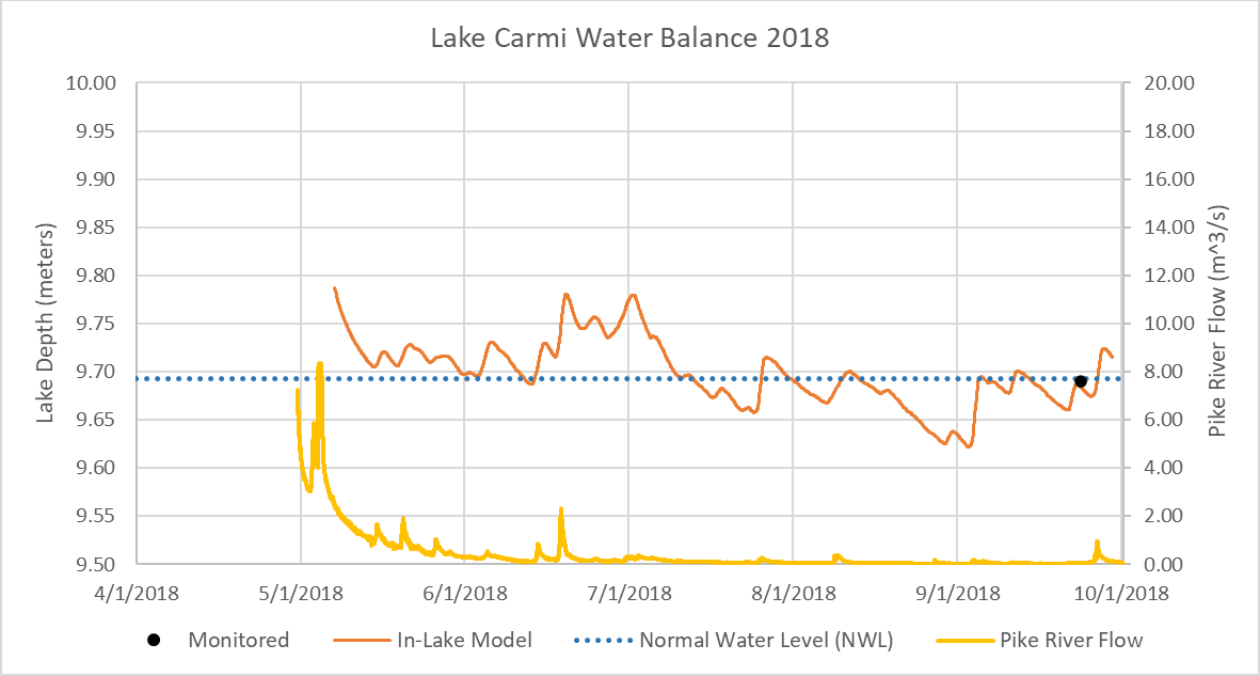

Figure F-1 2018 water surface elevation calibration

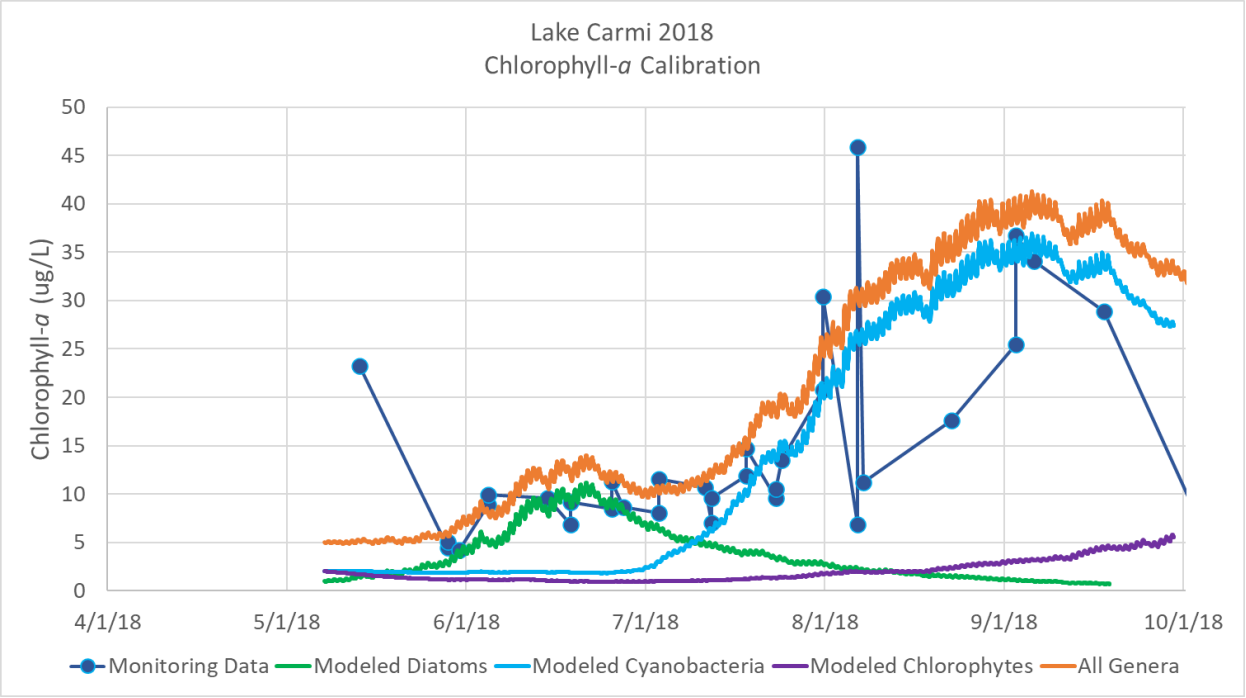

Figure F-2 2018 surface phytoplankton and chlorophyll-*a* calibration

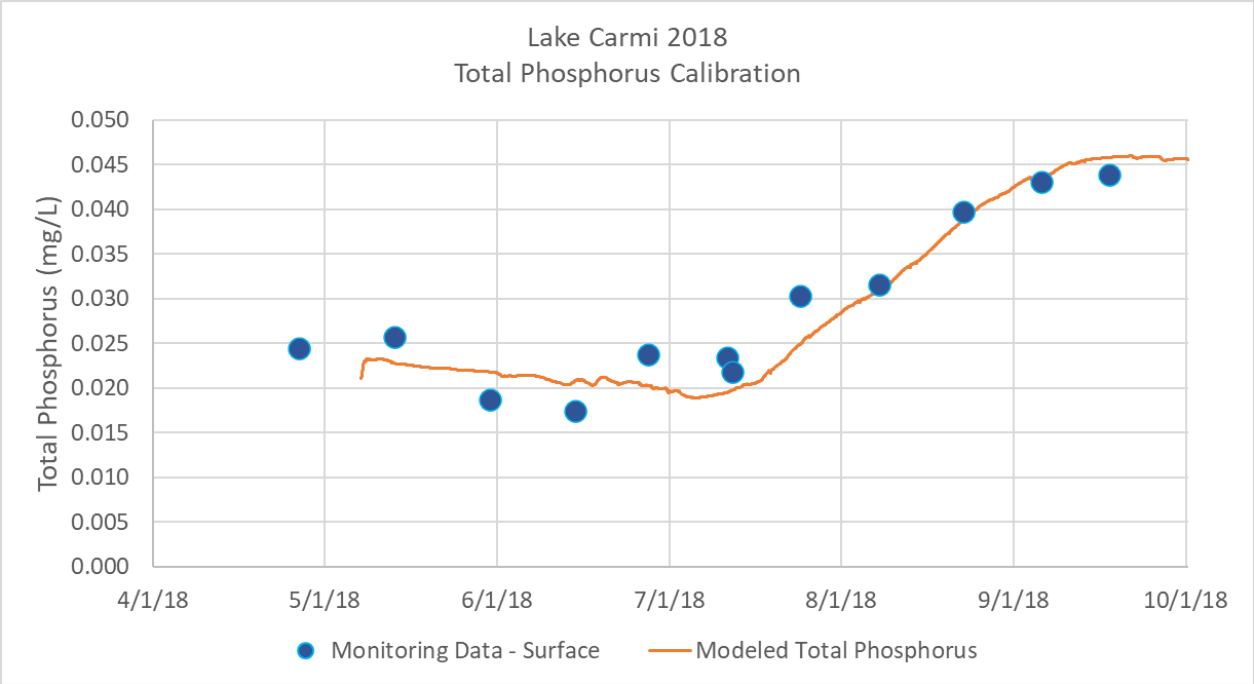

Figure F-3 2018 surface total phosphorus calibration

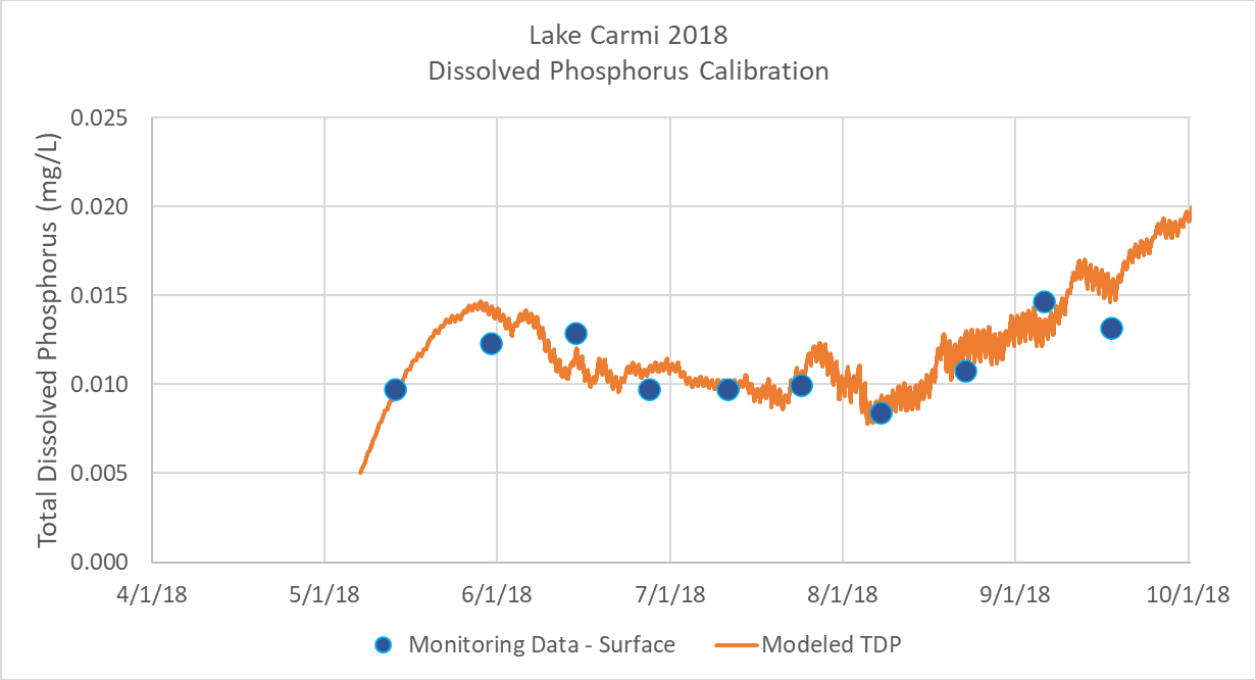

Figure F-4 2018 surface total dissolved phosphorus calibration

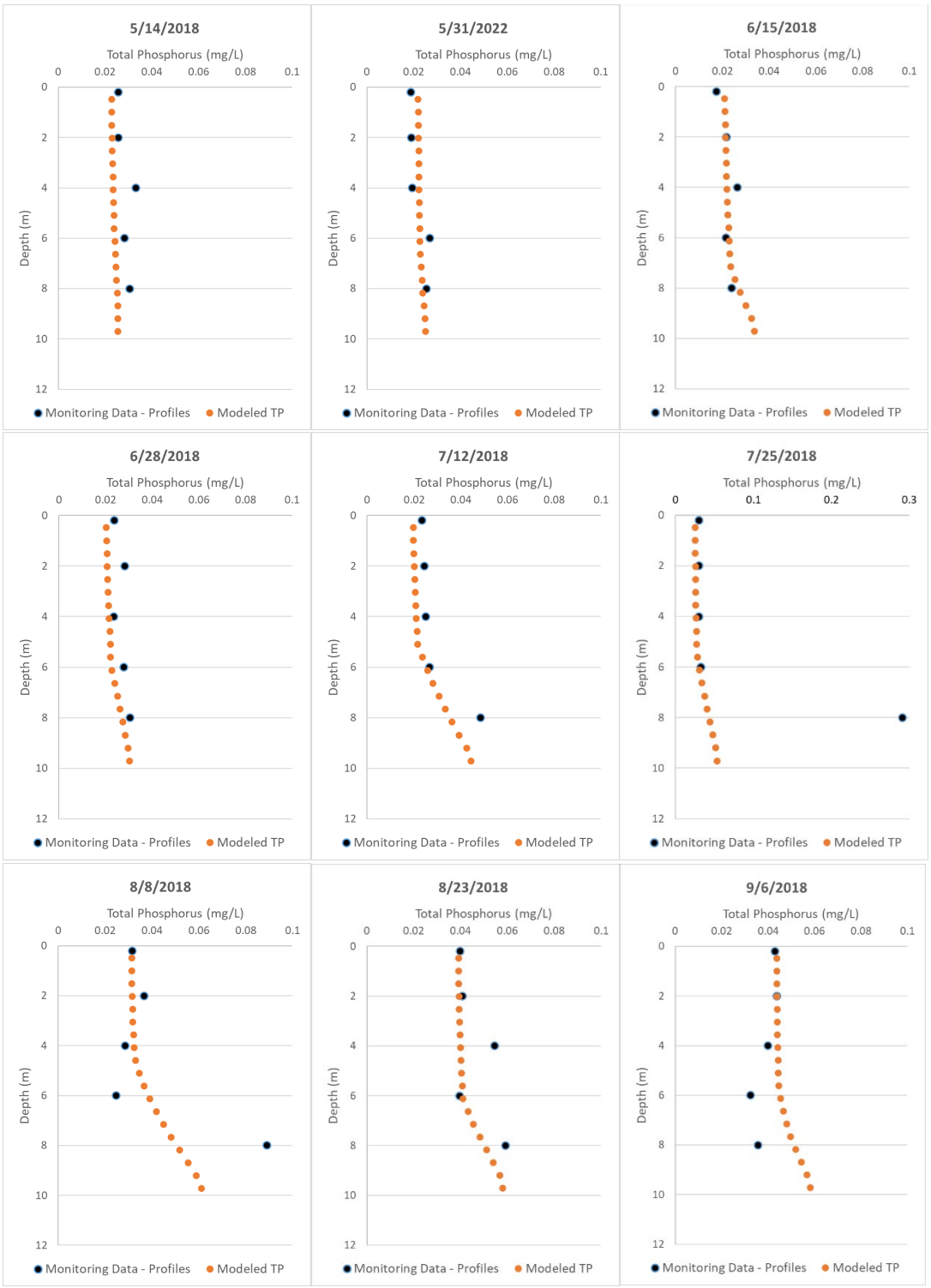

Figure F-5 2018 total phosphorus profile calibration

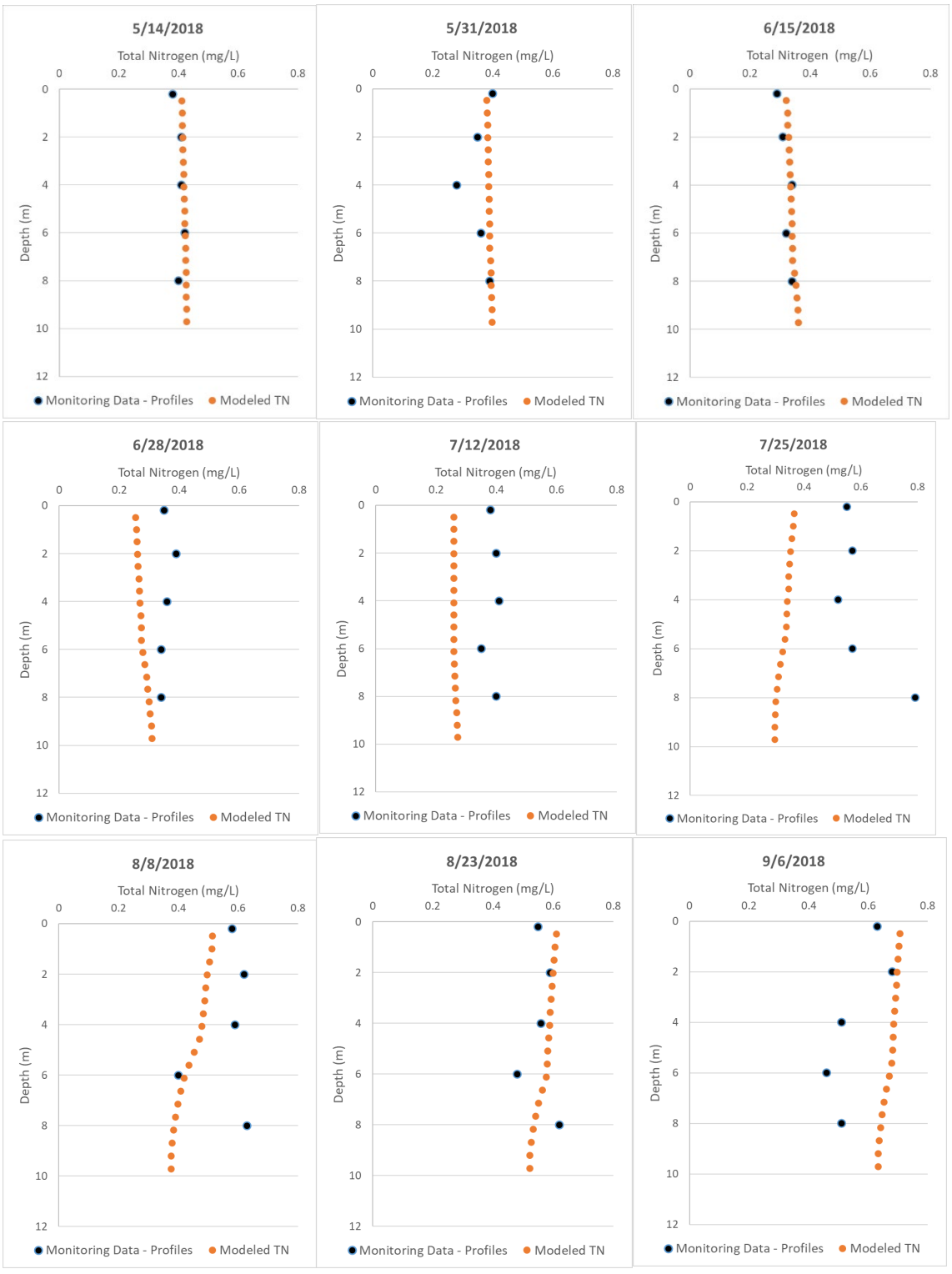

Figure F-6 2018 total nitrogen profile calibration

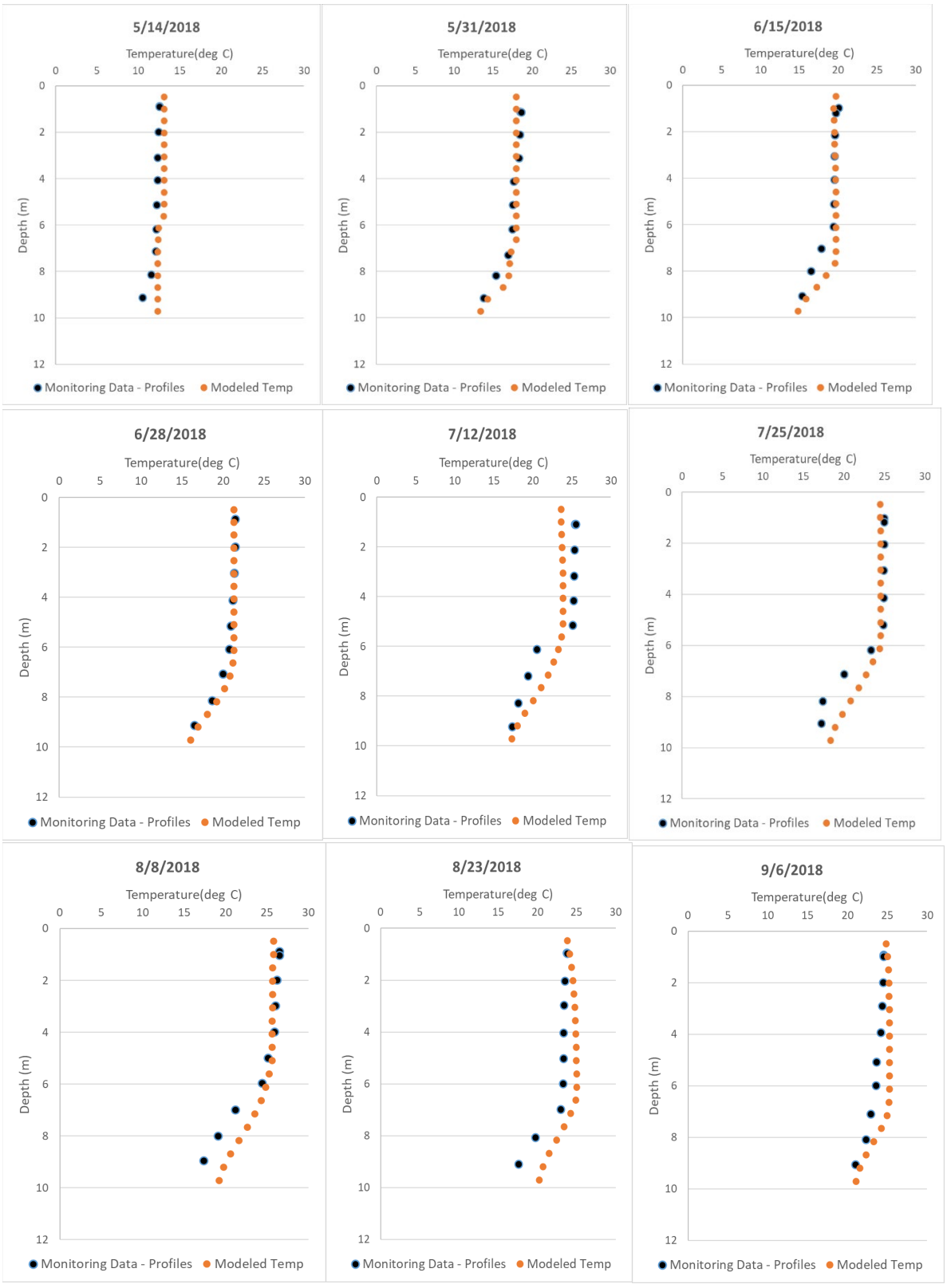

Figure F-7 2018 temperature profile calibration

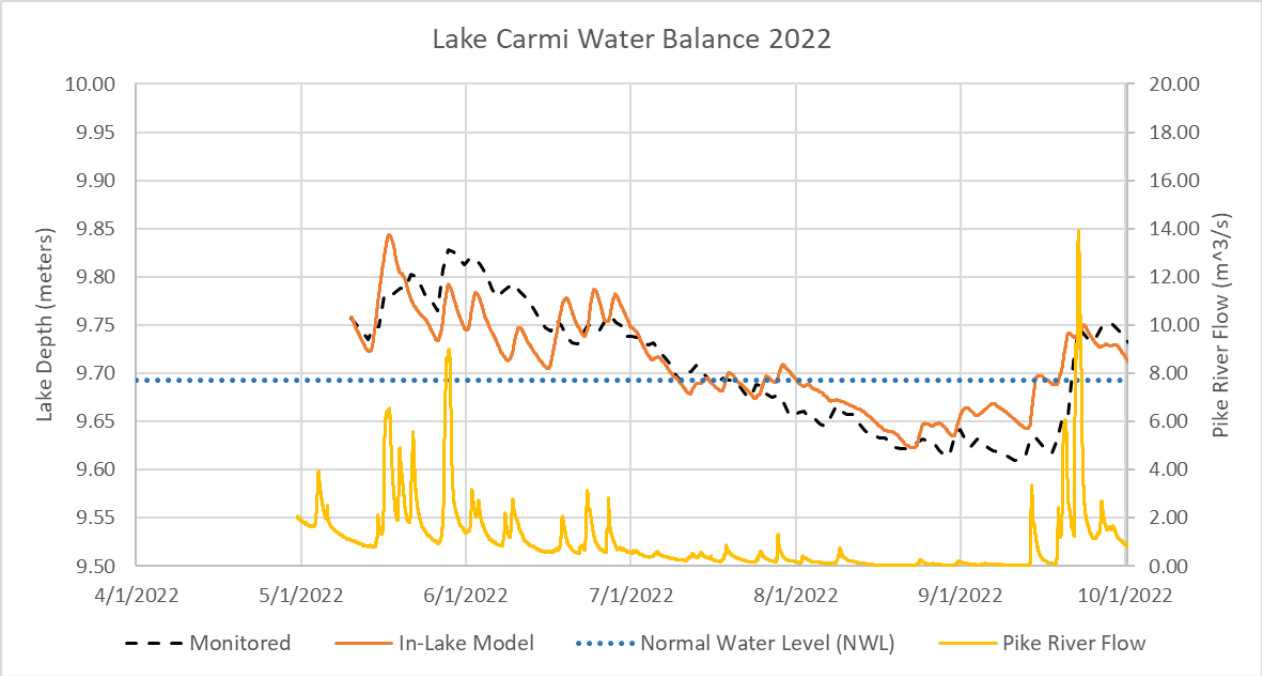

Figure F-8 2022 water surface elevation calibration

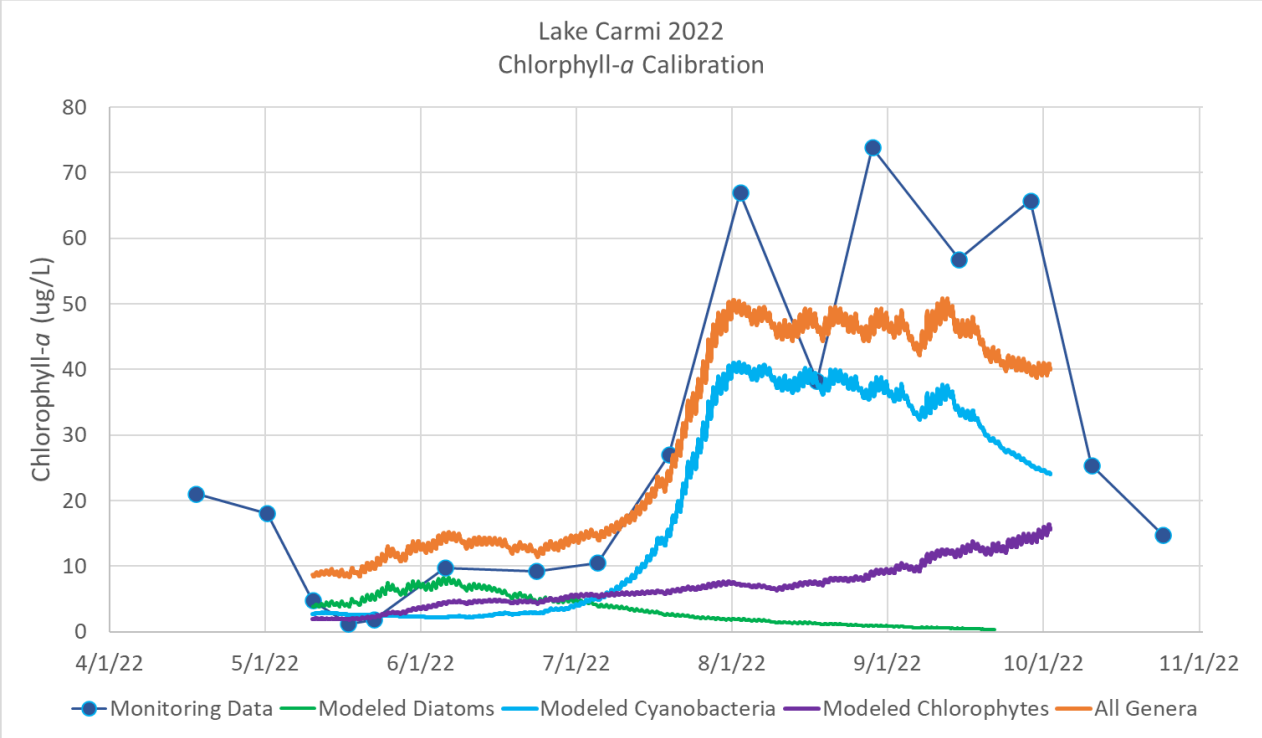

Figure F-9 2022 surface phytoplankton and chlorophyll-*a* calibration

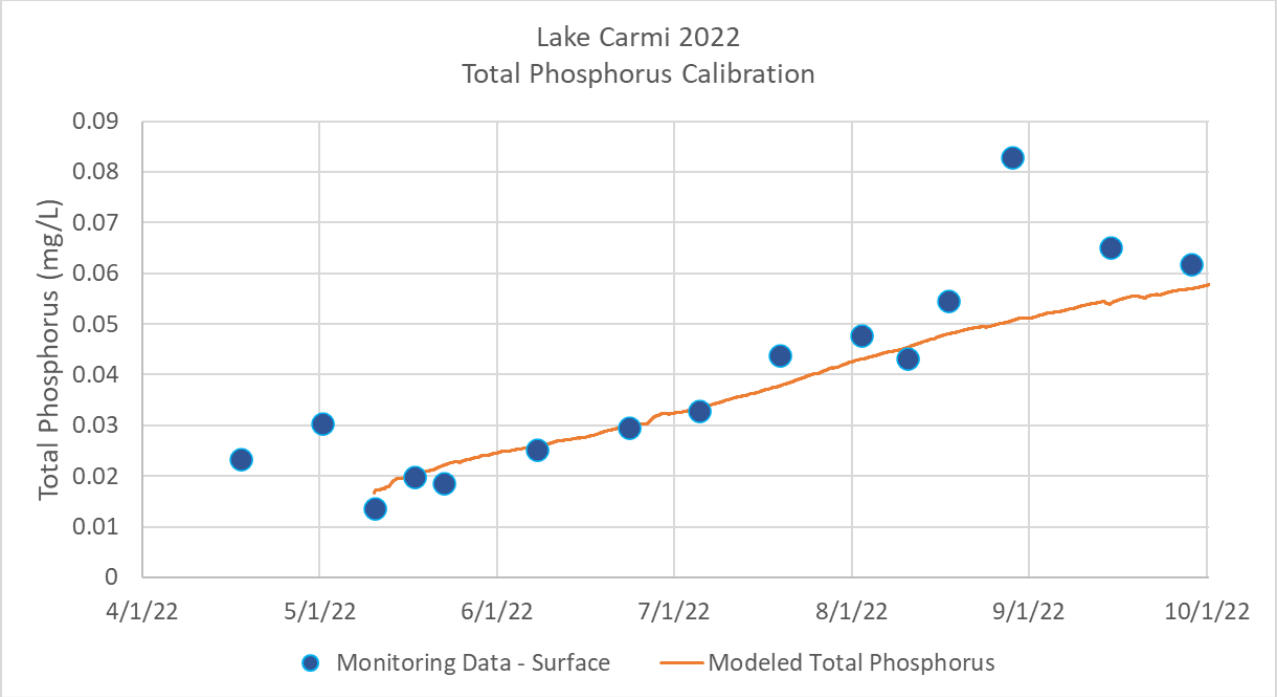

Figure F-10 2022 surface total phosphorus calibration

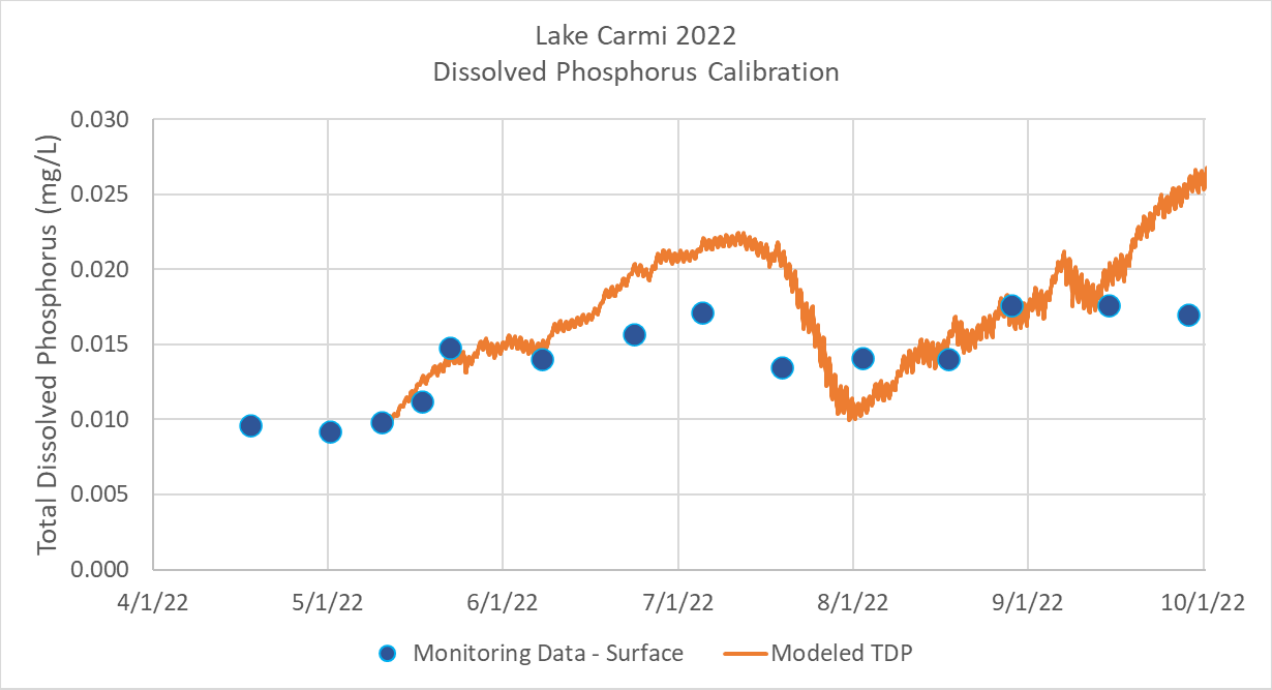

Figure F-11 2022 surface total dissolved phosphorus calibration

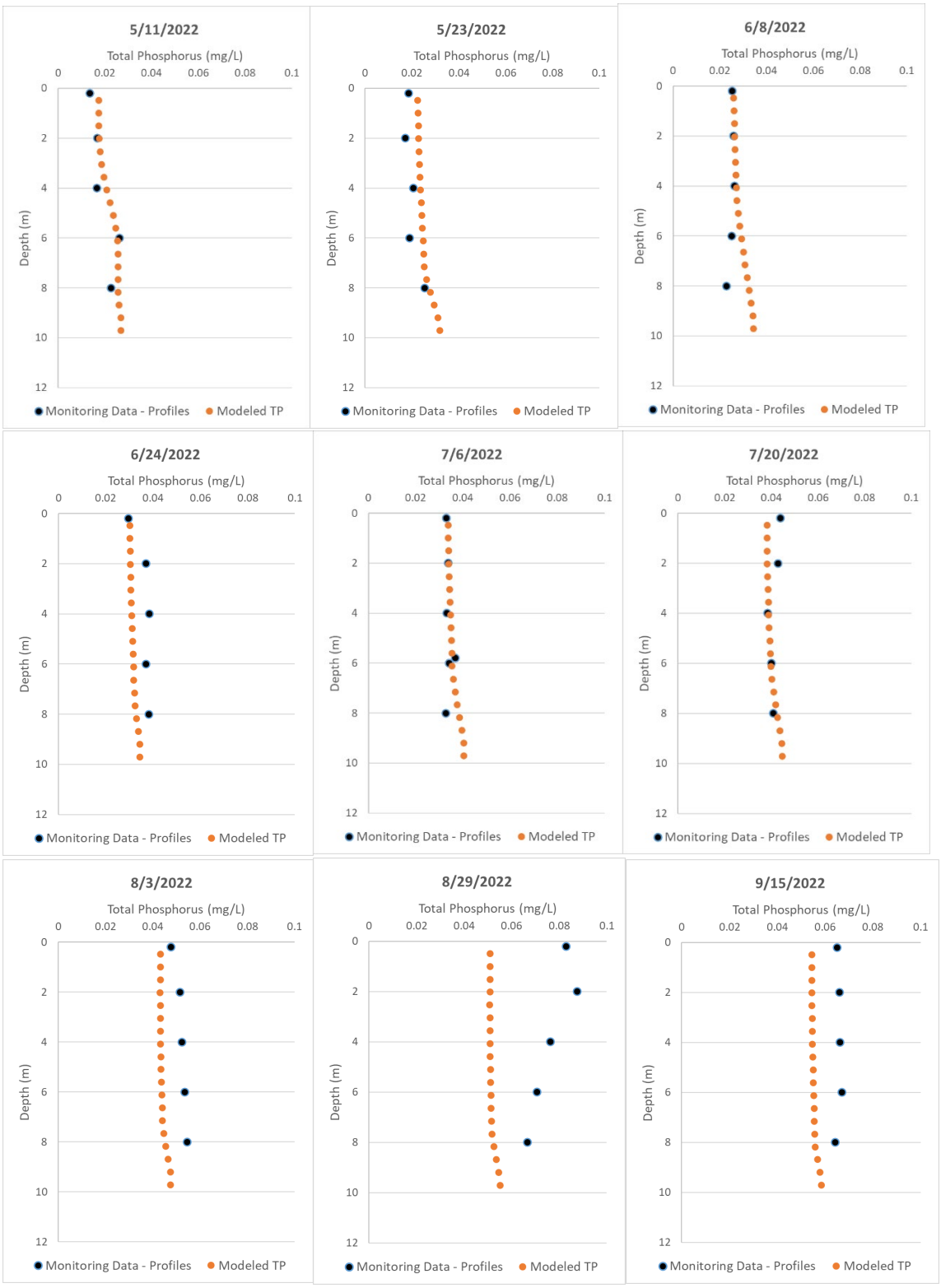

Figure F-12 2022 total phosphorus profile calibration

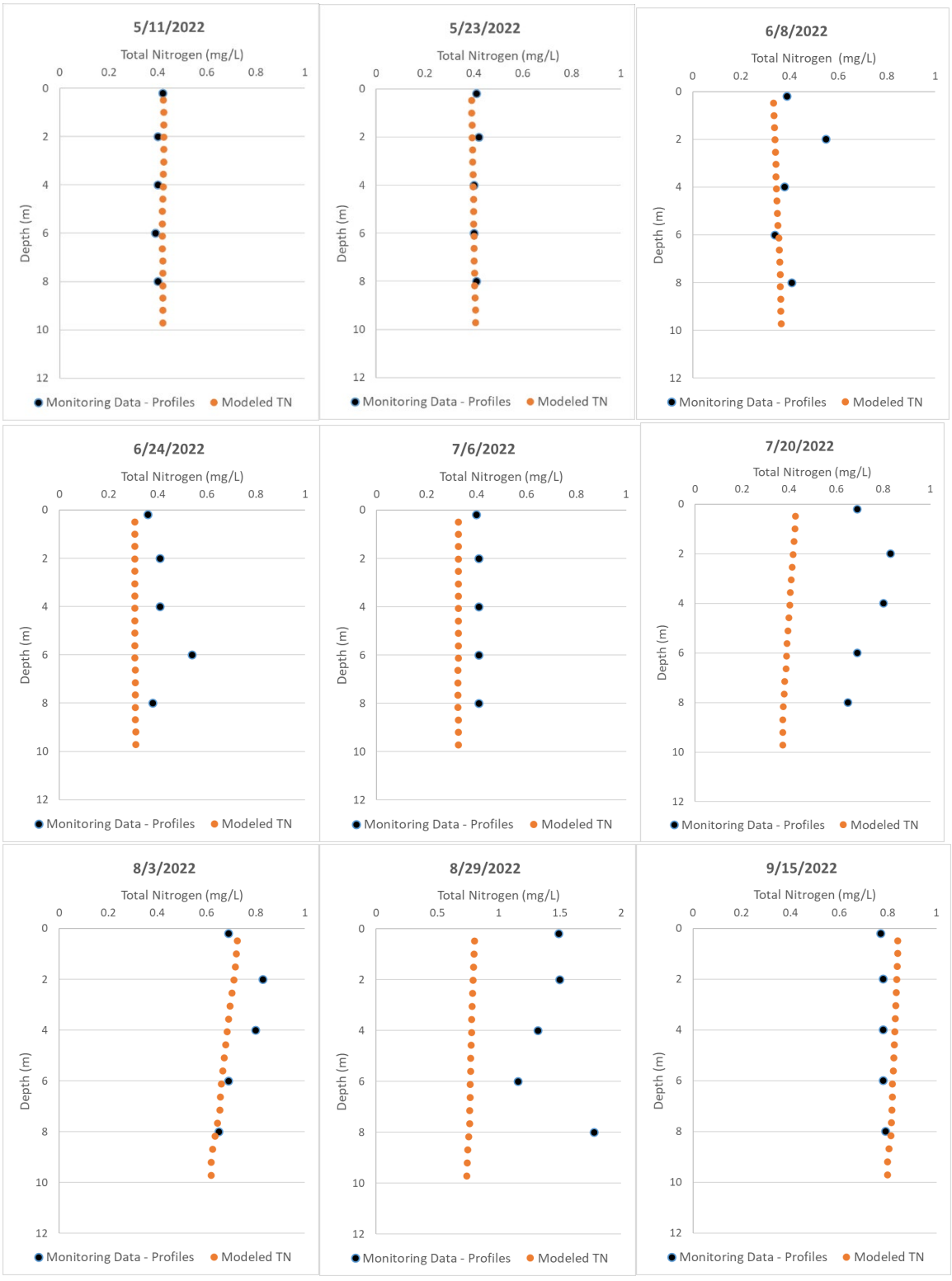

Figure F-13 2022 total nitrogen profile calibration

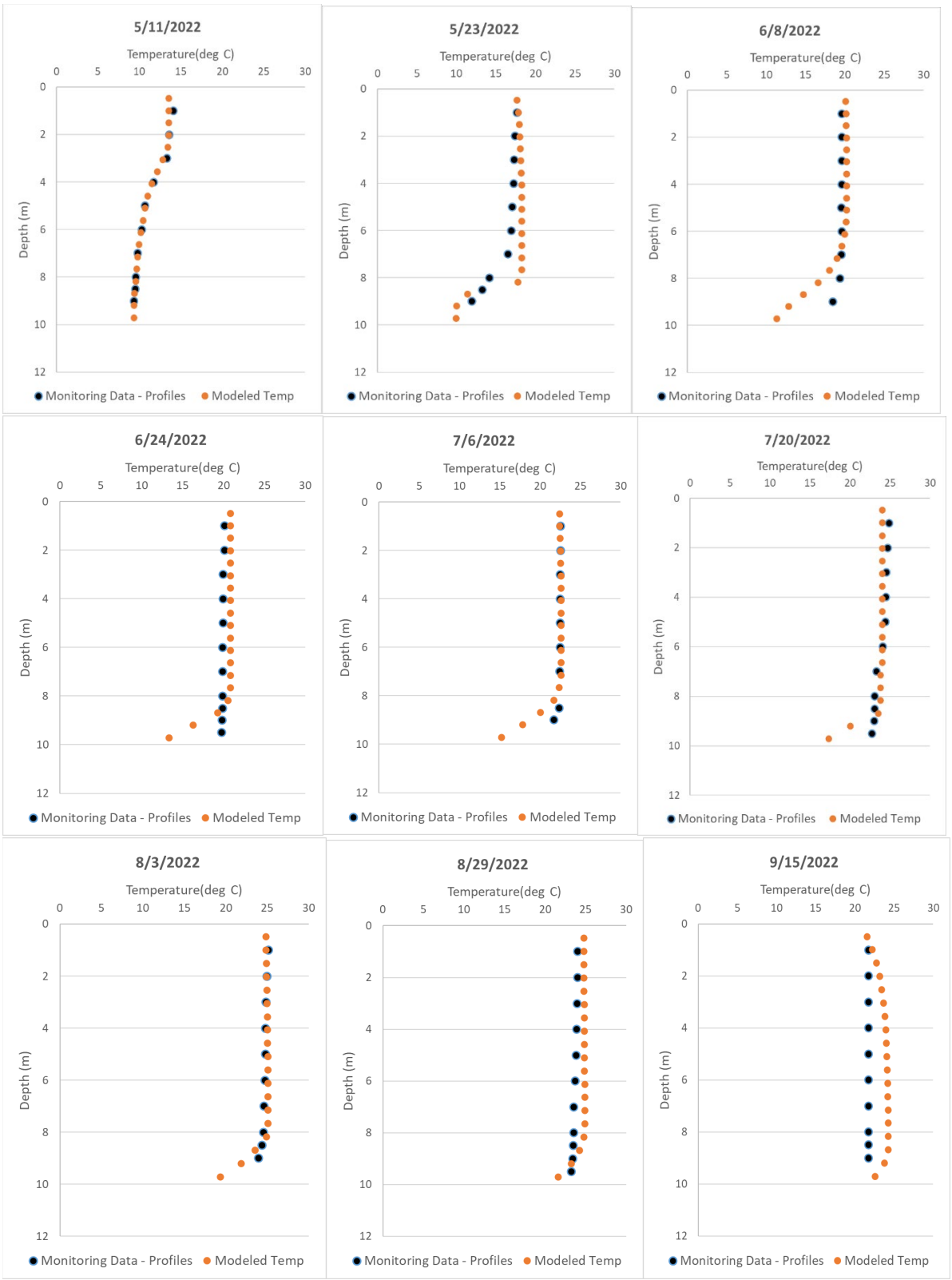

Figure F-14 2022 temperature profile calibration

Appendix G

Figures Showing Water Quality With Aluminum Treatment

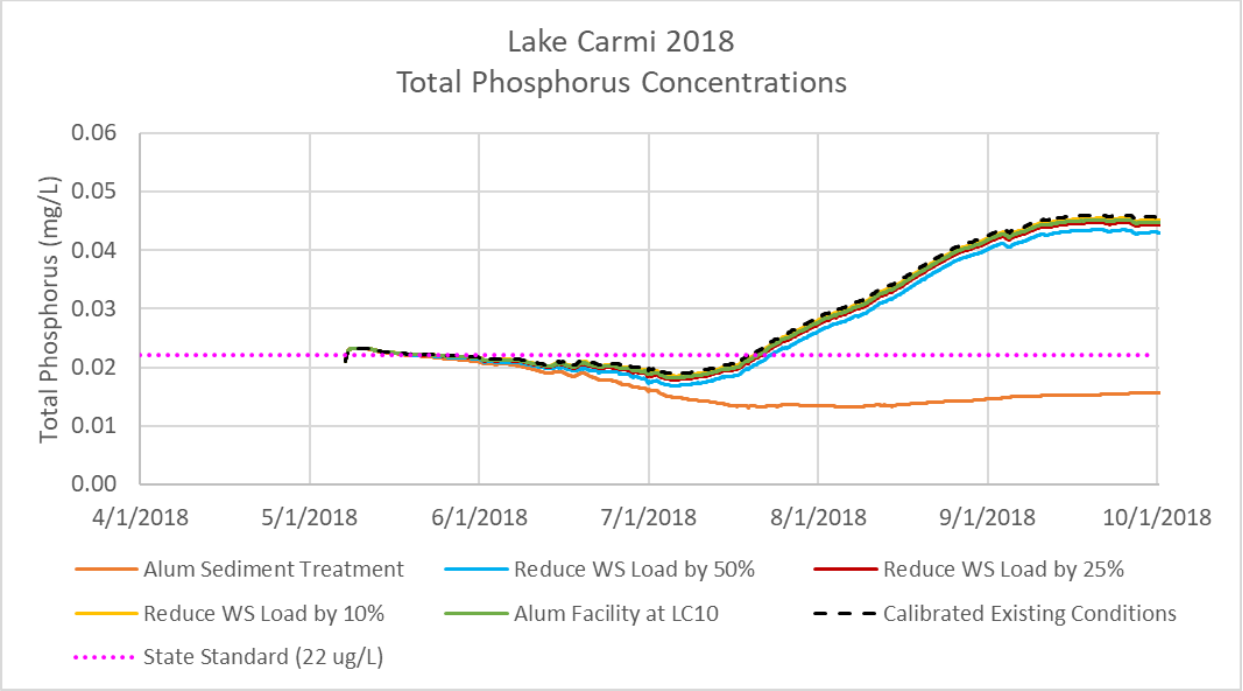

Figure G-1 **2018 Barr Model predicted changes to total phosphorus concentrations with implementation of BMPs**

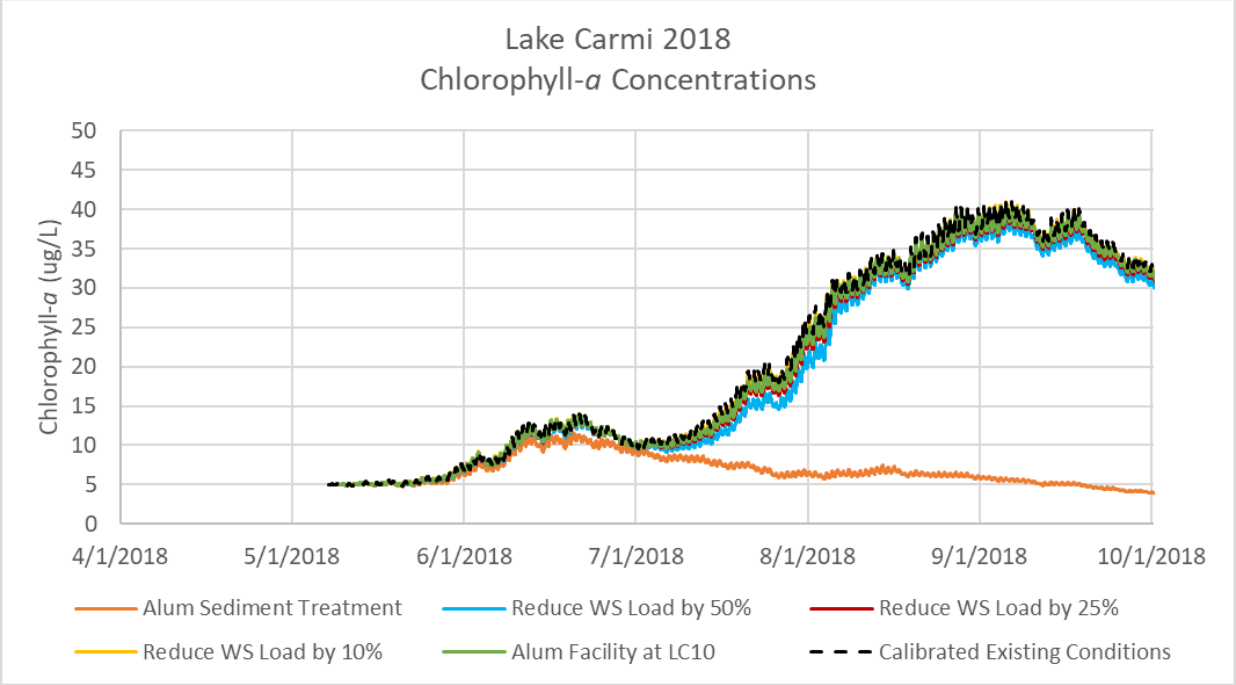

Figure G-2 **2018 Barr Model predicted changes to chlorophyll-*a* concentrations with implementation of BMPs**

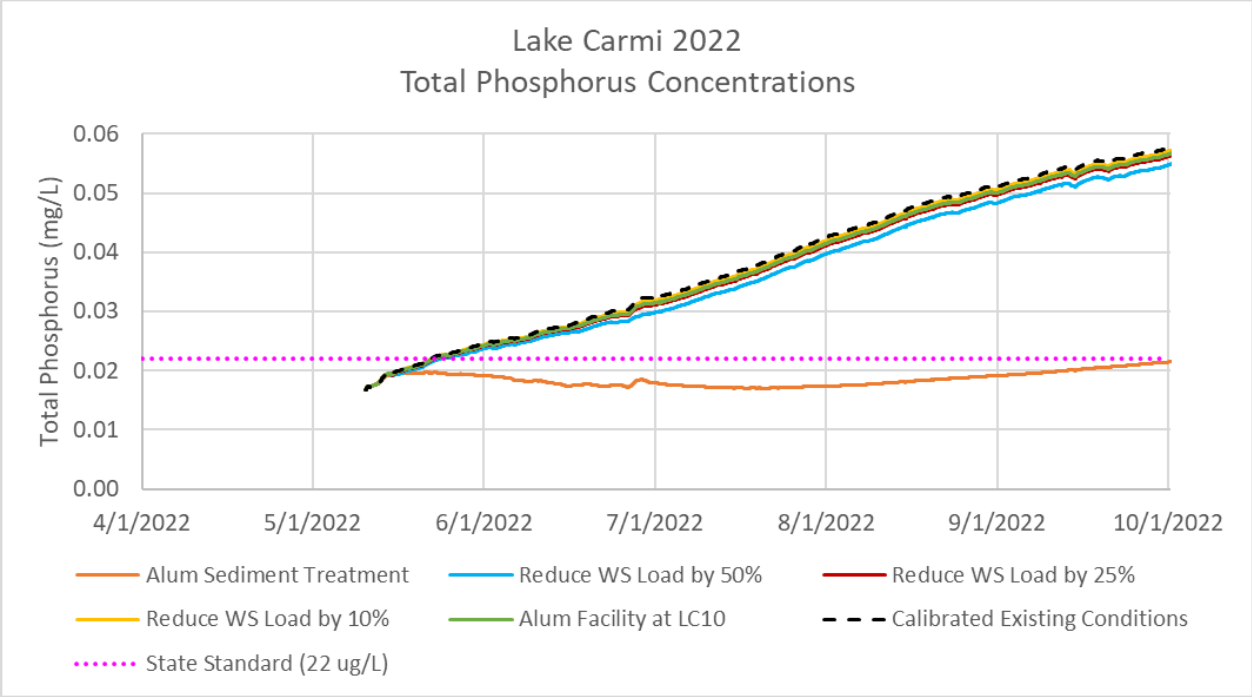

Figure G-3 **2022 Barr Model predicted changes to total phosphorus concentrations with implementation of BMPs**

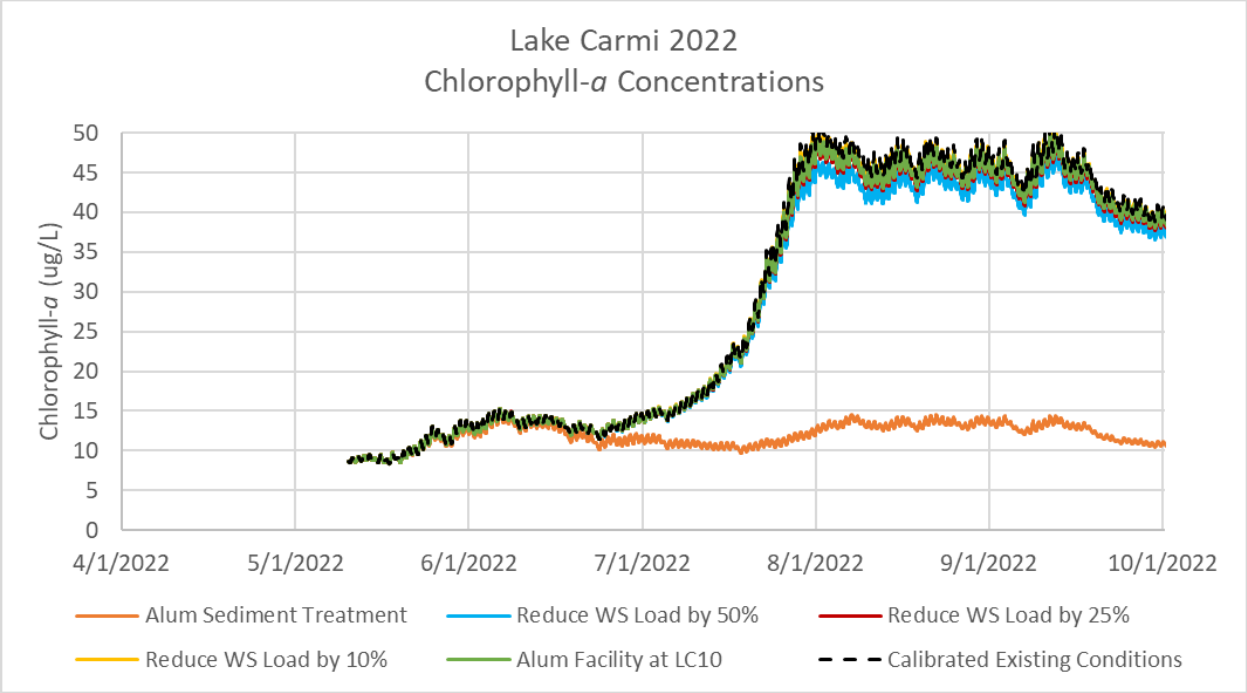

Figure G-4 **2022 Barr Model predicted changes to chlorophyll-*a* concentrations with implementation of BMPs**